

Heading for a glucose sensor : designing and testing a new principle

Citation for published version (APA):

Stroe-Biezen, van, S. A. M. (1993). *Heading for a glucose sensor : designing and testing a new principle*. [Phd Thesis 1 (Research TU/e / Graduation TU/e), Chemical Engineering and Chemistry]. Technische Universiteit Eindhoven. <https://doi.org/10.6100/IR407752>

DOI:

[10.6100/IR407752](https://doi.org/10.6100/IR407752)

Document status and date:

Published: 01/01/1993

Document Version:

Publisher's PDF, also known as Version of Record (includes final page, issue and volume numbers)

Please check the document version of this publication:

- A submitted manuscript is the version of the article upon submission and before peer-review. There can be important differences between the submitted version and the official published version of record. People interested in the research are advised to contact the author for the final version of the publication, or visit the DOI to the publisher's website.
- The final author version and the galley proof are versions of the publication after peer review.
- The final published version features the final layout of the paper including the volume, issue and page numbers.

[Link to publication](#)

General rights

Copyright and moral rights for the publications made accessible in the public portal are retained by the authors and/or other copyright owners and it is a condition of accessing publications that users recognise and abide by the legal requirements associated with these rights.

- Users may download and print one copy of any publication from the public portal for the purpose of private study or research.
- You may not further distribute the material or use it for any profit-making activity or commercial gain
- You may freely distribute the URL identifying the publication in the public portal.

If the publication is distributed under the terms of Article 25fa of the Dutch Copyright Act, indicated by the "Taverne" license above, please follow below link for the End User Agreement:

www.tue.nl/taverne

Take down policy

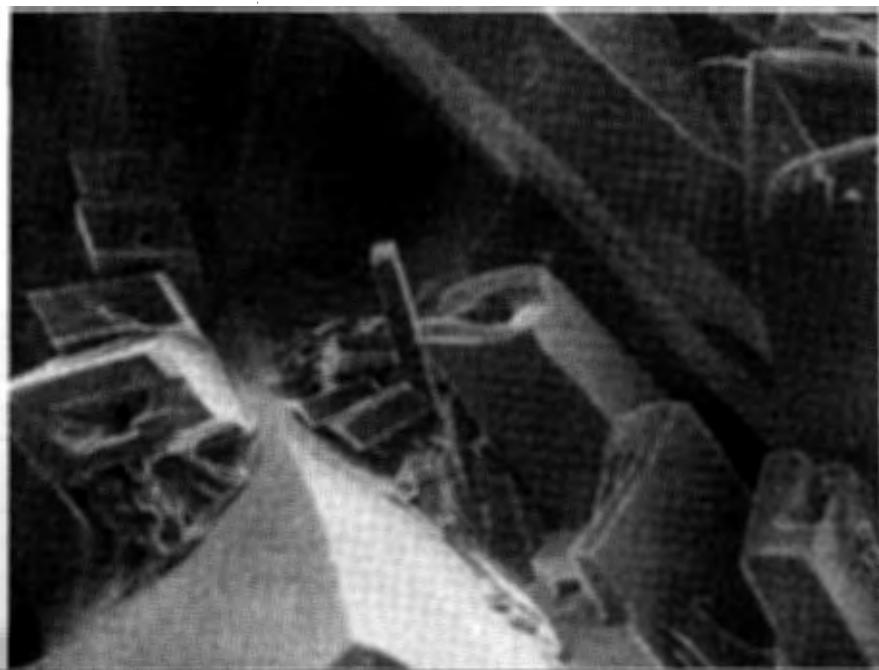
If you believe that this document breaches copyright please contact us at:

openaccess@tue.nl

providing details and we will investigate your claim.

Heading for a Glucose Sensor

Designing and testing a new principle



Saskia van Stroe-Biezen

Heading for a Glucose Sensor

Designing and testing a new principle

PROEFSCHRIFT

ter verkrijging van de graad van doctor aan de
Technische Universiteit Eindhoven, op gezag van
de Rector Magnificus, prof.dr. J.H. van Lint,
voor een commissie aangewezen door het College
van Dekanen in het openbaar te verdedigen op
dinsdag 21 december 1993 om 16.00 uur

door

SASKIA ANNA MARIA VAN STROE-BIEZEN

Geboren te Eindhoven



Dit proefschrift is goedgekeurd door de promotoren

prof.dr.ir. F.M. Everaerts

en

prof.dr.ir. C.A.M.G. Cramers

en de copromotor

dr. L.J.J. Janssen

Het in dit proefschrift beschreven onderzoek werd gefinancierd door de Stichting voor de Technische Wetenschappen (STW, projectnummer EST 99.1911 (OBS))

*...non est, crede mihi, sapientis dicere "vivam":
sera nimis vita est crastina: vive hodie.*

Martialis 1,15

Voor mijn ouders

Aan Alberto

Dankwoord

Op deze plaats wil ik iedereen bedanken die op een of andere manier heeft bijgedragen aan het tot stand komen van dit proefschrift. Mijn zes afstudeerders, mijn stagiaires, verschillende mensen die me met raad en daad hebben bijgestaan, de STW-gebruikerscommissie en mijn promotiecommissie, het zijn er teveel om op te noemen.

Toch wil ik een paar mensen met name noemen. Mijn ouders wil ik bedanken voor de mogelijkheden en de steun die ze me steeds geboden hebben om te studeren en te promoveren. Mijn copromotor, Jos Janssen, heeft me gedurende drie jaar op stimulerende wijze begeleid, waarbij hij de voor mij zo belangrijke zelfstandigheid niet heeft ondermijnd. Mijn promotor, Frans Everaerts, heeft steeds achter me gestaan. Ook al was de "afstand" groot, toch hebben we een goede relatie weten op te bouwen. Tot slot wil ik mijn man Alberto bedanken. Alberto, jouw steun, stimulans, hulp en begrip hebben mijn promotietijd tot een plezierige tijd gemaakt en hebben er toe geleid dat de promotie al op dit tijdstip kon plaatsvinden.

Cover: "Let's have a closer look at glucose"
Microprobe photograph of glucose crystals
by Alberto J. van Stroo
(magnification 700x, 15 keV, 10 nA)

CONTENTS

CHAPTER 1. GENERAL INTRODUCTION	1
1.1 The need for glucose sensors	1
1.2 Present glucose sensors	2
1.3 A new principle for a short-term <i>in vivo</i> glucose sensor	4
1.4 Scope of this thesis	7
References	9
CHAPTER 2. THE DIFFUSION COEFFICIENTS OF OXYGEN, HYDROGEN PEROXIDE AND GLUCOSE IN A HYDROGEL	10
2.1 Introduction	10
2.2 Theory	11
2.3 Experimental	17
2.4 Results and discussion	20
References	28
CHAPTER 3. THE KINETIC PARAMETERS OF SOLUBLE GLUCOSE OXIDASE	29
3.1 Introduction	29
3.2 The solubility of oxygen in glucose solutions	31
3.2.1 Theory	31
3.2.2 Experimental	32
3.2.3 Results and discussion	34
3.3 A kinetic study of soluble glucose oxidase using a rotating disc electrode	42
3.3.1 Theory	42
3.3.2 Experimental	43
3.3.3 Results and discussion	46
3.3.4 Conclusions	54
References	55

CHAPTER 4. THE INHERENT KINETIC PARAMETERS OF IMMOBILIZED GLUCOSE OXIDASE	57
4.1 Introduction	57
4.2 Theory	58
4.3 Experimental	67
4.4 Results and discussion	69
References	77
CHAPTER 5. TESTING THE PERFORMANCE OF A MACRO GLUCOSE SENSOR	78
5.1 The sensor simulation program	78
5.2 Calculations with the sensor simulation program	84
5.3 Macro-sensor experiments	87
5.3.1 Introduction	87
5.3.2 Experimental	89
5.3.3 Results and discussion	92
5.4 Concluding remarks	97
References	99
CHAPTER 6. THE USAGE OF MEMBRANES IN GLUCOSE SENSORS. A REVIEW	100
6.1 Immobilization of glucose oxidase for usage in a glucose sensor	100
6.1.1 Introduction	100
6.1.2 Immobilization of glucose oxidase	102
6.1.2.1 GO-immobilization by adsorption	102
6.1.2.2 GO-immobilization by gel entrapment	105
6.1.2.3 GO-immobilization by covalent binding	107
6.1.3 Non-immobilization method	114
6.1.4 Concluding remarks	114
6.2 Coating membranes in a glucose sensor	115
References	117

APPENDIX I	120
APPENDIX II	122
LIST OF SYMBOLS	132
SUMMARY	135
SAMENVATTING	137
CURRICULUM VITAE	139

CHAPTER 1. GENERAL INTRODUCTION

1.1 The need for glucose sensors

Many people suffer from the metabolism disease Diabetes mellitus. All over the world about 30 million diabetics are registered [1, 2]. In a healthy pancreas, β -cells in the islets of Langerhans produce and also store the hormone insulin. This hormone serves as a receptor to transport glucose into a cell, where it is metabolized. Insulin is also necessary for storing unneeded glucose as glycogen in muscle and tissue cells and to inhibit glucose release from liver cells. In diabetic patients the glucose concentration is badly regulated. Two types of diabetes can be distinguished. Type I (juvenile-onset type) is caused by a β -cell injury, which leads to an absolute deficiency of insulin. Type II (maturity-onset type) is caused by either a disturbed secretion of sufficient insulin from the β -cells or a failure of the insulin to carry out its important tasks. Type II diabetes is therefore related to a relative shortage of insulin. Whereas type II is often treated with a diet, type I diabetes is always treated through the administration of insulin.

The disturbed glucose metabolism of diabetics can cause severe complications, such as retinopathy, nephropathy, neuropathy and microvascular lesions [2, 3]. To keep the glucose level in blood within the normal range (3.5-6.5 mM), it is necessary to determine the optimal quantity and frequency of subcutaneously injected insulin. Even then, it is very difficult to achieve normoglycaemia, and so hyper and hypoglycaemic situations still occur [2].

To determine the optimal insulin administration, a blood sample is taken every three hours. The diabetic patient has to stay in the hospital for 24 hours. Apart from the inconvenience of this conventional method, the obtained glucose curve does not give a complete representation. Within the three-hour interval between two samples, a peak or a dip in the glucose concentration can occur which is not monitored. Furthermore, the glucose metabolism is highly dependent upon the activities of the

individual. Naturally, a glucose measurement taken while lying in a hospital bed does not reflect the glucose concentration of a person participating in the daily life. This difference in glucose metabolism is a nice demonstration of the continuous monitoring of the body itself.

It is easy to understand that a continuously measuring, ambulant monitoring device would eliminate the disadvantages of the present way of monitoring. An implantable glucose sensor (long-term *in vivo*) would fulfil these demands and could even be coupled to an insulin pump. This would in fact create an artificial β -cell [4-8]. For pacemakers it is already possible to have a long-term implantation. Here, encapsulation of the device by tissue growth is no obstruction to adequate performance. However, encapsulation of a glucose sensor would surely influence the measurements. Furthermore, long-term implantation of a glucose sensor would imply long-term stability of the enzyme used and also long-term supply of insulin from the co-implanted insulin pump. If the maximum life time of an implanted device (sensor plus pump) is, for example, one year, the advantage of the artificial β -cell would not be able to compete with the disadvantage of replacing the device each year. Therefore, aiming at a needle-type glucose sensor for the subcutaneous measurement of the day curve (short-term *in vivo*), seems to have more successful perspectives for the near future. As research on biocompatible materials has been greatly expanded over the last years, the possibilities for an artificial pancreas must certainly not be ruled out.

1.2 Present glucose sensors

Since the seventies, more and more research groups have become occupied with the design and development of an *in vivo* glucose sensor, either long-term or short-term [9]. Practically all these sensors are based on the enzymatically catalysed oxidation of glucose. The enzyme used for this purpose is the flavoprotein glucose oxidase (GO, E.C. 1.1.3.4), which contains two active flavin adenine dinucleotide (FAD)

centers (co-factor). The FAD centers are called the prosthetic group of the enzyme and is responsible for the redox properties of the enzyme. The FAD groups in GO are strongly bound to the apo-enzyme (enzyme without co-factor) to form a compact, spherical holo-enzyme (enzyme with co-factor). The enzyme GO is derived from either *Aspergillus niger*, *Penicillium amagakienses* or *Penicillium notatum*.

The enzyme is immobilized for usage in the sensor. The reaction is described as follows:



where GO-FAD is the oxidized form of the enzyme GO, and GO-FADH₂ the reduced form of GO. Reduced glucose oxidase can be re-oxidized by the transfer of electrons to an electrode. The current measured, in this case, is proportional to the glucose concentration. Electron transfer can be performed in three ways, which reflects the three generations of glucose sensors [10, 11]:

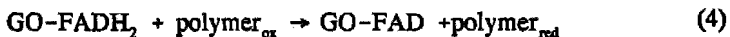
1. via oxygen (first generation):



2. via a mediator (second generation):



3. via a conducting polymer (third generation):



The first generation glucose sensor has the disadvantage that the oxygen concentration in blood is too low. Therefore, research groups have studied the possibility of

eliminating the necessity of oxygen by the use of mediators or conducting polymers. The second generation glucose sensor, however, has the disadvantage that the mediators are often highly toxic and therefore not suitable for *in vivo* applications, at least not when they are not covalently bound. Besides that, oxygen from the blood can interfere with the mediator system, which causes a decrease in the measuring current. The third generation glucose sensor has the same disadvantage of oxygen interference. Most research groups are therefore occupied with first generation glucose sensors. They try to solve the problem of oxygen deficiency by placing an extra membrane on top of the sensor, which inhibits glucose diffusion, relatively to that of oxygen. Still, no satisfying *in vivo* sensor is used for measuring a continuous glucose day curve. Problems, other than those related to oxygen deficiency or oxygen interference, are numerous. Immobilization of the enzyme GO causes a decrease in activity and long-term stability of the enzyme is difficult to reach. Furthermore, production of hydrogen peroxide in first generation sensors often occurs far apart from the detection electrode. Detection currents will be low and non-detected hydrogen peroxide leaks out of the sensor. Especially in low glucose concentration ranges, these low detection currents result in poor accuracy. It is not only in the case of measuring a glucose day curve that this can lead to the danger of overlooking hypoglycaemia. Also during surgery, where the glucose metabolism can dramatically change, the timely discovery of hypoglycaemia is essential. In these situations, a new and accurate short-term *in vivo* glucose sensor would be a enormous improvement.

To overcome these problems or at least to get a better insight into the bottlenecks of glucose monitoring, a new approach to designing a short-term *in vivo* glucose sensor is proposed in this thesis.

1.3 A new principle for a short-term *in vivo* glucose sensor

To obtain the highest possible electrochemical signal of a first generation glucose sensor, it is important that hydrogen peroxide production occurs in the direct vicinity of the detection electrode. The only way to control the hydrogen peroxide production is to have a clear notion of the concentration profiles of the participating species. Creating a counter-current diffusion of oxygen and glucose through an enzyme-containing layer is the major issue in this approach. The diffusion coefficients of glucose, oxygen and hydrogen peroxide and the kinetic parameters of the enzymatic reaction determine the place and dimension of the volume element in the enzyme layer, where hydrogen peroxide production takes place.

Fig. 1.1 shows the schematic design of the new glucose sensor.

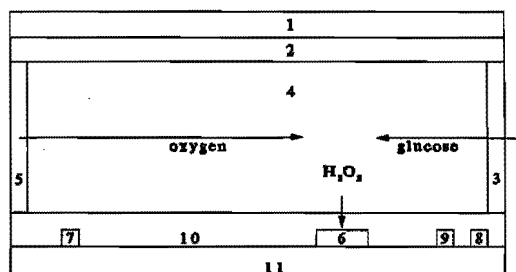


Figure 1.1: Design of the new glucose sensor with a counter-current principle of participating compounds.

The coating layer (1) is a biocompatible layer that prevents blood cells and blood macromolecules from entering the sensor. The second layer (2) is a hydrophobic membrane, which is impermeable for glucose. However, the sensor contains a window (3), which is permeable for glucose. This construction only allows glucose to enter the sensor at a defined spot. The third layer (4) consists of a hydrogel in

which GO is covalently bound via a cross-linker. An oxygen-producing electrode (5) solves the problem of oxygen deficiency. The detection electrode (6) is placed in the direct vicinity of hydrogen peroxide production. In addition, a counter electrode (7) for the oxygen electrode is present, as well as a counter electrode (8) and a reference electrode (9) for the detection electrode. All electrodes are separated from the GO containing layer by an extra non-GO-containing layer (10). The whole configuration is placed onto a non-conducting SiO₂-on-Si wafer. The concentration profiles of all participating species in the enzyme containing layer are shown in Fig. 1.2. The concentration profile for hydrogen peroxide is drawn symmetrically, but the kinetics of the enzymatic reaction are not symmetrical (i.e., glucose dominates the reaction). The profile will therefore be asymmetrical in reality.

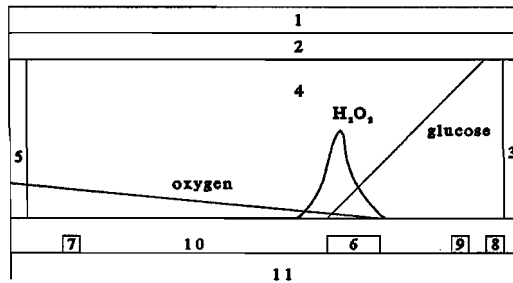
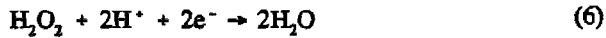


Figure 1.2: The concentration profiles of oxygen, glucose and hydrogen peroxide in the sensor.

As a result of the concentration profiles, one could easily decide to alter the first design with respect to the enzyme layer. Actually, GO is only needed in the region where the reaction occurs. Also, to be sure that the detection electrode is large enough to cover up the whole reaction region, one could make the choice to use a detection electrode of almost the full sensor length.

Naturally, the reaction plane shifts when the glucose concentration of the sample

changes. To prevent this, the oxygen evolution should be related to the signal of the detection electrode. This can be achieved via a feed-back control. Of course, oxygen from blood entering through the glucose window is another feature that disturbs the concentration profiles. In addition, the reaction product gluconolactone accumulates in the sensor, as it only can leave the sensor through the "glucose window". This might lead to the phenomenon of product inhibition [12, 13]. However, this need not have a great impact on the performance of the sensor. After all, one of the advantages of the new principle is that diffusion is limiting and kinetics are not. Furthermore, a discussion could arise concerning the detection of hydrogen peroxide. Hydrogen peroxide can either be oxidized or reduced:



The disadvantage of the oxidation of hydrogen peroxide is the production of oxygen, which causes a disturbance of the oxygen profile and so a shift of the reaction plane. On the other hand, applying a reduction potential would not only reduce hydrogen peroxide but oxygen as well. As the oxygen concentration in the vicinity of the detection electrode is not very high, this would only mean a small increase in the detection current. Maybe the wisest solution would be to alternate the detection potential between the limiting reduction region and the limiting oxidation region. As reduction consumes oxygen and oxidation produces oxygen, the concentration profile of oxygen is damaged less.

1.4 Scope of this thesis

To design and develop a glucose sensor as described on the preceding pages, a knowledge of the diffusional patterns and the enzyme kinetics is essential. Therefore, the main goal of this thesis is to determine these parameters and to use them to

verify the principle of the sensor and to estimate its practical usability.

The determination of the diffusion coefficients of oxygen, hydrogen peroxide and glucose in a hydrogel with and without GO is presented in Chapter 2.

Chapter 3 deals with the determination of the intrinsic kinetics of the soluble enzyme, whereas Chapter 4 describes the inherent kinetic parameters of the immobilized enzyme. The effect of the immobilization technique on the activity of GO is revealed in this way, while diffusional effects due to immobilization are eliminated.

To describe the concentration profiles of the main species, the use of a simulation program is indispensable. In Chapter 5 a comparison is made between the computer calculations and the measurements with a macro-sensor. The comparison evaluates the proposed sensor model, and gives rise to new ideas concerning the design of the sensor.

In Chapter 6, a literature survey of possible immobilization techniques for GO is given, because the technique used in this study need not be the ideal one. Chapter 6 also gives a short introduction on the usage of sensor coating membranes.

A knowledge of the diffusion coefficients and the kinetic parameters appears to be essential for the design of the glucose sensor described in this thesis. Moreover, it seems to be a powerful tool to get an insight into the processes that take place in the glucose sensor. Naturally, this might be useful for other designs of glucose sensors as well. The fact is that other research groups have wrongly neglected these issues, which have a great impact on the operational qualities of a sensor.

Lastly, a remark should be made on the use of the unit for the concentration. As different journals and research groups demand and/or use different nomenclatures, the unit for the concentration in this thesis is not always according to the S.I.. Use is made of mol m^{-3} as well as mol l^{-1} ($= \text{M}$, mol dm^{-3} or kmol m^{-3}).

References

1. J. Pickup and D. Rothwell, *Med. & Biol. Eng. & Comput.*, 22 (1984) 385.
2. A.P.F. Turner and J.C. Pickup, *Biosensors*, 1 (1985) 85.
3. E. van Ballegooie and R.J. Heine (Eds.), *Diabetes Mellitus*, Scientific Publisher Bunge, Utrecht, the Netherlands, (1991).
4. S.P. Besmann, J.M. Hellyer, E.C. Layne, G. Takada, L.J. Thomas jr. and D. Sayler, *Diabetes Excepta Medica-International Congress Series*, 413 (1977) 496.
5. E.F. Pfeiffer, *Artif. Organs*, 12 (1988) 310.
6. W. Schubert, P. Baur Schmidt, J. Nagel, R. Thull and M. Schaldach, *Med. & Biol. Eng. & Comput.*, 18 (1980) 527.
7. P. Abel, A. Müller and U. Fischer, *Biomed. Biochim. Acta*, 43 (1984) 577.
8. M. Shichiri, R. Kawamori, N. Hakui, N. Asakawa, Y. Yamasaki and H. Abe, *Biomed. Biochim. Acta*, 43 (1984) 561.
9. Chapter 6 of this thesis.
10. C.G.J. Koopal, Thesis, University of Nijmegen, (1992).
11. H. Gunasingham, C.-H. Tan and T.-C. Aw, *Anal. Chim. Acta*, 234 (1990) 321.
12. C. Walsh, *Enzymatic Reaction Mechanisms*, W.H. Freeman and Company, San Francisco, (1979), p. 220.
13. S.A.M. van Stroe-Biezen, A.P.M. Janssen and L.J.J. Janssen, *Bioelectr. and Bioeng.*, *in press*.

CHAPTER 2. THE DIFFUSION COEFFICIENTS OF OXYGEN, HYDROGEN PEROXIDE AND GLUCOSE IN A HYDROGEL

2.1 Introduction

For the design of the new glucose sensor, as described in Chapter 1, a knowledge of the diffusion behaviour of all participating compounds (oxygen, glucose and hydrogen peroxide) in the enzyme-containing hydrogel is needed.

For the determination of the diffusion coefficients of the electrochemically active oxygen and hydrogen peroxide, a rotating disc electrode (RDE) is used. An RDE consists of a disc-shaped electrode (e.g., Pt) with a teflon holder. With a stirring motor, the rotation speed of the RDE can be adjusted. The stirring creates a well-defined hydrodynamic profile, the thickness of the stagnant diffusion layer adjacent to the disc is uniform and the current density is equal over the entire disc surface. An RDE covered with the same hydrogel layer as used in the glucose sensor appears to be a suitable method to determine the effective diffusion coefficients (D_{eff}) of oxygen and hydrogen peroxide in the hydrogel.

As glucose is not electroactive, another method has to be used to determine its diffusion coefficient. For this purpose, a diffusion cell can be used, where hydroquinone and glucose simultaneously diffuse through a hydrogel membrane. With data from diffusion cell experiments, the ratio of the diffusion coefficients of glucose and hydroquinone is calculated. The diffusion coefficient of hydroquinone can be determined with the formerly mentioned RDE-hydrogel method.

The methods described in this chapter are used to determine important parameters, needed for the design of the glucose sensor. Whereas the methods themselves do not have any relation with the sensor, the data obtained certainly do.

2.2 Theory

A rotating disc electrode (RDE) covered with a hydrogel layer appears to be an accurate means of measuring diffusion coefficients of electrochemically active compounds [1, 2]. Fig. 2.1 shows schematically the concentration profile for electroactive species.

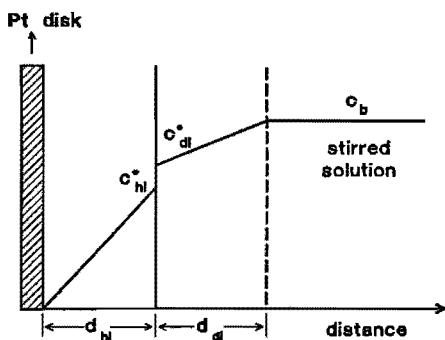


Figure 2.1: Schematic profiles the concentration of electroactive species vs. the distance from the platinum disc surface. Hydrogel layer thickness is denoted by d_{hl} and Nernst diffusion layer by d_{dl} .

Under steady-state conditions the flux J ($\text{mol m}^{-2} \text{s}^{-1}$) in both the hydrogel layer (J_{hl}) and the Nernst diffusion layer (J_{dl}) is the same

$$J = J_{hl} = J_{dl} \quad (1)$$

From the definition for J and assuming a linear concentration profile, it follows that

$$J_{hl} = J_{dl} \Leftrightarrow D_{hl} \frac{\Delta C_{hl}}{d_{hl}} = D_{dl} \frac{\Delta C_{dl}}{d_{dl}} \quad (2)$$

At the hydrogel layer - Nernst diffusion layer interface a jump in the concentration of the active component can take place. The partition coefficient α is defined by

$$\alpha = \frac{c_{hl}^*}{c_{dl}^*} \quad (3)$$

where the asterisk refers to the interface.

The concentration of the electroactive species at the electrode surface will be virtually zero, as a sufficiently high overpotential is applied. In this case, from Eqns. (2) and (3) the following expression is derived:

$$D_{hl} \frac{\alpha c_{dl}^*}{d_{hl}} = D_{dl} \frac{c_b - c_{dl}^*}{d_{dl}} \quad (4)$$

where c_b is the bulk concentration (mol m^{-3}).

From Eqn. (4), it follows that

$$c_{dl}^* = \frac{D_{dl} \frac{c_b}{d_{dl}}}{\frac{\alpha D_{hl}}{d_{hl}} + \frac{D_{dl}}{d_{dl}}} \quad (5)$$

As $J = D_{hl} \frac{\alpha c_{dl}^*}{d_{hl}}$ and using (4), it is found that

$$J = \frac{\frac{\alpha D_{hl}}{d_{hl}} \frac{D_{dl}}{d_{dl}} c_b}{\frac{\alpha D_{hl}}{d_{hl}} + \frac{D_{dl}}{d_{dl}}} \quad (6)$$

The permeabilities P_{hl} and P_{dl} are defined by

$$P_{hl} = \frac{\alpha D_{hl}}{d_{hl}} = \frac{D_{eff}}{d_{hl}} \quad (7)$$

and

$$P_{dl} = \frac{D_{dl}}{d_{dl}} \quad (8)$$

where D_{eff} is the effective diffusion coefficient ($m^2 s^{-1}$).

Combining Eqns. (6), (7) and (8) and using

$$I_{lim} = nFA_c J \quad (9)$$

where I_{lim} is the limiting current (A), n the number of electrons involved in the electrode reaction, F the faraday, i.e., the charge on one mole of electrons (C), and A_c the geometrical electrode area (m^2), the following equation can be derived:

$$\frac{1}{I_{lim}} = \frac{1}{nFA_c c_b P_{hl}} + \frac{1}{nFA_c c_b P_{dl}} \quad (10)$$

The limiting current depends on two serial diffusional resistances. The total diffusional resistance ($1/k$) is defined by

$$\frac{1}{k} = \frac{1}{k_{nl}} + \frac{1}{k_{dl}} = \frac{1}{P_{nl}} + \frac{1}{P_{dl}} \quad (11)$$

where k is the total mass transfer coefficient (m s^{-1}).

The first term ($1/k_{nl}$) is independent of the rotation speed. The second term ($1/k_{dl}$), however, is proportional to the reciprocal of the square root of the angular rotation rate (ω) of the RDE as P_{dl} is inversely proportional to d_{dl} . From the theory of mass transfer to an RDE [3], it is well known that

$$d_{dl} = 1.61 (D_{dl}/\nu_{dl})^{1/3} (\nu_{dl}/\omega)^{1/2} \quad (12)$$

and so

$$P_{dl} = \frac{D_{dl}}{1.61 (D_{dl}/\nu_{dl})^{1/3} (\nu_{dl}/\omega)^{1/2}} \quad (13)$$

where ν_{dl} is the kinematic viscosity of the diffusion layer ($\text{m}^2 \text{s}^{-1}$).

Hence, if the reverse of the limiting current is plotted against the reverse of the square root of the angular rotation rate, a linear plot is obtained, the slope of which and the intercept give information about the permeability of the solution (Levich-slope [3]) and the permeability of the hydrogel layer, respectively.

In this way effective diffusion coefficients of oxygen and hydrogen peroxide can be determined electrochemically. However, glucose is electrochemically inactive and its diffusion coefficient has to be determined by the diffusion cell method. A comparison between the effective diffusion coefficients of hydroquinone (electrochemically determined) and glucose can be made by simultaneous diffusion through a membrane made of the same hydrogel material as used for the RDE experiments, which is

The diffusion coefficients of oxygen, hydrogen peroxide and glucose in a hydrogel

strengthened by a filter-paper on each side of the membrane. The concentration profile is shown in Fig. 2.2. In this method two stirred solutions, A and B, where $c_A > c_B$, were separated.

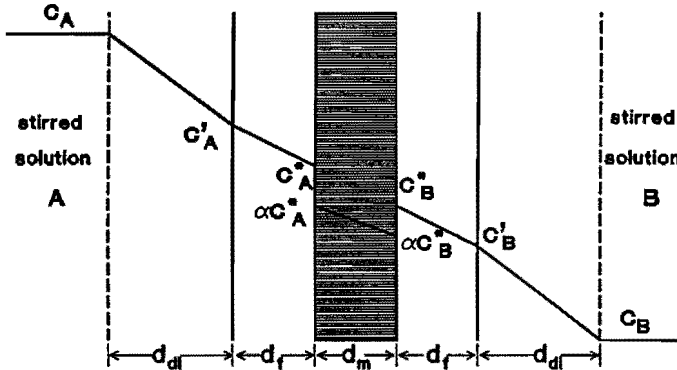


Figure 2.2: Concentration profiles through a hydrogel membrane (d_m) with a filter-paper (d_f) on each side, placed between two compartments, A and B. Nernst diffusion layers are denoted by d_{dl} .

For relatively short times the total flux J through the various layers is constant:

$$J = k \Delta c \tag{14}$$

where Δc is equal to $c_A - c_B \approx c_A$ and k is, similarly to Eqn. (11), the total mass transfer coefficient ($m s^{-1}$).

Again, the diffusional resistance is built up of several terms:

$$\begin{aligned}\frac{1}{k} &= \frac{1}{k_m} + \frac{2}{k_{dl}} + \frac{2}{k_f} \\ &= \frac{d_m}{D_{eff}} + \frac{2d_{dl}}{D_{dl}} + \frac{2d_f}{D_f}\end{aligned}\tag{15}$$

where the subscripts m, dl and f refer to the membrane, the Nernst diffusion layer and the filter-paper, respectively. Combining Eqns. (14) and (15) gives

$$J = \frac{\Delta c}{\left[\frac{2d_{dl}}{D_{dl}} + \frac{2d_f}{D_f} + \frac{d_m}{D_{eff}} \right]}\tag{16}$$

The total amount of glucose or hydroquinone transported from compartment A to compartment B can now be written as

$$c_B V = JA_m t\tag{17}$$

and so the rate of the increase of the concentration in solution B is

$$\frac{dc_B}{dt} = \frac{JA_m}{V} = \frac{1}{\left[\frac{2d_{dl}}{D_{dl}} + \frac{2d_f}{D_f} + \frac{d_m}{D_{eff}} \right]} \Delta c \frac{A_m}{V}\tag{18}$$

By comparing the slope of the plots of c_B vs. time, the ratio of the effective diffusion coefficients of hydroquinone and glucose in the membrane can be determined. However, first the diffusional resistance of the Nernst diffusion layers and the two filter-papers for both hydroquinone and glucose have to be checked and inserted in Eqn. (18).

In this diffusion cell method, imperfections of the gel do not matter as the two

compounds diffuse simultaneously through the same membrane. Thickness and area of the membrane are also of no importance.

2.3 Experimental

Reagents

The hydrogel used for these experiments was made of poly(vinyl alcohol) (PVA) from Denka Poval (B24) and cross-linked with glutaraldehyde (25%, w/w, aqueous solution; Merck) and the photosensitive DTS-18 (polyazonium salt from PCAS, Longjumeau, France). Mowiol PVA was obtained from Hoechst (04/M1).

$\text{NaH}_2\text{PO}_4 \cdot 2\text{H}_2\text{O}$ and $\text{Na}_2\text{HPO}_4 \cdot 2\text{H}_2\text{O}$, used for the buffer solution, were purchased from Merck.

Hydrogen peroxide (30%, w/w, aqueous solution) was obtained from Chempro Pack, hydroquinone from Merck and D-glucose from Janssen Chimica.

Glucose detection was performed with a Sigma glucose kit (No. 635), based on the reaction of glucose with *o*-toluidine, which yields a blue-green complex.

Glucose oxidase (GO) from *Aspergillus niger* (E.C. 1.1.3.4, M=150,000 Dalton, lyophil, GO/catalase min 2000) was obtained from Serva.

All solutions were prepared with demineralized, distilled water.

Instrumentation

For the RDE experiments a Wenking POS 73 potentiostat was used, equipped with a digital multimeter (Fluke 8600 A, Philips Nederland B.V., Tilburg, Netherlands) and a Motomatic E-550-M stirring motor. Recording was carried out with an *x,y* recorder (Philips 8120). A circulation water-bath (Colora NB-32981, Oortmerssen B.V., The Hague) was used for temperature control of the one-compartment cell.

Diffusion cell experiments were performed with a magnetic stirrer in both compartments, which were thermostatically controlled with a Colora NB-32981 circulating waterbath.

For the determination of the glucose concentration an LKB Biochrom Ultrospec II Type 4050 spectrophotometer was used for detecting the glucose-*o*-toluidine complex at 635 nm. The same spectrophotometer was used to determine the hydroquinone concentration at 290 nm.

A Talysurf 4 roughness meter from Rank Precision Instruments was used to measure the thickness of the gel layers.

Preparation of gel layers

A 10-g amount of PVA was slowly added to 90 cm³ of demineralized water and stirred. The solution was heated for 1.5 h at 80 °C until all the PVA had dissolved and a homogenous solution was obtained. The solution was cooled to room temperature. Just before the spinning procedure, 0.20 g (0.2%, w/w) of DTS-18 and 0.16 or 0.40 g of 25% (w/w) aqueous glutardialdehyde were added. In the case of a GO-containing gel layer 0.40 g glutardialdehyde and 4 ml of a 12.8 mg/ml GO-solution was added. With a pipette an aliquot of the resulting solution was placed on the required surface (glass plate covered with a water-soluble 30% Mowiol PVA layer or electrode surface). After spinning for 5 s at 1000 rpm and for 25 s at 3000 rpm, the gel layer was dried for 30 min at 40 °C. For the GO-containing gel layer a vacuum pump was used to dry the layer. The spinning and drying procedure was repeated until enough layers had been spun on the surface. Thereafter the gel layer was irradiated with UV radiation at room temperature for 90 s. The gel layer was developed in demineralized water for 2 min and unreacted reactants were washed away. Finally, the gel layer was dried for at least 1 h at 60 °C, while cross-linking with glutardialdehyde was finished. The GO-containing layers were allowed to dry for at least 24 h at 4 °C.

The thickness of the gel layer on both platinum electrodes and glass plates (control measurement) was measured with a roughness meter, connected with a thermograph. The thickness of a swollen gel layer (after contact with an aqueous solution) could also be measured with this technique.

The diffusion coefficients of oxygen, hydrogen peroxide and glucose in a hydrogel

To loosen the membrane from the glass plates, the plates were put in demineralized, distilled water for at least 8 h to solve the Mowiol PVA layer. After drying the membrane, it was easily torn off the glass plates.

Procedures

For all electrochemical experiments a polished platinum electrode was used as the working electrode ($A_e=0.50 \cdot 10^{-4} \text{ m}^2$). Further, a platinum counter electrode with a surface area of $5 \cdot 10^{-4} \text{ m}^2$ and a saturated calomel reference electrode (SCE) with Luggin capillary were placed in the one-compartment cell. A circulating water-bath was used to keep the temperature constant. As supporting electrolyte 0.1 M sodium phosphate buffer (pH=6.7) was used with a kinematic viscosity of $0.9 \cdot 10^{-6} \text{ m}^2 \text{ s}^{-1}$ at 25 °C and $0.7 \cdot 10^{-6} \text{ m}^2 \text{ s}^{-1}$ at 37 °C [4].

For oxygen measurements the buffer solution was saturated with oxygen (1 atm) for at least 30 min. This yields an oxygen concentration of 1.1 mol m^{-3} at 25 °C and 0.9 mol m^{-3} at 37 °C [5]. A voltammogram was recorded from +600 to -650 mV (vs. SCE) at a rotation speed varying from 1 to 49 s^{-1} (Pt electrode experiment) or from 0.5 to 16 s^{-1} (Pt-PVA electrode experiment).

For hydrogen peroxide measurements ($7\text{-}8 \text{ mol m}^{-3}$) the buffer solution was saturated with argon before adding hydrogen peroxide and voltammograms were scanned from +300 to -650 mV (vs. SCE). The rotation speed for both the Pt electrode and the Pt-PVA electrode experiments varied between 1 and 9 s^{-1} .

Hydroquinone studies (2 mol m^{-3}) were performed with an argon-saturated buffer solution with hydroquinone added before saturation. Anodization from -550 to +1200 mV (vs. SCE) was conducted at various rotation rates (Pt electrode $1\text{-}36 \text{ s}^{-1}$; Pt-PVA electrode $0.5\text{-}9 \text{ s}^{-1}$).

For all three compounds the electrode was rotated at high speed ($> 50 \text{ s}^{-1}$ for a Pt electrode and $> 16 \text{ s}^{-1}$ for a Pt-PVA electrode) for about 20 s before a new scan was made. The scan rate varied between 25 and 50 mV s^{-1} for Pt electrode experiments and between 2 and 10 mV s^{-1} for Pt-PVA electrode experiments.

With a diffusion cell containing two compartments, the ratio of the effective diffusion coefficients of glucose and hydroquinone was determined. Compartment A of the cell contained 100 cm³ of 0.1 M sodium phosphate buffer with 1.00 kmol m⁻³ glucose and 0.100 kmol m⁻³ hydroquinone. Initially compartment B contained only 100 cm³ of phosphate buffer. Between the two compartments a cross-linked PVA membrane (13.2 cm²) was placed with a filter-paper (Rotband, Schleicher and Schüll) on each side for solidity purposes. Thereafter both compartments were simultaneously filled with the solution.

The concentration increase in compartment B was followed for 5 h, with UV spectroscopy for hydroquinone and with a glucose-kit [6] and visible spectroscopy for glucose. Although only samples from compartment B were analyzed, an equal amount of sample was taken from compartment A to keep the solution levels in both compartments equal and to prevent forced diffusion through the membrane and destruction of the membrane.

The influence of the two filter-papers and the Nernst diffusion layers was checked by conducting a comparative experiment with only the two filter-papers placed between the two compartments.

The temperature was maintained at 25 °C with a circulating water-bath for all diffusion cell experiments and both compartments were stirred magnetically.

2.4 Results and discussion

Properties of the gel layer on an RDE

Several PVA gel layers with different degrees of cross-linking were used to investigate the diffusion behaviour of oxygen, hydrogen peroxide and hydroquinone.

In Table 2.1 properties of gels A-E are given, such as thickness, percentage of glutardialdehyde added and swelling factor after saturation with buffer solution (i.e., $d_{\text{w}}(\text{wet})/d_{\text{w}}(\text{dry})$). All gels were made on different days. Gel E is the only gel containing the enzyme glucose oxidase (GO). Although gel solutions A, B and C

The diffusion coefficients of oxygen, hydrogen peroxide and glucose in a hydrogel

were made with the same procedure, the thickness of one spun layer varied substantially.

Table 2.1: Properties of the various hydrogels used for diffusion measurements on an RDE (GA = glutardialdehyde)

Gel	No. of layers	GA (25% w/w) added (g)	GO added (mg)	d_{hl} (dry) (μm)	Swelling factor
A	4	0.16	-	13.5	2.3
B	2	0.16	-	8.0	2.3
C	4	0.16	-	26.0	2.3
D	4	0.40	-	13.0	2.1
E	2	0.40	51.2	4.8	2.2

If the same gel solution (i.e., gel A) was spun on several surfaces (platinum discs or glass plates), it was found that the spinning and cross-linking procedure provided layers of reproducible thickness and degree of cross-linking. This means that the difference in the behaviour of the gel layers is due to the gel solution preparation.

Determination of the diffusion coefficients

Plots of I_{lim}^{-1} versus $\omega^{-1/2}$ gave straight lines, as expected, for measurements with both the Pt electrodes and the Pt-PVA electrodes (Figs. 2.3 and 2.4).

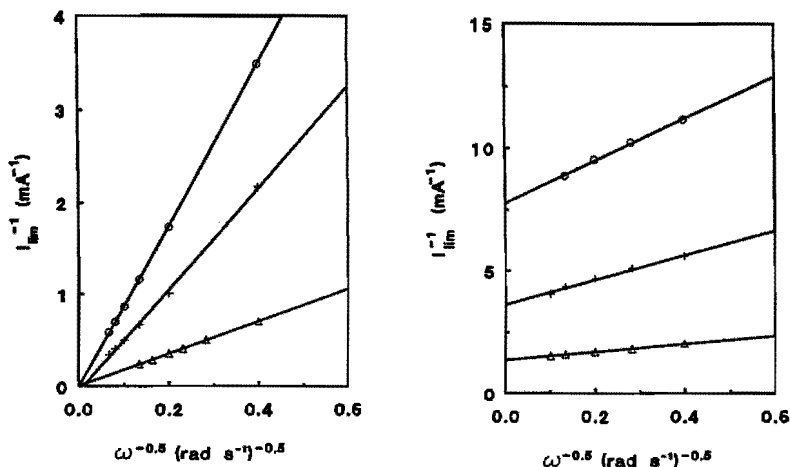


Figure 2.3: Rotating disc electrode data with a Pt electrode ($T=25\text{ }^{\circ}\text{C}$) for (Δ) H_2O_2 , (+) O_2 and (\circ) hydroquinone.

Figure 2.4: Rotating disc electrode data with a Pt-PVA electrode ($T=25\text{ }^{\circ}\text{C}$) for (Δ) H_2O_2 , (+) O_2 and (\circ) hydroquinone.

Table 2.2 shows the diffusion coefficients in the buffer solution and the effective diffusion coefficients in the gel layer for various gels and at two temperatures (25 °C and 37 °C). The ratio D_{eff}/D_{dl} is also given.

For oxygen, hydrogen peroxide and hydroquinone the D_{eff}/D_{dl} ratios are virtually identical and depend on the properties of the gel and temperature. This means that the ratio of the effective diffusion coefficients for the three compounds in the hydrogel layer is almost identical with this ratio in the buffer solution. No difference in behaviour was observed between gels with and without enzyme.

The diffusion coefficients of oxygen, hydrogen peroxide and glucose in a hydrogel

Table 2.2: Diffusion coefficients in the buffer solution and effective diffusion coefficients in the various gels for O₂, H₂O₂ and hydroquinone (HQ) at two temperatures (Unreliable measurement, gel destroyed)*

	T (°C)	25			37		
		O ₂	H ₂ O ₂	HQ	O ₂	H ₂ O ₂	HQ
Buffer	D_{di} (10 ⁻⁹ m ² s ⁻¹)	1.93	1.43	0.89	2.46	1.83	1.17
Gel A	D_{eff} (10 ⁻⁹ m ² s ⁻¹)	0.40	0.31	0.20	0.60	0.45	0.27*
	$\frac{D_{eff}}{D_{di}}$	0.21	0.21	0.22	0.25	0.25	0.23*
Gel B	D_{eff} (10 ⁻⁹ m ² s ⁻¹)	0.68	0.50	0.31	0.99	0.73	0.43*
	$\frac{D_{eff}}{D_{di}}$	0.35	0.35	0.35	0.40	0.40	0.37*
Gel C	D_{eff} (10 ⁻⁹ m ² s ⁻¹)	0.55	0.40	0.25	0.82	0.58	-
	$\frac{D_{eff}}{D_{di}}$	0.28	0.28	0.28	0.33	0.31	-
Gel D	D_{eff} (10 ⁻⁹ m ² s ⁻¹)	0.36	0.27	0.18	0.54	0.37	-
	$\frac{D_{eff}}{D_{di}}$	0.19	0.19	0.20	0.22	0.22	-
Gel E	D_{eff} (10 ⁻⁹ m ² s ⁻¹)	0.37	0.27	0.17	0.57	0.42	-
	$\frac{D_{eff}}{D_{di}}$	0.19	0.19	0.19	0.23	0.23	-

Simultaneous diffusion of glucose and hydroquinone through two filter-papers shows a linear increase of c_B/c_A for both species (Fig. 2.5).

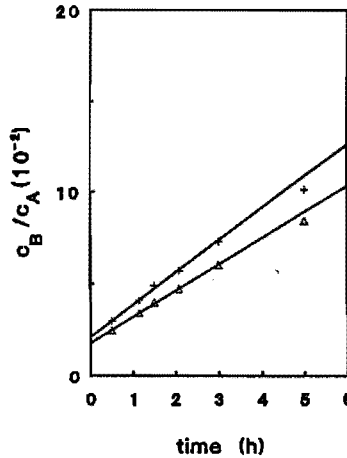


Figure 2.5: Data for a diffusion cell with two filter-papers. c_B/c_A plotted against time for (+) hydroquinone and (Δ) glucose. $T=25^\circ\text{C}$.

c_B was divided by c_A ($\approx \Delta c$) to correct for the different starting concentrations. The slopes of the lines of glucose and hydroquinone have a ratio of 0.81. Washburn [4] gave a diffusion coefficient of $0.52 \cdot 10^{-9} \text{ m}^2 \text{ s}^{-1}$ for glucose in pure water at 15°C and of $0.66 \cdot 10^{-9} \text{ m}^2 \text{ s}^{-1}$ for hydroquinone. The ratio of the diffusion coefficients under these conditions is 0.79, which makes it acceptable to consider the two filter-papers as a stagnant layer of buffer solution with a diffusion coefficient equal to that in the Nernst diffusion layer. The diffusional resistance of the Nernst diffusion layer and the filter-paper (Eqn. (15)) can be considered as one resistance of a buffer solution layer:

$$\frac{2}{k_{dl}} + \frac{2}{k_r} = \frac{1}{k_{bl}} = \frac{d_{bl}}{D_{bl}} = \frac{d_{bl}}{D_{dl}} \quad (19)$$

where the subscript bl refers to the buffer solution layer.

As the diffusion coefficient of hydroquinone in 0.1 M phosphate buffer at 25 °C is $0.89 \cdot 10^{-9} \text{ m}^2 \text{ s}^{-1}$, it can be calculated that the diffusion coefficient of glucose under the same conditions is $0.72 \cdot 10^{-9} \text{ m}^2 \text{ s}^{-1}$. Also, k_{bl} can be calculated for both compounds using the slopes of Fig. 2.5, as in this case

$$\frac{dc_B}{dt} = \frac{k_{bl} \Delta C A_f}{V} \text{ with } A_f = A_m$$

$= 13.2 \cdot 10^{-4} \text{ m}^2$. For hydroquinone a value of $k_{bl} = 3.6 \cdot 10^{-7} \text{ m s}^{-1}$ was found and for glucose $k_{bl} = 2.9 \cdot 10^{-7} \text{ m s}^{-1}$.

A gel D membrane, together with a filter-paper on each side, was placed between the two compartments and also gave straight lines (Fig. 2.6).

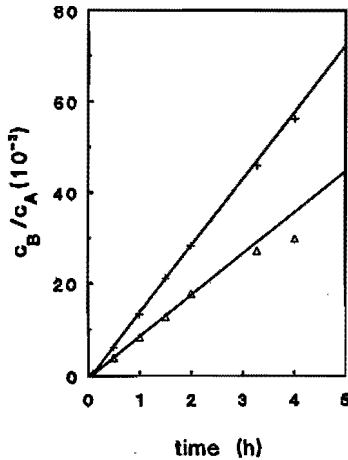


Figure 2.6: Data for a diffusion cell with a hydrogel membrane and two filter-papers. c_B/c_A plotted against time for (+) hydroquinone and (Δ) glucose. $T = 25 \text{ °C}$.

The diffusion coefficients of oxygen, hydrogen peroxide and glucose in a hydrogel

Now the slopes have a ratio of 0.61, which means that glucose is slowed by the membrane to a greater extent than hydroquinone. The ratio of 0.61 can also be seen as the ratio of the total mass transfer coefficients of hydroquinone and glucose, so

$$\frac{\left[\frac{1}{k_m} + \frac{1}{k_{bl}} \right]_{\text{hydroquinone}}}{\left[\frac{1}{k_m} + \frac{1}{k_{bl}} \right]_{\text{glucose}}} = 0.61 \quad (20)$$

Inserting the value of k_{bl} for both glucose and hydroquinone, the ratio of the effective diffusion coefficients is found to be 0.28. $(D_{eff}/D_{dl})_{\text{hydroquinone}}=0.20$ whereas $(D_{eff}/D_{dl})_{\text{glucose}}=0.071$ (Table 2.3).

For a less cross-linked gel C membrane the same ratio of the slopes of 0.61 is found (Table 2.3). The ratio of the effective diffusion coefficients is 0.28, and $(D_{eff}/D_{dl})_{\text{hydroquinone}}=0.28$ whereas $(D_{eff}/D_{dl})_{\text{glucose}}=0.097$.

The conclusion can be drawn that glucose is slowed more than hydroquinone and also than oxygen and hydrogen peroxide, because of an interaction of glucose with the gel matrix. In both gels glucose is slowed 2.9 times more than hydroquinone (0.071 vs. 0.20 and 0.097 vs. 0.28). A size-exclusion effect can be excluded because, although gel D is far more cross-linked than gel C, this has evidently no influence.

Also a gel E membrane (with GO) exhibits the same behaviour. $(D_{eff}/D_{dl})_{\text{hydroquinone}}=0.19$ whereas $(D_{eff}/D_{dl})_{\text{glucose}}=0.065$, which means that again glucose is slowed 2.9 times more than hydroquinone.

Further, a gel with GO (gel E) and a similar gel without GO (gel D) behave alike.

The diffusion coefficients of oxygen, hydrogen peroxide and glucose in a hydrogel

Table 2.3: Diffusion coefficients in the buffer solution and effective diffusion coefficients in two gels with different degrees of cross-linking for hydroquinone and glucose at 25 °C

		hydroquinone	glucose
Buffer	D_{ai} ($10^{-9} \text{m}^2 \text{s}^{-1}$)	0.89	0.72
gel C	D_{eff} ($10^{-9} \text{m}^2 \text{s}^{-1}$)	0.25	0.070
	$\frac{D_{eff}}{D_{ai}}$	0.28	0.097
gel D	D_{eff} ($10^{-9} \text{m}^2 \text{s}^{-1}$)	0.18	0.051
	$\frac{D_{eff}}{D_{ai}}$	0.20	0.071
gel E	D_{eff} ($10^{-9} \text{m}^2 \text{s}^{-1}$)	0.17	0.047
	$\frac{D_{eff}}{D_{ai}}$	0.19	0.065

Acknowledgment

I wish to acknowledge drs.ir. M.W.C.M. Nieuwesteeg, ing. G. Steeghs and ing. M.H. Kuijpers from Dräger Medical Electronics, Best, Netherlands, for their contribution to this chapter.

References

1. D.A. Gough and J.K. Leypoldt, *Anal. Chem.*, 52 (1980) 1126.
2. C.A. Marrese, O. Miyawaki and L.B. Wingard, Jr., *Anal. Chem.* 59 (1987) 248.
3. V.G. Levich, *Physicochemical Hydrodynamics*, Prentice Hall, Englewood Cliffs, NJ, (1962).
4. E.W. Washburn, *International Critical Tables*, 1st edn., McGraw-Hill, New York, (1929).
5. M.L. Hitchman, *Measurement of Dissolved Oxygen*, Chemical Analysis, Vol. 49, John Wiley & Sons, New York, (1978).
6. J.E. Middleton, *Clin. Chim. Acta*, 31 (1968) 433.

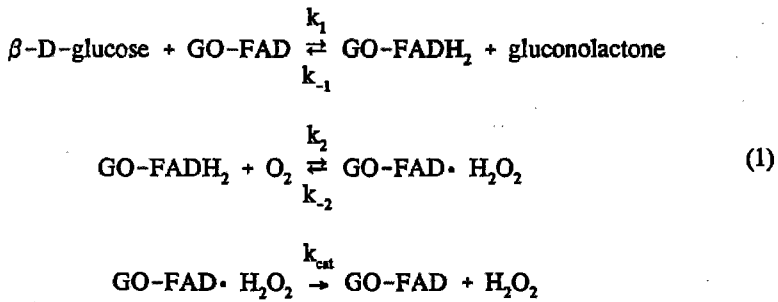
CHAPTER 3. THE KINETIC PARAMETERS OF SOLUBLE GLUCOSE OXIDASE

3.1 Introduction

To describe the concentration profiles of oxygen, glucose and hydrogen peroxide, besides the diffusion coefficients of these compounds (Chapter 2), the kinetic parameters of the enzymatic reaction must be known.

The enzyme glucose oxidase (GO) is immobilized in a hydrogel layer, which can have a great impact on the activity of the enzyme. To specify this impact, this chapter deals with the kinetic parameters of the soluble enzyme, whereas Chapter 4 deals with the kinetic parameters of immobilized GO.

The enzyme GO catalyses the glucose oxidation in the presence of oxygen according to the ping-pong mechanism [1]:



With the formation of hydrogen peroxide as the rate-determining step the following equation can be derived for steady-state conditions [2]:

$$\frac{1}{v_0} = \frac{1}{V_{\text{max}}} \left[1 + \frac{k_m(\text{O})}{c_{\text{ox}}} + \frac{k_m(\text{G})}{c_{\text{f}}} \right] \quad (2)$$

where v_0 is the initial velocity of product formation ($M \text{ min}^{-1}$), V_{\max} the maximal initial velocity ($M \text{ min}^{-1}$), $k_m(o)$ and $k_m(g)$ the Michaelis constants (M) for oxygen and glucose respectively, and c_{ox} and c_g the initial concentrations of these species (M). Furthermore,

$$V_{\max} = k_{cat} * c_{GO} \quad (3)$$

$$k_m(o) = \frac{k_{-2} + k_{cat}}{k_2} \quad (4)$$

$$k_m(g) = \frac{k_{-1} + k_{cat}}{k_1} \quad (5)$$

where c_{GO} is the total concentration of enzyme present (M).

A primary plot for this mechanism can be obtained by plotting the reciprocal initial velocity versus the reciprocal initial oxygen concentration at a constant glucose concentration. A set of parallel lines is obtained, each corresponding to a fixed glucose concentration. A secondary plot can be deduced by plotting the intercepts of the primary plot ($c_{ox} \rightarrow \infty$) as a function of the reciprocal glucose concentration. The intercept of this secondary plot ($c_g \rightarrow \infty$) denotes V_{\max}^{-1} . To accurately determine V_{\max} (and so $k_m(o)$ and $k_m(g)$), usage of measurements at high glucose concentrations is essential. In this way, the intercept of the secondary plot is closely approached.

The major problem in obtaining the primary and secondary plots, is measurement of the initial reaction rate v_0 . Measurements should be performed under pseudo-steady-state conditions, i.e., the concentration of glucose and oxygen should remain virtually constant. The electrochemical technique of using a Rotating Disc Electrode (RDE) is suitable for this purpose. A glucose solution is saturated with pure oxygen or an oxygen/nitrogen mixture. At time zero, an aliquot of GO is added and the RDE measures the increase in hydrogen peroxide concentration with time. Measur-

ing the hydrogen peroxide concentration with an RDE requires, however, a knowledge of the diffusion coefficient in the glucose solution and the kinematic viscosity of the glucose solution. Of course, also the solubility of oxygen in a solution with a particular glucose concentration must be known, because the hydrogen peroxide production rate is not only related to the glucose concentration, but also to the oxygen concentration.

Paragraph 3.2 describes the determination of the diffusion coefficients, viscosity and oxygen solubility as a function of the glucose concentration. With the obtained values, the kinetic parameters of soluble GO are determined in paragraph 3.3.

3.2 The solubility of oxygen in glucose solutions

3.2.1 Theory

The determination of the solubility of oxygen can be carried out by using an RDE. The well-known Levich relation is used for RDE experiments [3]:

$$I_{\text{lim}} = 0.62nFA_c c_b D^{2/3} \nu^{-1/6} \omega^{1/2} \quad (6)$$

where I_{lim} is the limiting current (A), n the number of electrons involved in the electrode reaction, F the faraday constant, i.e., the charge on one mole of electrons (C), A_s the electrode area (m^2), c_b the bulk concentration of the electroactive species (mol m^{-3}), D the diffusion coefficient of the electroactive species ($\text{m}^2 \text{s}^{-1}$), ν the kinematic viscosity of the solution ($\text{m}^2 \text{s}^{-1}$) and ω the angular rotation speed (rad s^{-1}).

D and ν will alter as a result of changes in glucose concentration.

To solve this problem, a Stokes-Einstein-type relationship is used [4]:

$$\eta D = \text{constant} \quad (7)$$

where η is the dynamic viscosity of the solution ($\text{kg m}^{-1} \text{s}^{-1}$). From data for the dynamic viscosity and the density (ρ), the kinematic viscosity ν ($=\eta/\rho$) as a

function of the glucose concentration was obtained. As the diffusion coefficient of oxygen in the absence of glucose is well-known, it is possible to determine the diffusion coefficient of oxygen for several glucose concentrations from Eqn. (7). Eqn. (6) can be applied to calculate the solubility of oxygen.

The validity of Eqn. (7) was checked for two electroactive species, viz., hydrogen peroxide and hydroquinone, because for these species the concentrations in the glucose solution are chosen. However, this is not the case for oxygen, as here both the diffusion coefficient and the concentration are unknown.

3.2.2 Experimental

Reagents

Phosphate-buffered saline (PBS) was prepared with $\text{NaH}_2\text{PO}_4 \cdot 2\text{H}_2\text{O}$, $\text{Na}_2\text{HPO}_4 \cdot 2\text{H}_2\text{O}$ and NaCl purchased from Merck. Hydrogen peroxide (30%, w/w, aqueous solution) was obtained from Chempro Pack, hydroquinone from Merck and D-glucose from Janssen Chimica. Platinum black electrodes were made with a solution of $\text{H}_2\text{PtCl}_6 \cdot 6\text{H}_2\text{O}$ from H. Drijfhout & Sons and PbCl_2 from Merck.

All solutions were prepared with demineralized, distilled water.

Instrumentation

For the RDE experiments a Wenking POS 73 potentiostat was used, equipped with a digital multimeter (Fluke 8600 A) and a Motomatic E-550-M stirring motor. Recording was carried out with either an *x,y* recorder (Philips 8120) for polished platinum RDE cyclic voltammograms or an *x,t* recorder (Kipp & Sons BD40) for platinum black RDE experiments. A circulating waterbath (Colora NB-32981) was used for temperature control of the one-compartment cell.

For preparation of the platinum black electrodes, a Delta Elektronika Power Supply E 030-1 was used, connected with a sliding resistance (Albert van der Perk) and an amperometer (Gossen).

Preparation of a platinum black RDE

A polished platinum RDE was scanned from -1500 to +1500 mV (vs. SCE) with a scan rate of 1 V s^{-1} in a 2 M H_2SO_4 solution to remove all impurities. The electrode was immersed in a 3% (w/w) H_2PtCl_6 solution (with 0.02%, w/w, PbCl_2) and connected as the cathode with a platinum sheet as the anode. A current of about 5 mA was used to prepare a platinum black layer on the platinum RDE within 10 min. Subsequently the platinum black electrode (platinized electrode) was washed in running tap water for at least 30 min and then washed with distilled, demineralized water for 5 min.

Procedures

For all experiments a platinum RDE (polished or platinized) was used as the working electrode ($A_e = 0.50 \cdot 10^{-4} \text{ m}^2$). Further, a platinum counter electrode with a surface area of $5 \cdot 10^{-4} \text{ m}^2$ and a saturated calomel reference electrode (SCE) with a Luggin capillary were placed in the one-compartment cell. A circulating water-bath was used to keep the temperature constant. As supporting electrolyte PBS (0.050 M NaH_2PO_4 , 0.050 M Na_2HPO_4 and 0.16 M NaCl , pH=7) was used. Glucose concentrations in this electrolyte varied from 0 to 1.0 M.

Hydroquinone experiments ($2\text{-}3 \text{ mol m}^{-3}$) were performed with an argon-saturated (1 atm) glucose solution. Hydroquinone was added before passing argon through. A cyclic voltammogram was recorded from -550 to +1200 mV (vs. SCE) at various rotation rates ($1\text{-}9 \text{ s}^{-1}$). Rotation rates were varied in random order. A scan rate of 50 mV s^{-1} was used. After every set of measurements belonging to one glucose concentration the RDE was cleaned by scanning from -1500 to +1500 mV (vs. SCE) in 2 M H_2SO_4 with a scan rate of 1 V s^{-1} .

For hydrogen peroxide measurements ($3\text{-}4 \text{ mol m}^{-3}$) the glucose solution was saturated with argon (1 atm) before adding hydrogen peroxide and cyclic voltammograms were scanned cathodically from +300 to -750 mV (vs. SCE) at 50 mV s^{-1} . Again the rotation speeds were varied in random order and the RDE was cleaned in

2 M H₂SO₄ after each set of measurements. Hydrogen peroxide diffusion coefficients were also determined by using a platinized RDE. An oxidation potential of +700 mV vs. SCE was applied and the electrode was allowed to reach a steady background current for a glucose solution without hydrogen peroxide at a certain rotation speed. Thereafter an aliquot of a hydrogen peroxide stock solution was added while leaving the potential at +700 mV. The solution was stirred magnetically for a few seconds to make it homogeneous and a steady current was obtained.

Oxygen measurements were carried out with a platinum black electrode. Glucose solutions were saturated with argon to determine the background current at -580 mV vs. SCE at a certain rotation speed. Subsequently the solution was saturated with oxygen (1 atm) while leaving all other conditions unchanged. After about 10 min a steady reduction current could be measured.

Measurements for all three compounds were carried out at 25 °C and 37 °C. The temperature was controlled with a circulating water-bath.

3.2.3 Results and discussion

From the dynamic viscosity η [5] and the density ρ [6] as a function of the weight percentage of glucose, the dynamic viscosity was calculated as a function of the molar glucose concentration (Fig. 3.1), taking into account the influence of NaCl, NaH₂PO₄ and Na₂HPO₄.

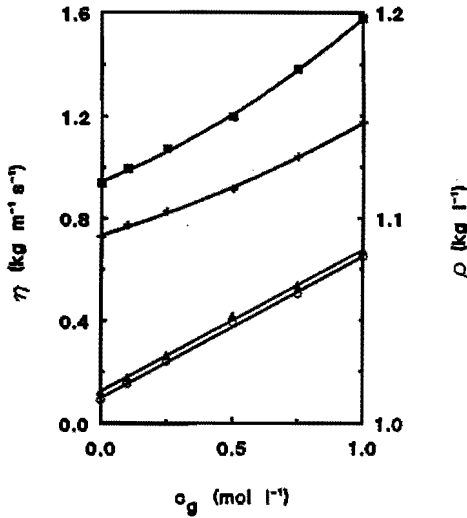


Figure 3.1: Dynamic viscosity (■ = 25 °C, + = 37 °C) and density (▲ = 25 °C, ○ = 37 °C) as a function of the glucose concentration in PBS.

If mutual interactions between the salt ions and glucose are neglected, the Grunberg-Nissan relation can be used [7]:

$$\log \eta_s = x_w \log \eta_w + x_1 \log \eta_1 + x_2 \log \eta_2 + x_3 \log \eta_3 \quad (8)$$

where x_w is the mole fraction of water, x_i is the mole fraction of compound i ($i = 1, 2$ or 3), η_s and η_w the dynamic viscosity of the overall solution and pure water, respectively, and η_i is the apparent dynamic viscosity of compound i . Further,

$$\log \eta_a = x_{w,a} \log \eta_w + x_{1,a} \log \eta_1 \quad (9)$$

$$\log \eta_b = x_{w,b} \log \eta_w + x_{2,b} \log \eta_2 \quad (10)$$

$$\log \eta_c = x_{w,c} \log \eta_w + x_{3,c} \log \eta_3 \quad (11)$$

where the subscripts a, b and c refer to aqueous solutions of NaCl, sodium phosphate and glucose, respectively. When x_i is assumed to be equal in Eqn. (8) and in Eqns. (9)-(11) (viz., $x_{1,a} = x_1$; $x_{2,b} = x_2$; $x_{3,c} = x_3$) it follows

$$\begin{aligned} x_w + x_1 + x_2 + x_3 &= 1 && \text{(from Eqn. 8)} \\ x_{w,a} + x_1 &= 1 && \text{(from Eqn. 9)} \\ x_{w,b} + x_2 &= 1 && \text{(from Eqn. 10)} \\ x_{w,c} + x_3 &= 1 && \text{(from Eqn. 11)} \end{aligned} \quad (12)$$

From this set of equations, the following can easily be derived

$$x_w - x_{w,a} - x_{w,b} - x_{w,c} = -2 \quad (13)$$

Combining Eqns. (8)-(11) and (13) gives

$$\eta_a = \frac{\eta_a * \eta_b * \eta_c}{\eta_w^2} \quad (14)$$

Values for η_w , η_a , η_b and η_c can be found in the literature [5, 8]. The same procedure can be followed for calculating the density for the glucose-PBS solutions [6, 9].

Cyclic voltammograms of hydrogen peroxide and hydroquinone in the glucose solutions had similar shapes to those in pure PBS. Plots of I_{lim} versus $\omega^{1/2}$ gave

straight lines although at higher rotation rates a small deviation is observed owing to kinetic limitations. Therefore, a reciprocal plot was made, which was linear even for high rotation rates. If, however, the original I_{lim} versus $\omega^{1/2}$ plot has an intercept (I^*), a correction should be performed by subtracting I^* from all measured limiting currents. Only from these corrected values can a proper reciprocal plot be obtained (see Figs. 3.2 and 3.3).

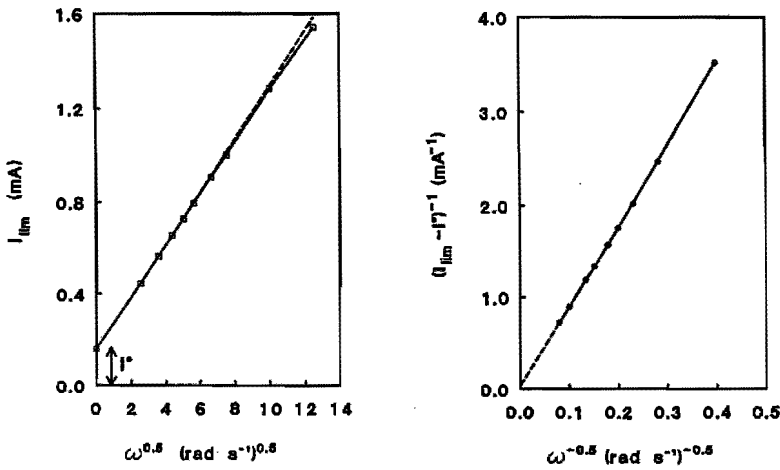


Figure 3.2: The current as a function of the square root of the angular rotation rate for 2 mM hydroquinone in PBS at 25 °C. The continuous line follows the measured curve and the dashed line is the linear curve for rotation speeds from 1 to 5 s⁻¹. I^* denotes the intercept.

Figure 3.3: The reciprocal of the corrected current $((I_{lim} - I^*)^{-1})$ as a function of the reciprocal of the square root of the angular rotation rate for 2 mM hydroquinone in PBS at 25 °C.

Contamination of the polished platinum electrodes easily occurs, especially in

solutions with a high glucose concentration (≥ 0.5 M). Cleaning of the electrodes in sulphuric acid was necessary after every set of measurements ($1-9$ s⁻¹) for one glucose concentration. If measurements were performed going from a low to a high rotation speed, the Levich slope was different from measurements going from a high to a low rotation speed (Fig. 3.4). This effect was not observed in a glucose-free solution (Fig. 3.4). The average of the two slopes, however, gave good results. A random order of measuring while alternating low and high rotation speeds yielded the same results. This is shown in Fig. 3.5 for hydroquinone and hydrogen peroxide.

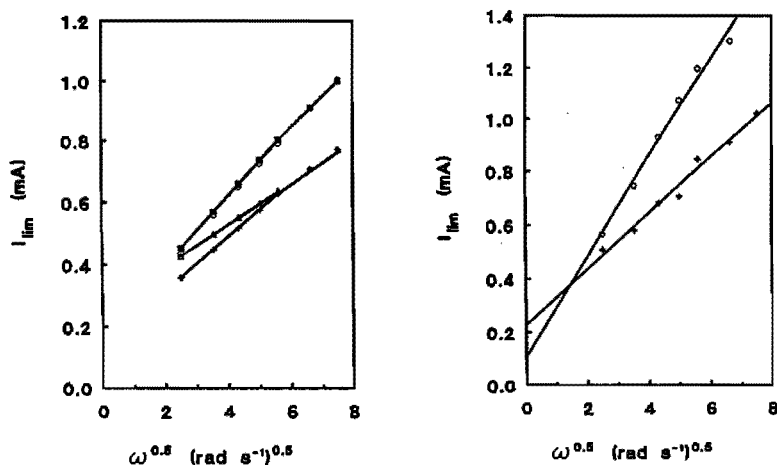


Figure 3.4: *The current plotted against the square root of the angular rotation rate for 2 mM hydroquinone at 25 °C. Measurements were performed in PBS with (○) rising and (■) falling rotation speeds and in PBS containing 1 M glucose with (+) rising or (Δ) falling rotation speeds.*

Figure 3.5: *Plot of the current versus the square root of the angular rotation rate. Rotation rates were varied in random order for (○) 3.77 mM hydrogen peroxide and (+) 2.89 mM hydroquinone. $c_s=1$ M, $T= 25$ °C.*

To check the validity of this adjusted method, experiments with a platinized electrode were carried out. With a platinized electrode, however, it is not possible to obtain a voltammogram showing a limiting current, even if a low scan rate of 1 mV s^{-1} is used. Therefore, a potential at which a limiting current appears was directly applied. For a hydrogen peroxide-free medium it took 1-3 h (depending on the glucose concentration) to reach a background current at $+700 \text{ mV}$. The results for the platinum black electrode were consistent with those for the polished platinum electrode. The advantage of the platinum black electrode is that the limiting current remains constant for at least 15 min.

Fig. 3.6 shows the factor ηD for both hydrogen peroxide and hydroquinone as a function of glucose concentration. It can be clearly seen that within the examined range of glucose concentration ηD does not change significantly.

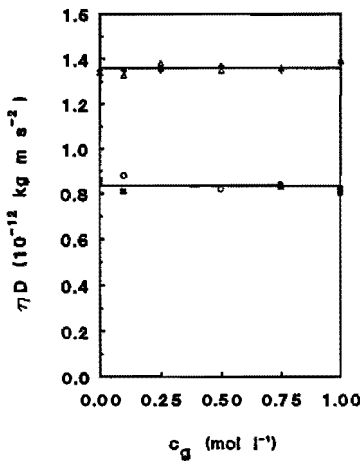


Figure 3.6: ηD for hydrogen peroxide at (+) 25°C and (Δ) 37°C as a function of the glucose concentration in PBS, and for hydroquinone at (O) 25°C and (\blacksquare) 37°C .

Therefore it is assumed that ηD for oxygen does not depend on the glucose concentration either. It is known that oxygen, hydrogen peroxide and hydroquinone behave similarly when diffusing through a hydrogel layer [10]. Further, it is known that the Stokes-Einstein relationship is valid for oxygen in NaCl solutions [11].

As the diffusion coefficient of oxygen in PBS is measured as $1.94 \cdot 10^{-9} \text{ m}^2 \text{ s}^{-1}$ [10] and η for this solution is known to be $0.938 \cdot 10^{-3} \text{ kg m}^{-1} \text{ s}^{-1}$ (Fig. 3.1), ηD can be calculated as $1.82 \cdot 10^{-12} \text{ kg m s}^{-2}$. At $37 \text{ }^\circ\text{C}$, ηD becomes $2.47 \cdot 10^{-9} \cdot 0.728 \cdot 10^{-3} = 1.80 \cdot 10^{-12} \text{ kg m s}^{-2}$. From these values for ηD and the values for η (Fig. 3.1), the diffusion coefficient of oxygen (D_{ox}) was calculated as a function of the glucose concentration (Fig. 3.7).

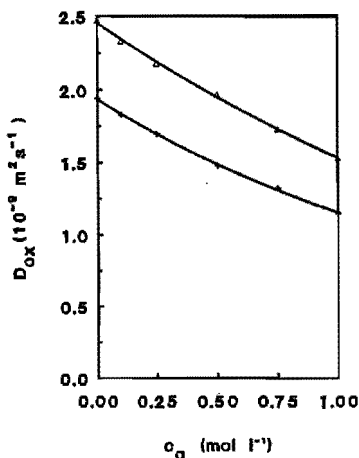


Figure 3.7: Diffusion coefficient of oxygen as a function of the glucose concentration in PBS at (+) 25 °C and (Δ) 37 °C.

With a platinum black electrode the solubility of oxygen in glucose solutions was determined, using the diffusion coefficients from Fig. 3.7. The results are presented

in Fig. 3.8 for 25 °C and 37 °C.

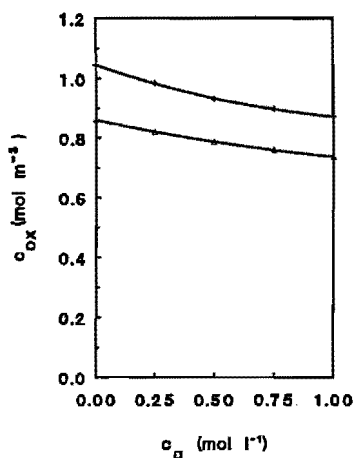


Figure 3.8: Solubility of oxygen as a function of the glucose concentration in PBS at (+) 25 °C and (Δ) 37 °C.

The solubility of oxygen is likely to be slightly changed by the presence of salt ions (salting out effect [12]).

The solubility of oxygen as a function of the glucose concentration for both 25 °C and 37 °C is given by

$$c_{ox} = 1.045 - 0.2687c_g + 0.09714c_g^2 \quad (15)$$

$$c_{ox} = 0.8607 - 0.1689c_g + 0.04571c_g^2 \quad (16)$$

respectively. These fitted relationships are applicable to a glucose concentration range of 0-1 M. The deviation between the measured values and values calculated

with Eqn. (15) or (16) is $\leq 0.3\%$.

Although significant changes in diffusion coefficients, viscosity and solubility of oxygen only occur at glucose concentrations that are so high that they are physiologically irrelevant, the data determined in this paragraph are necessary to determine the kinetic parameters of soluble GO (*vide infra*, paragraph 3.3).

3.3 A kinetic study of soluble glucose oxidase using a rotating disc electrode

3.3.1 Theory

The initial velocity can be determined by measuring the concentration of hydrogen peroxide as a function of time after addition of the enzyme GO. As hydrogen peroxide is an electrochemically active species an RDE is used. Levich [3] deduced a simple equation for the measured diffusion-controlled limiting current, I_{lim} (A), as a function of the concentration c_b (M) of the electroactive species in the bulk of the solution and the angular velocity ω (rad s^{-1}) of the RDE:

$$I_{\text{lim}} = 0.62 n F A_e c_b D^{2/3} \nu^{-1/6} \omega^{1/2} \quad (17)$$

where n is the number of electrons involved in the electrode reaction, F the faraday constant, i.e., the charge on one mole of electrons (Coulombs), A_e the geometric electrode area (m^2), D the diffusion coefficient of the electroactive species ($\text{m}^2 \text{s}^{-1}$) and ν the kinematic viscosity of the solution ($\text{m}^2 \text{s}^{-1}$).

Eqn. (17) is only valid for diffusion-controlled conditions, i.e., the applied potential is high enough to lower the concentration of the electroactive species at the electrode surface to virtually zero. If I_{lim} is plotted versus $\omega^{1/2}$ a straight line is obtained from the slope of which D [10] or c_b [13] can be calculated.

In the case of glucose oxidation the concentration of the electroactive product, H_2O_2 ,

in the bulk solution will increase linearly with time and so will I_{lim} , at a fixed ω . The plot of I_{lim} versus time (and hence the hydrogen peroxide concentration versus time) is called a progress curve. The initial velocity v_0 can be calculated from the initial slope of the curve using the Levich equation. After some minutes the progress curve starts to show a clear deviation from linear behaviour, as a result of product inhibition, significant substrate consumption and/or enzyme instabilization. At this stage the pseudo-steady-state condition no longer exists. As the RDE technique is able to measure the product formation continuously, it is possible to calculate the initial, pseudo-steady-state reaction rate.

3.3.2 Experimental

Reagents

Glucose oxidase from *A. niger* (E.C. 1.1.3.4, M=150.000, lyophil, GO/catalase min 2000) was purchased from Serva. Phosphate-buffered saline (PBS) was made with $NaH_2PO_4 \cdot 2H_2O$, $Na_2HPO_4 \cdot 12H_2O$ and NaCl purchased from Merck. D-glucose monohydrate was obtained from Janssen Chimica. Product inhibition experiments were carried out with hydrogen peroxide (30%, w/w, aqueous solution) from Chempro Pack and gluconolactone from Sigma.

Platinum black electrodes were prepared with a solution of $H_2PtCl_6 \cdot 6H_2O$ from H. Drijfhout & Sons and $PbCl_2$ from Merck.

All solutions were prepared using demineralized, distilled water.

Preparation of a platinum black electrode

A polished platinum RDE was scanned from -1500 to +1500 mV (vs. a saturated calomel electrode (SCE)) with a scan rate of 1 V s^{-1} in a 2 M H_2SO_4 solution to remove all impurities from the electrode. The electrode was immersed in a 3% (w/w) H_2PtCl_6 solution (with 0.02%, w/w, $PbCl_2$) and connected as the cathode with a platinum sheet as the anode. A current of about 5 mA was used to deposit a

platinum black layer on the platinum RDE over a period of 10 min.

The platinum black electrode (platinized electrode) was then washed with running tap water for at least 30 min and with distilled, demineralized water for a further 5 min.

Preparation of the enzyme stock solution

A 0.065 M acetate buffer (pH=4.4) was prepared by mixing 1.525 ml of a 4 M acetic acid solution and 0.53 g $\text{CH}_3\text{COONa}\cdot 3\text{H}_2\text{O}$ and diluting to 100 ml with distilled, demineralized water.

Approximately 3 mg of the lyophilized enzyme was weighted exactly and dissolved in 10 ml of the acetate buffer. The solution was homogenized in an ultrasonic bath (Struers) for 5 min.

Preparation of the glucose solutions

Glucose-containing PBS was prepared by adding the appropriate amount of glucose to 9.22 g NaCl (0.16 mol), 17.8 g $\text{Na}_2\text{HPO}_4\cdot 12\text{H}_2\text{O}$ (0.050 mol) and 8.00 g $\text{NaH}_2\text{PO}_4\cdot 2\text{H}_2\text{O}$ (0.050 mol), and diluting to 1000 ml with distilled, demineralized water. The pH was adjusted to either 7.0 or 7.4 with 4 M NaOH. The glucose solutions were allowed to mutarotate for at least 3 h before usage.

Measuring the time course of hydrogen peroxide concentration

A platinum black RDE was used as the working electrode ($A_e=0.50 \times 10^{-4} \text{ m}^2$) in all experiments. Further, a platinum counter electrode with a surface area of $5 \times 10^{-4} \text{ m}^2$ and a saturated calomel reference electrode (SCE) with a Luggin capillary were placed in the one-compartment cell. A circulating water-bath (Colora NB-32981) was used to keep the temperature constant (25 °C or 37 °C). PBS (0.050 M NaH_2PO_4 , 0.050 M Na_2HPO_4 and 0.16 M NaCl, pH=7.0 or 7.4) was used as supporting electrolyte. Glucose concentrations varied from 0 to 0.5 M. A Wenking POS 73 potentiostat, equipped with a digital multimeter (Fluke 8600 A) and a Motomatic E-

550-M stirring motor, was used to carry out the RDE measurements. The rotation rate was chosen to be 2 s^{-1} ($=12.6 \text{ rad s}^{-1}$).

Before the enzyme was added and the time course of hydrogen peroxide concentration was measured, the glucose solution was allowed to reach a constant temperature. The solution was saturated with argon. The diffusion-controlled background current of oxygen reduction was measured

at -580 mV (vs. SCE). Thereafter, the solution was saturated with oxygen or a nitrogen/oxygen mixture for at least 30 min while leaving the applied potential unchanged. In this way the diffusion-controlled current for oxygen reduction could be determined and the oxygen concentration in the bulk solution calculated.

During experiments the appropriate gas was passed over the saturated solution, because bubbling through the solution would disturb the hydrodynamic profile created by the RDE.

After measurement of the oxygen concentration, the potential was changed to $+700 \text{ mV}$ (vs. SCE) and the diffusion-controlled background current of hydrogen peroxide oxidation was allowed to reach a steady value. Then, an aliquot of the GO stock solution was pipetted into the solution (final concentration 1.12 mg l^{-1}) and the solution was stirred vigorously for a few seconds, with the potential kept at $+700 \text{ mV}$ (vs. SCE). Immediately after adding the enzyme the increase in hydrogen peroxide concentration was measured. The time course was recorded on a Kipp & Zonen x,t recorder (BD40) and followed until a clear deviation from linearity was observed.

For gluconolactone inhibition experiments the glucose solution also contained the required gluconolactone concentration. For hydrogen peroxide inhibition experiments an aliquot of a hydrogen peroxide stock solution was added after measuring the background current. After determination of this basal hydrogen peroxide level, GO was added and the time course was recorded.

3.3.3 Results and discussion

Measurements of progress curves

Before adding GO to a particular glucose solution the oxygen concentration was measured using the RDE. The solubility of oxygen appears to be affected by the glucose concentration [13]. For times below zero the background current was measured. At time zero the enzyme GO was added. At this point, the RDE was removed from the solution for a few seconds because there was no special pipette entry port in the cell. During this period the current dropped to zero. After returning the RDE into the solution, a large peak in the current occurred, which is due to charging of the electrochemical double layer. After this peak a virtually linear progress curve is shown (pseudo-steady state), followed by a clear deviation from linear behaviour. The exact duration of the pseudo-steady state varied slightly. At a fixed oxygen concentration, the pseudo-steady-state time is shorter at higher glucose concentrations (Fig. 3.9). Owing to a higher reaction rate at high glucose concentrations, significant consumption of oxygen occurs earlier. Furthermore, progress curves start to show deviation from linearity sooner when, at a fixed glucose concentration, the oxygen concentration is set at a low value.

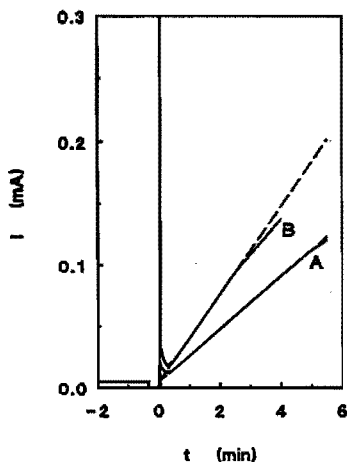


Figure 3.9: Continuous time courses for the hydrogen peroxide concentration after addition of GO. $T=25\text{ }^{\circ}\text{C}$ and $\text{pH}=7.0$, $c_{\text{ox}}=1.1\text{ mM}$, $c_{\text{s}}=20\text{ mM}$ (curve A) or 100 mM (curve B). The slope of the dashed line is equal to the initial slope of the progress curve.

The fact that the pseudo-steady-state time is not well reproducible indicates that kinetic experiments, performed by taking a sample after a fixed time interval, can be very risky. The chance of measuring a sample outside pseudo-steady-state conditions is considerably large. However, taking a sample within a very short time to ensure pseudo-steady-state conditions can cause difficulties with analysis as only a small amount of hydrogen peroxide has been formed.

The initial reaction rate for a fixed glucose and oxygen concentration was calculated from the initial slope of the progress curve using the Levich relation. Two electrons are transferred per mole of hydrogen peroxide ($n=2$). The rotation speed was chosen to be 2 s^{-1} ($= 12.6\text{ rad s}^{-1}$) and the electrode had a surface area of $0.50 \cdot 10^{-4}\text{ m}^2$. Use of the Levich relation requires knowledge of the kinematic viscosity of the solution and the diffusion coefficient of the electroactive species. As the kinematic

viscosity starts to increase significantly and the diffusion coefficient starts to decrease at higher glucose concentrations ($c_g \geq 100$ mM), it was necessary to determine these parameters for solutions with such a high glucose concentration [13]. Fig. 3.9 can now serve as a calculation example. The initial slope of curve A ($c_g=20$ mM, $c_{ox}=1$ mM) is equal to 0.0216 mA min⁻¹. For a kinematic viscosity of 0.95×10^{-6} m² s⁻¹ and a hydrogen peroxide diffusion coefficient of 1.43×10^{-9} m² s⁻¹, the initial increase (v_0) in the hydrogen peroxide concentration with time is calculated to be 0.078 mM min⁻¹. Curve B is a progress curve for $c_g=100$ mM and $c_{ox}=1$ mM. The initial slope of this curve is equal to 0.358 mA min⁻¹. For a kinematic viscosity of 0.98×10^{-6} m² s⁻¹ and a hydrogen peroxide diffusion coefficient of 1.39×10^{-9} m² s⁻¹, v_0 is calculated to be 0.135 mM min⁻¹.

Both initial velocities were used to construct the primary plot for $T=25$ °C and $pH=7.0$ (*vide infra*).

In this study a platinum black electrode was used to measure the progress curves. The advantages of this electrode are its high catalytic activity and its resistance to poisoning. A polished platinum electrode is easily poisoned by organic substances. However, the disadvantage of the platinum black electrode is the long "lag" period before a steady background current is reached. This period can be as long as 1 h.

To optimize the RDE procedure, the choice of the electrode material can be varied. Nowadays, research is carried out on new electrode materials for hydrogen peroxide detection. Carbon electrodes have the disadvantage of high overvoltages [14] and gold electrodes do not show hydrogen peroxide oxidation at $pH < 9$ [15]. Ti/IrO₂ electrodes seem to give reproducible results and show high stability [16].

Product inhibition behaviour

To verify the assumption of a ping-pong mechanism the product inhibition behaviour was studied. According to this mechanism hydrogen peroxide is a competitive inhibitor for glucose and a non-competitive inhibitor for oxygen. Gluconolactone is a competitive inhibitor for oxygen and a non-competitive inhibitor for glucose [2].

Other possible mechanisms for the oxidation of glucose in the presence of GO are tabulated in Table 3.1, together with their product inhibition properties [2].

Table 3.1: Primary plot and product inhibition behaviour for various BiBi mechanisms. G, L, O and H denote glucose, gluconolactone, oxygen and hydrogen peroxide, respectively. C indicates competitive inhibition and N indicates noncompetitive inhibition.

Mechanism	Primary plot	Product inhibition behaviour			
		G vs. L	G vs. H	O vs. L	O vs. H
Random sequential	Intersecting lines	C	C	C	C
Ordered sequential	Intersecting lines	N	C	N	N
Ping-pong	Parallel lines	N	C	C	N

Only the ping-pong mechanism produces parallel lines when a double-reciprocal plot is constructed from initial velocity experiments. However, it is sometimes difficult to state parallelism as there is always the possibility of an intersection in the far third quadrant. Therefore it is worth examining the product inhibition behaviour. In this work, three inhibition cases were studied: gluconolactone versus glucose, gluconolactone versus oxygen and hydrogen peroxide versus oxygen (Figs. 3.10, 3.11 and 3.12). Competitive inhibition is shown by intersection of the double-reciprocal lines on the ordinate. Non-competitive inhibition is indicated by intersection on the negative abscissa. The product inhibition behaviour shown in Figs. 3.10-3.12, together with parallel lines in the primary double-reciprocal plots, indicates a ping-

pong mechanism, or at least a very close approximation. Each point in Figs. 3.10-3.12 was calculated from a separate measurement of a progress curve.

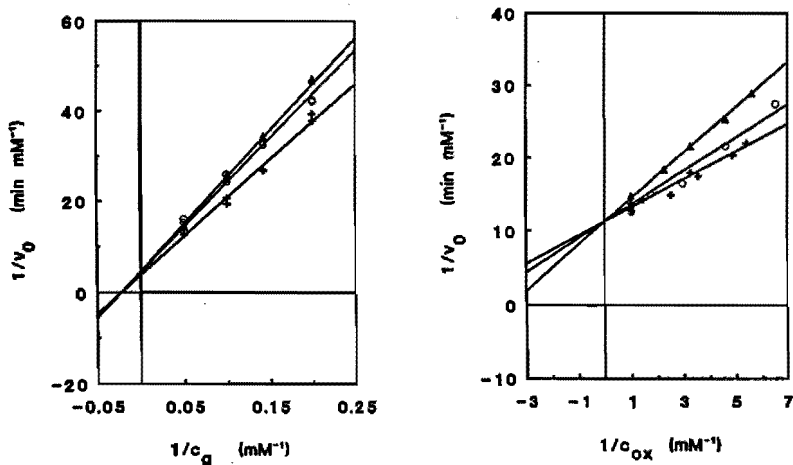


Figure 3.10: Product inhibition behaviour of gluconolactone versus glucose.
 $T=25$ °C, $\text{pH}=7.0$ and $c_{ox}=1.1$ mM. Initial gluconolactone concentrations used are: 0 mM (+), 50 mM (O) and 100 mM (\blacktriangle).

Figure 3.11: Product inhibition behaviour of gluconolactone versus oxygen.
 $T=25$ °C, $\text{pH}=7.0$ and $c_g=20$ mM. Initial gluconolactone concentrations used are: 0 mM (+), 10 mM (O) and 200 mM (\blacktriangle).

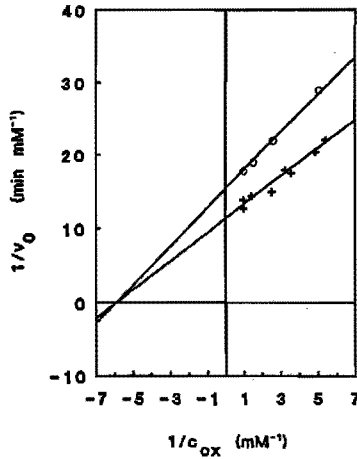


Figure 3.12: Product inhibition behaviour of hydrogen peroxide versus oxygen. $T=25\text{ }^{\circ}\text{C}$, $\text{pH}=7.0$ and $c_g=20\text{ mM}$. Initial hydrogen peroxide concentrations used are: 0 mM (+) and 0.75 mM (O).

The kinetic parameters of GO-catalysed glucose oxidation at $T=25\text{ }^{\circ}\text{C}$ and $\text{pH}=7.0$

The hydrogen peroxide production was examined for several combinations of substrate concentrations at the standard conditions of $T=25\text{ }^{\circ}\text{C}$ and $\text{pH}=7.0$. Fig. 3.13 shows the results of all measurements. A set of parallel lines is obtained. However, at $c_g \geq 100\text{ mM}$, the well-known phenomenon of substrate inhibition [17] is observed, i.e., the reduced enzyme complexes with glucose, which makes glucose a competitive inhibitor for oxygen. The mechanism allows gluconolactone to bind the reduced enzyme, but as glucose is incorporated into gluconolactone, it is possible that glucose binds the reduced enzyme at the gluconolactone site. Owing to substrate inhibition the lines for $c_g = 100$ and 500 mM exhibit a different slope to that obtained for lower glucose concentrations, but the intercepts (i.c. [Fig.3.13]) can still be used to construct the secondary plot, which is represented by the equation

$$\text{i.c. [Fig. 3.13]} = 2.38 + 167 * c_g^{-1} \quad (18)$$

which has a regression coefficient of 0.9993.

The intercept of the secondary plot (Eqn. (18)) gives the reciprocal V_{\max} . V_{\max} determined in this way is related to an infinite concentration for glucose as well as oxygen and has a value of 0.42 mM min^{-1} . As the GO concentration is chosen to be 1.12 mg l^{-1} , k_{cat} is calculated to be $3.74 \times 10^{-4} \text{ mol (mg GO)}^{-1} \text{ min}^{-1}$ or 935 s^{-1} (turnover number). The Michaelis constants $k_m(\text{o})$ and $k_m(\text{g})$ are 0.80 mM and 70 mM , respectively. These values indicate that the glucose concentration determines the reaction rate almost completely.

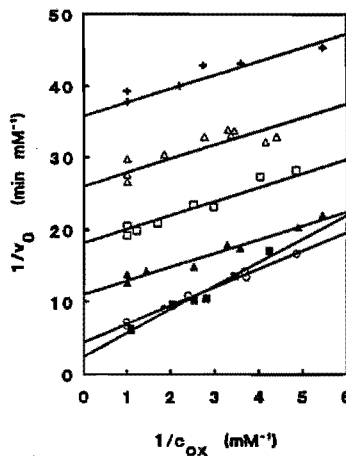


Figure 3.13: Double-reciprocal plots (v_0^{-1} versus c_{ox}^{-1}) for initial velocity experiments with the enzyme GO ($T=25 \text{ }^\circ\text{C}$, $\text{pH}=7.0$). Each line corresponds to a fixed initial glucose concentration: 5 mM (+), 7 mM (Δ), 10 mM (\square), 20 mM (\blacktriangle), 100 mM (\circ) and 500 mM (\blacksquare).

The kinetic parameters of GO-catalysed glucose oxidation at $T=37\text{ }^{\circ}\text{C}$ and $\text{pH}=7.4$

In the same way as for $T=25\text{ }^{\circ}\text{C}$ and $\text{pH}=7.0$ a primary and secondary plot can be constructed from measurements of the rate of hydrogen peroxide production for $T=37\text{ }^{\circ}\text{C}$ and $\text{pH}=7.4$ (Fig. 3.14). These physiological conditions will occur when the glucose sensor is used *in vivo*. Again, the ping-pong mechanism seems to be obeyed, as a set of parallel lines is obtained.

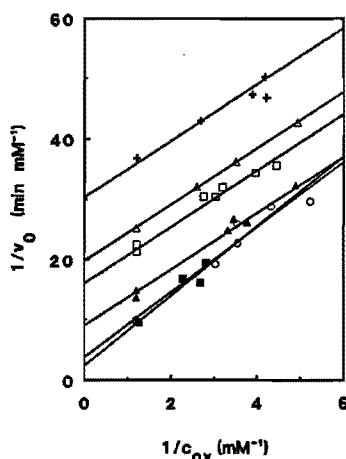


Figure 3.14: Double-reciprocal plots (v_0^{-1} versus c_{ox}^{-1}) for initial velocity experiments with the enzyme GO ($T=37\text{ }^{\circ}\text{C}$, $\text{pH}=7.4$). Each line corresponds to a initial fixed glucose concentration: 5 mM (+), 7 mM (Δ), 10 mM (\square), 20 mM (\blacktriangle), 100 mM (\circ) and 500 mM (\blacksquare).

Eqn. (19) represents the secondary plot derived from the intercepts of Fig. 3.14 (i.e. [Fig. 3.14]) and has a regression coefficient of 0.9974:

$$\text{i.c. [Fig. 3.14]} = 1.96 + 138 * c_g^{-1} \quad (19)$$

V_{\max} has a value of 0.51 mM min^{-1} for infinite concentrations of glucose as well as oxygen. The catalytic constant k_{cat} is equal to $4.56 \times 10^{-4} \text{ mol (mg GO)}^{-1} \text{ min}^{-1}$ or $1140 \text{ mol s}^{-1} (\text{mol GO})^{-1}$. The Michaelis constants $k_m(\text{o})$ and $k_m(\text{g})$ in this case are determined to be 2.4 mM and 70 mM respectively.

Again, substrate inhibition is observed at a glucose concentration above 100 mM .

The temperature change from 25 to $37 \text{ }^\circ\text{C}$ combined with a pH change from 7.0 to 7.4 seems to have no effect on $k_m(\text{g})$, and V_{\max} only changes slightly. The only parameter that changes significantly is $k_m(\text{o})$. Gibson *et al.* [1] also observed a change in V_{\max} and $k_m(\text{o})$ due to temperature changes, but not in $k_m(\text{g})$.

3.3.4 Conclusions

The RDE method appears to be very useful for determining the kinetic parameters of the GO-catalysed oxidation of glucose. The continuous measurement of the time course for hydrogen peroxide concentration makes it possible to determine the initial velocity. The method is also applicable to other (enzymatic) reactions, provided that one of the products is electrochemically active. If one of the substrates is electroactive, its consumption can be recorded as a function of time. In either case, there should be no interference from any of the other compounds present.

To optimize the procedure in the case of hydrogen peroxide detection, another electrode material can be chosen.

Acknowledgment

I wish to express my gratitude to Dr. H.J.M. Kocken and Prof. Dr. L.A.Æ. Sluyterman for their contribution to this chapter.

References

1. Q.H. Gibson, B.E.P. Swoboda and J. Massey, *J. Biol. Chem.*, 239 (1964) 3927.
2. C. Walsh, *Enzymatic Reaction Mechanisms*, W.H. Freeman and Company, San Francisco, (1979), p.220-224.
3. V.G. Levich, *Physicochemical Hydrodynamics*, Prentice Hall, Englewood Cliffs, NJ, (1962), p.60-72.
4. J. Joseph, E. Ackerman and R.L. Berger, *J. Am. Chem. Soc.*, 78 (1956) 2979.
5. *International Critical Tables of Numerical Data, Physics, Chemistry and Technology*, E.W. Washburn (Ed.), Vol. V, Mc Graw-Hill Book Company, Inc., New York, 1st edn., (1929).
6. *International Critical Tables of Numerical Data, Physics, Chemistry and Technology*, E.W. Washburn (Ed.), Vol. II, Mc Graw-Hill Book Company, Inc., New York, 1st edn., (1927).
7. R.H. Perry, *Perry's Chemical Engineers' Handbook*, Mc Graw-Hill Book Company, New York, 6th edn., (1984).
8. Landolt-Börnstein, *Zahlenwerte und Funktionen aus Physik, Chemie, Astronomie, Geophysik und Technik*, 5.Teil, Bandteil 5, Springer-Verlag, Berlin, (1969).
9. V.M.M. Lobo and J.L. Quaresma, *Handbook of Electrolyte Solutions, Physical Sciences Data 41, Part B*, Elsevier, Amsterdam, (1989).
10. S.A.M. van Stroe-Biezen, F.M. Everaerts, L.J.J. Janssen and R.A. Tacken, *Anal. Chim. Acta*, 273 (1993) 553.
11. J.C.P.A. Brock, *Report Eindhoven University of Technology, Eindhoven*, (1981).
12. R. Battino and H.L. Clever, *Chem. Revs.*, 66 (1966) 395.

13. S.A.M. van Stroe-Biezen, A.P.M. Janssen and L.J.J. Janssen, *Anal. Chim. Acta*, *Anal. Chim. Acta*, 280 (1993) 217.
14. B.E. Conway, J.O'M. Bockris and R.E. White (Eds.), *Modern Aspects of Electrochemistry*, Vol. 19, Plenum Press, New York, (1989), p.317.
15. *Gmelins Handbuch der Anorganischen Chemie*, Vol. 7, 8th edn., Verlag Chemie, GmbH Weinheim, (1966), p.2240.
16. A. Nerini and C. Comninellis, *Abstracts of the 42nd Meeting of the International Society of Electrochemistry*, Montreux, (1991), p.6-15.
17. H.J. Fromm, *Molecular Biology, Biochemistry and Biophysics*, Vol. 22: *Initial Rate Enzyme Kinetics*, Springer-Verlag, Berlin, (1975), p.150.

CHAPTER 4. THE INHERENT KINETIC PARAMETERS OF IMMOBILIZED GLUCOSE OXIDASE

4.1 Introduction

The activity of an immobilized enzyme differs from that of the native enzyme due to [1, 2]:

- conformational changes
- steric hindrance
- enzyme-matrix interaction
- diffusional resistance
- partition effects

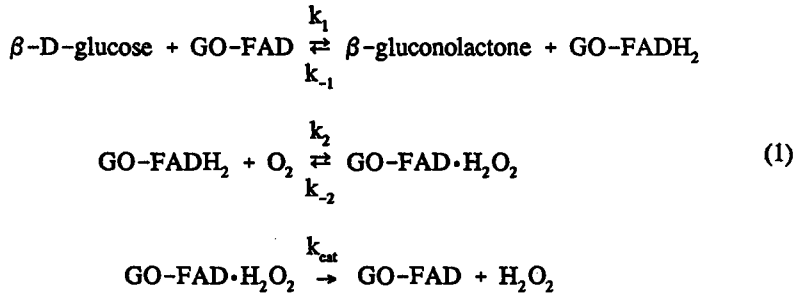
These effects cause a change in the effective kinetics of the enzyme. Generally, Michaelis-Menten kinetic behaviour is no longer observed in the presence of diffusional limitations [3]. The diffusional limitations can be divided into internal and external diffusion. External diffusion implies the diffusion of the substrate from a bulk solution to the enzyme layer. Internal diffusion implies the diffusion of the substrate through the enzyme layer to the enzyme. If diffusional limitations are separated, one obtains the inherent kinetic parameters. Here, partition effects are still playing a role. Substrate concentrations in the bulk solution are different from those in the enzyme layer. If, however, the partition effects are also removed, the intrinsic parameters are obtained. Only these parameters can be compared with the (intrinsic) parameters for the soluble enzyme. Diffusional and partition effects are actually influencing the substrates, whereas conformational changes, steric hindrance and enzyme-matrix interactions are effecting the enzyme itself. Therefore, the true kinetic behaviour of immobilized enzymes is reflected in the intrinsic kinetic

parameters.

In this chapter, a method is described to eliminate diffusional effects in order to obtain the inherent kinetic parameters of immobilized glucose oxidase (GO). Also, a relation between the inherent and the intrinsic parameters is deduced. If the partition coefficients of the substrates are known, the intrinsic parameters can be calculated. A knowledge of the partition coefficients of the products of the reaction is superfluous, because the method used does not measure the product formation to elucidate the kinetic parameters.

4.2 Theory

The enzyme glucose oxidase (GO) from *Aspergillus niger* catalyses the oxidation of glucose by oxygen, as also shown in Chapter 3:



Most research groups that are involved in research on glucose sensors want to study the influence of immobilization on the activity of the enzyme, but they actually compare the effective kinetic parameters of the bound enzyme with the intrinsic kinetic parameters of the soluble enzyme. As they determine the kinetics by measuring the substrate decrease or product increase in the bulk solution, the obtained values include internal and external diffusion of substrates and/or products

as well as partition effects.

A way to eliminate diffusional effects is to make use of a diffusion cell [4-7]. The cell consists of two compartments, compartment A containing a solution with a higher glucose concentration than compartment B. Between the compartments an enzyme-containing membrane is mounted. Glucose will diffuse from compartment A through the enzyme membrane to compartment B. When the compartments are saturated with oxygen (or an oxygen/nitrogen mixture), reaction will take place in the enzyme membrane.

This case of simultaneous diffusion and reaction kinetics can be represented by Fig. 4.1.

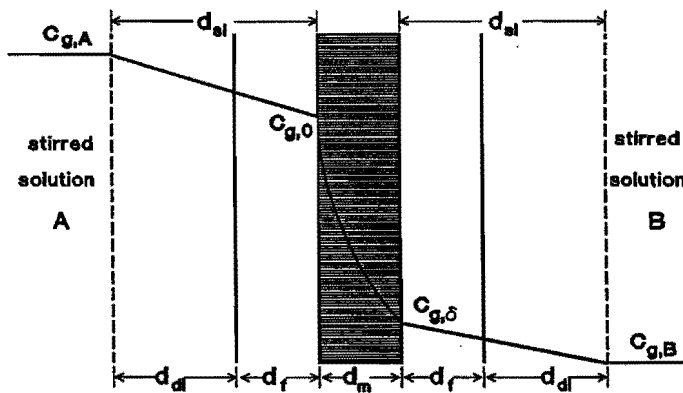


Figure 4.1: The concentration profile of glucose in the case of simultaneous diffusion and enzymatic reaction in the GO-containing membrane (d_m). d_{dl} , d_f and d_{sl} denote a diffusion layer, a filter-paper and a solution layer, respectively.

In the model shown in Fig. 4.1, a stagnant solution layer is visible. Although both compartments are stirred by a magnetic stirrer as well as by bubbling gas through (oxygen or an oxygen/nitrogen mixture), there will always be a diffusional resistance

of solution. In addition, the diffusion layer contains an artificially created diffusion layer by placing a filter-paper on each side of the membrane. This is carried out for solidity purposes. The diffusion layer and the filter-paper are considered as one diffusional resistance of solution.

A differential equation can be deduced for the glucose concentration in the membrane under pseudo-steady-state conditions:

$$D_m \frac{\delta^2 c_g}{\delta x^2} = v_0 \quad (2)$$

where D_m is the diffusion coefficient of glucose in the membrane ($m^2 s^{-1}$), c_g the concentration of glucose in the membrane, with the partition coefficient not taken into account ($mol m^{-3}$), x the distance from the boundary between filter-paper and membrane (m) and v_0 the reaction velocity of the enzymatic reaction ($mol m^{-3} s^{-1}$). For the enzyme glucose oxidase the reaction velocity can be written as [8, 9]:

$$v_0 = \frac{k_{cat}^* c_{GO} c_{ox} c_g}{k_m^*(o) c_g + k_m^*(g) c_{ox} + c_{ox} c_g} \quad (3)$$

where k_{cat}^* is the inherent turnover number ($mol (mol GO)^{-1} s^{-1}$), c_{GO} the total GO concentration in the membrane ($mol m^{-3}$), c_{ox} the concentration of oxygen in the membrane with the partition coefficient not taken into account ($mol m^{-3}$) and $k_m^*(o)$ and $k_m^*(g)$ the inherent Michaelis constants of oxygen and glucose ($mol m^{-3}$), respectively.

Therefore,

$$D_m \frac{d^2 c_g}{dx^2} = \frac{k_{cat}^* c_{GO} c_{ox} c_g}{k_m^*(o) c_g + k_m^*(g) c_{ox} + c_g c_{ox}} \quad (4)$$

and $z = (k_m^*(o) + c_{ox})y + k_m^*(g)c_{ox}$, so that

$$y'' = \frac{k_{cat}^* c_{GO} c_{ox}}{D_m} \frac{y}{z} \quad (5)$$

Further, while $z'' = (k_m^*(o) + c_{ox})y''$ and $y = \frac{z - k_m^*(g)c_{ox}}{k_m^*(o) + c_{ox}}$, it follows that

$$z'' = \frac{k_{cat}^* c_{GO} c_{ox}}{D_m} \left[\frac{z - k_m^*(g)c_{ox}}{z} \right] \quad (6)$$

and so

$$z' z'' = \frac{k_{cat}^* c_{GO} c_{ox}}{D_m} z' - \frac{k_{cat}^* c_{GO} c_{ox}^2 k_m^*(g)}{D_m} \frac{z'}{z} \quad (7)$$

Mathematically, this differential equation is best solved by using

$$\int z' z'' = \frac{1}{2} z'^2 + C \quad (8)$$

and so

$$\frac{1}{2} z'^2 = \frac{k_{cat}^* c_{GO} c_{ox}}{D_m} z - \frac{k_{cat}^* c_{GO} c_{ox}^2 k_m^*(g)}{D_m} \ln(z) - C \quad (9)$$

While $z' = (k_m^*(o) + c_{ox})y' = -\frac{k_m^*(o) + c_{ox}}{D_m} J$ it can be deduced that

$$\frac{1}{2} J^2 = \frac{D_m k_{cat}^* c_{GO} c_{ox}}{(k_m^*(o) + c_{ox})^2} *$$

$$\left((k_m^*(o) + c_{ox}) c_g + k_m^*(g) c_{ox} - k_m^*(g) c_{ox} \ln \frac{(k_m^*(o) + c_{ox}) c_g + k_m^*(g) c_{ox}}{(k_m^*(o) + c_{ox}) c_{g,0} + k_m^*(g) c_{ox}} \right) - C \quad (10)$$

The boundary conditions are:

$$x=0: \quad J=J_0 \quad \text{and} \quad c_g=c_{g,0}$$

$$x=\delta: \quad J=J_\delta \quad \text{and} \quad c_g=c_{g,\delta}$$

so that

$$\frac{1}{2} (J_0^2 - J_\delta^2) = \frac{D_m k_{cat}^* c_{GO} c_{ox}}{(k_m^*(o) + c_{ox})^2} *$$

$$\left[(k_m^*(o) + c_{ox})(c_{g,0} - c_{g,\delta}) + k_m^*(g) c_{ox} \ln \frac{(k_m^*(o) + c_{ox}) c_{g,\delta} + k_m^*(g) c_{ox}}{(k_m^*(o) + c_{ox}) c_{g,0} + k_m^*(g) c_{ox}} \right] \quad (11)$$

The enzyme concentration c_{GO} (mol m⁻³) is defined as $m_{GO}/(d_m A_m)$, with m_{GO} being the number of moles of enzyme in the membrane. Eqn. (11) now becomes

$$\frac{1}{2} (J_0^2 - J_\delta^2) = \frac{P_{eff} k_{cat}^* m_{GO} c_{ox}}{A_m (k_m^*(o) + c_{ox})^2} *$$

$$\left[(k_m^*(o) + c_{ox})(c_{g,0} - c_{g,\delta}) + k_m^*(g) c_{ox} \ln \frac{(k_m^*(o) + c_{ox}) c_{g,\delta} + k_m^*(g) c_{ox}}{(k_m^*(o) + c_{ox}) c_{g,0} + k_m^*(g) c_{ox}} \right] \quad (12)$$

with P_{eff} ($=D_{eff}/d_m = \alpha_g D_m/d_m$) being the effective permeability of glucose in the

membrane ($m\ s^{-1}$) and $k_{cat}^{**} = k_{cat}^*/\alpha_g$, where α_g is the partition coefficient of glucose.

So when J_0 and J_s are measured, for known values of $c_{g,0}$ and $c_{g,b}$, the kinetic parameters can be calculated. However, a few problems arise. The thickness of the wetted membrane, d_m , is not known. Further, $c_{g,0} \neq c_{g,A}$ and $c_{g,b} \neq c_{g,B}$. This means that the diffusional resistance of both the solution layer (stagnant diffusion layer and filter-paper) and the enzyme-containing membrane should be determined. Therefore, two extra experiments are necessary.

Diffusional resistance of solution layer

Fig. 4.2 shows the situation where only a diffusional resistance of solution layer is present. This means that the enzymatic membrane is absent.

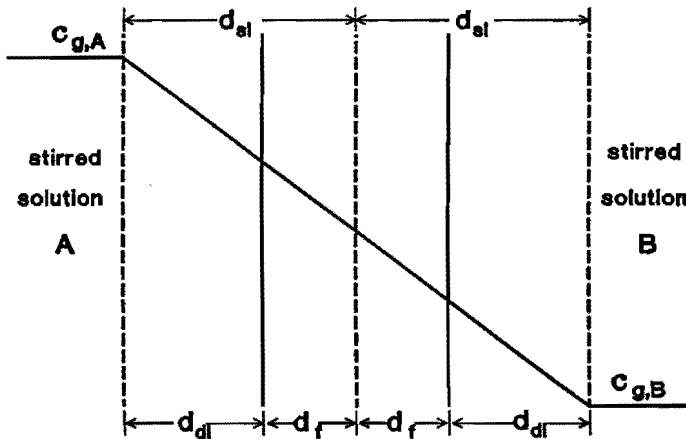


Figure 4.2: The concentration profile of glucose over a stagnant solution layer ($2d_{sl}$), which consists of two diffusion layers ($2d_{dl}$) and two filter-papers ($2d_f$).

Naturally, it is easy to deduce the following equation:

$$J_A = J_B = -D_{st} \frac{dc_g}{dx} = D_{st} \frac{c_{g,A} - c_{g,B}}{2d_{st}} \quad (13)$$

where J_A is the flux leaving compartment A and J_B the flux entering compartment B. The filter-papers are considered to behave like the stagnant diffusion layer, as stated before [10].

As $c_{g,A}$ and $c_{g,B}$ are chosen and the fluxes can be measured, D_{st}/d_{st} (i.e., the permeability of glucose through the solution layer) can be calculated.

In the case shown in Fig. 4.1 J_0 is equal to the flux through the solution layer adjacent to compartment A (J_A) and J_s is equal to the flux through the solution layer adjacent to compartment B (J_B). With the permeability (D_{st}/d_{st}) known, $c_{g,0}$ and $c_{g,s}$ can be calculated according to

$$\begin{aligned} J_A = J_0 &= \frac{D_{st}}{d_{st}}(c_{g,A} - c_{g,0}) \\ J_B = J_s &= \frac{D_{st}}{d_{st}}(c_{g,s} - c_{g,B}) \end{aligned} \quad (14)$$

Diffusional resistance of the membrane

To determine the diffusional resistance of the membrane, the same construction as shown in Fig. 4.1 can be used. Now, the compartments and the membrane are not saturated with oxygen, but with nitrogen. Enzymatic reaction is ruled out this way (see Fig. 4.3).

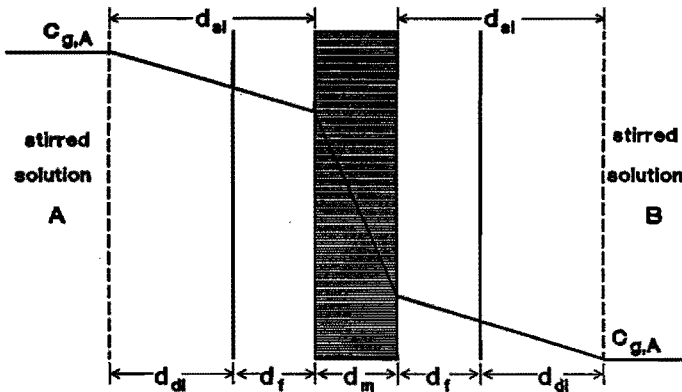


Figure 4.3: The concentration profile of glucose over a stagnant solution layer and a GO-containing membrane. Enzymatic reaction is eliminated by saturation with nitrogen.

The flux through the solution layer adjacent to compartment A (J_A), the flux through the membrane (J_m) and the flux through the solution layer adjacent to compartment B (J_B) are equal. The diffusional resistances of the three layers are in series. Therefore,

$$J_A = J_m = J_B = k(c_{g,A} - c_{g,B}) \quad (15)$$

with

$$\frac{1}{k} = \frac{d_{st}}{D_{st}} + \frac{d_m}{D_{eff}} + \frac{d_{st}}{D_{st}} \quad (16)$$

and k being the total permeability (total mass transfer coefficient) of glucose through the three layers ($m\ s^{-1}$). Furthermore, D_{eff} is the effective diffusion coefficient of glucose in the membrane ($D_{eff} = \alpha_g D_m$, with α_g being the partition coefficient of glucose). The flux can be measured, and as D_{st}/d_{st} is known, D_{eff}/d_m can be calculated.

The thickness of the enzyme-containing membrane is hard to determine. The one-

dimensional swelling factor is known to be 2.2 (Chapter 2, [10]), but also the surface area of the membrane will expand. As mounting the membrane between two filter-papers will prevent the expansion of the surface area, the membrane will fold itself. Therefore, it is hard to measure the exact thickness. However, the average thickness can be calculated, because D_{eff} is known (Chapter 2, [10]).

The relation between the inherent and the intrinsic kinetic parameters

Lastly, the relation between the inherent and the intrinsic parameters can be deduced. If partition coefficients are written explicitly, Eqn. (16) will change into

$$\frac{1}{2} \alpha_g^2 (J_0^2 - J_b^2) = \frac{P_m k_{\text{cat}} m_{\text{GO}} \alpha_{\text{ox}} c_{\text{ox}}}{A_m (k_m(o) + \alpha_{\text{ox}} c_{\text{ox}})^2} * \left[\alpha_g (k_m(o) + \alpha_{\text{ox}} c_{\text{ox}}) (c_{g,0} - c_{g,b}) + k_m(g) \alpha_{\text{ox}} c_{\text{ox}} \ln \frac{(k_m(o) + \alpha_{\text{ox}} c_{\text{ox}}) \alpha_g c_{g,b} + k_m(g) \alpha_{\text{ox}} c_{\text{ox}}}{(k_m(o) + \alpha_{\text{ox}} c_{\text{ox}}) \alpha_g c_{g,0} + k_m(g) \alpha_{\text{ox}} c_{\text{ox}}} \right] \quad (17)$$

with α_{ox} and α_g being the partition coefficients of oxygen and glucose, respectively, and $P_m (=D_m/d_m)$ the permeability of glucose in the membrane (m s^{-1}).

From Eqn. (17) it can be deduced that

$$\begin{aligned} k_{\text{cat}}^* &= \frac{k_{\text{cat}}}{\alpha_g} \\ k_{\text{cat}}^{**} &= \frac{k_{\text{cat}}}{\alpha_g^2} \\ k_m^*(o) &= \frac{k_m(o)}{\alpha_{\text{ox}}} \\ k_m^*(g) &= \frac{k_m(g)}{\alpha_g} \end{aligned} \quad (18)$$

If the partition coefficients are known, the intrinsic kinetic parameters are easily calculated from the inherent ones, and they can be compared with the intrinsic parameters of the soluble enzyme.

If the enzyme content (m_{GO}) is not known, Eqn. (16) must be written as

$$\frac{1}{2}(J_0^2 - J_s^2) = \frac{D_{eff} V_{max}^{**} c_{ox}}{(k_m^*(o) + c_{ox})^2} * \left[(k_m^*(o) + c_{ox})(c_{g,0} - c_{g,s}) + k_m^*(g)c_{ox} \ln \frac{(k_m^*(o) + c_{ox})c_{g,s} + k_m^*(g)c_{ox}}{(k_m^*(o) + c_{ox})c_{g,0} + k_m^*(g)c_{ox}} \right] \quad (19)$$

so that V_{max}^{**} ($= k_{cat}^{**} c_{GO}$) is determined.

4.3 Experimental

Reagents

Glucose oxidase from *Aspergillus niger* (E.C. 1.1.3.4, M=150000, lyophil, GO/catalase min 2000) was purchased from Serva. Phosphate-buffered saline (PBS) was prepared with $NaH_2PO_4 \cdot 2H_2O$, $Na_2HPO_4 \cdot 2H_2O$ and NaCl purchased from Merck. D-glucose was obtained from Janssen Chimica.

The enzymatic membrane was made of polyvinyl alcohol (PVA) from Denka Poval (B24) and cross-linked with glutaraldehyde (25%, w/w, aqueous solution, Merck) and the photosensitive DTS-18 (polyazonium salt from PCAS, Longjumeau, France). The Mowiol PVA was obtained from Hoechst (04/M1).

Glucose detection was performed with a Sigma glucose kit (No. 635), based on the reaction of glucose with *o*-toluidine, which yields a blue-green complex.

All solutions were prepared with demineralized, distilled water.

Preparation of the enzyme-containing membrane

A 10-g amount of PVA was slowly added to 90 cm³ of demineralized water and stirred. The solution was heated for 1.5 h at 80 °C until all the PVA had dissolved and a homogenous solution was obtained. The solution was cooled to room temperature. Just before the spinning procedure, 0.20 g (0.2%, w/w) of DTS-18, 0.40 g of 25% (w/w) aqueous glutardialdehyde and 1 ml of a 12.8 mg/ml GO-solution were added. With a pipette an aliquot of the resulting solution was placed on the required surface (glass plate covered with a 30% Mowiol PVA gel layer). After spinning for 5 s at 1000 rpm and for 25 s at 3000 rpm, the gel layer was dried in a vacuum pump. The spinning and drying procedure was repeated until enough layers had been spun on the surface. Thereafter the gel layer was irradiated with UV radiation at room temperature for 90 s. The gel layer was developed in demineralized water for 2 min and unreacted reactants were washed away. Finally, the gel layer was dried and cross-linked by glutardialdehyde for at least 24 hours at 4 °C.

The thickness of the gel layer on the glass plates was measured with a roughness meter, connected with a thermograph. The thickness of a swollen gel layer (after contact with an aqueous solution) could also be measured with this technique.

To loosen the membranes from the glass plates, the plates were immersed in demineralized, distilled water for at least 8 h to solve the Mowiol PVA layer. After drying the membrane, it was easily torn off the glass plate.

Preparation of the glucose solutions

Glucose-containing PBS was prepared by adding the appropriate amount of glucose to 9.22 g NaCl (0.16 mol), 17.8 g Na₂HPO₄·12H₂O (0.050 mol) and 8.00 g NaH₂PO₄·2H₂O (0.050 mol), and diluting to 1000 ml with distilled, demineralized water. The pH was adjusted to 7.0 with 4 M NaOH. The glucose solutions were allowed to mutarotate for at least 3 h before usage.

Diffusion cell experiments

Between two double-walled glass compartments a GO-containing membrane (13.2 cm²) was placed with a filter-paper (Rotband, Schleicher & Schüll) on each side for solidity purposes. Compartments A and B were filled with oxygen, oxygen/nitrogen or nitrogen-saturated glucose solutions (100 ml each). The glucose concentration in compartment A was always higher than that in compartment B. The compartments themselves were saturated before pouring in the glucose solutions. The gas inlet was placed in front of the membrane, to minimize the thickness of the stagnant solution layer. Further, a magnetic stirrer was used to create a uniform glucose concentration in the bulk solution. During several hours, samples were taken from both compartments. The samples were measured with a glucose kit and visible spectrophotometry (LKB Biochrom Ultraspec II, type 4050). A glucose concentration versus time plot was made, and the pseudo-steady-state region was used to calculate J_A and J_B . During the measurements, the temperature was maintained at 25 °C via water circulation through the double-walled compartments, using a Colora NB-32981 water-bath.

4.4 Results and discussion

Diffusional resistance of the solution layer

The glucose concentration as a function of time in both compartments for an experiment as shown in Fig. 4.2 is presented in Fig. 4.4.

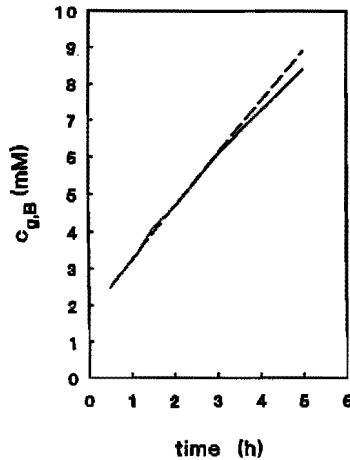


Figure 4.4: The glucose concentration in compartment B of the diffusion cell as a function of time in the case that only two filter-papers were mounted between the two compartments.

From the initial slope (h_B) of the curve the flux can be calculated:

$$J_B = \frac{V}{A_m} h_B \quad (20)$$

where V is the volume of a compartment (m^3) and A_m is the geometric surface area of the membrane (m^2).

With the use of Eqn. (20), the flux J_B is calculated to be $2.9 \cdot 10^{-5} \text{ mol m}^{-2} \text{ s}^{-1}$. As $c_{g,A} - c_{g,B}$ is equal to 100 mol m^{-3} , and the decrease in concentration difference is neglected, the diffusional resistance of both the solution layers ($2d_s/D_s$) is calculated to be $3.4 \cdot 10^6 \text{ s m}^{-1}$. Although the glucose concentration in the solution layer adjacent to compartment A is higher than that in the solution layer adjacent to compartment B, the diffusional resistance of both solution layers can be considered equal, because the experiments were carried out with glucose concentrations $\leq 100 \text{ mol m}^{-3}$.

Diffusional resistance of the membrane

The results of experiments as shown in Fig. 4.3 are presented in Fig. 4.5.

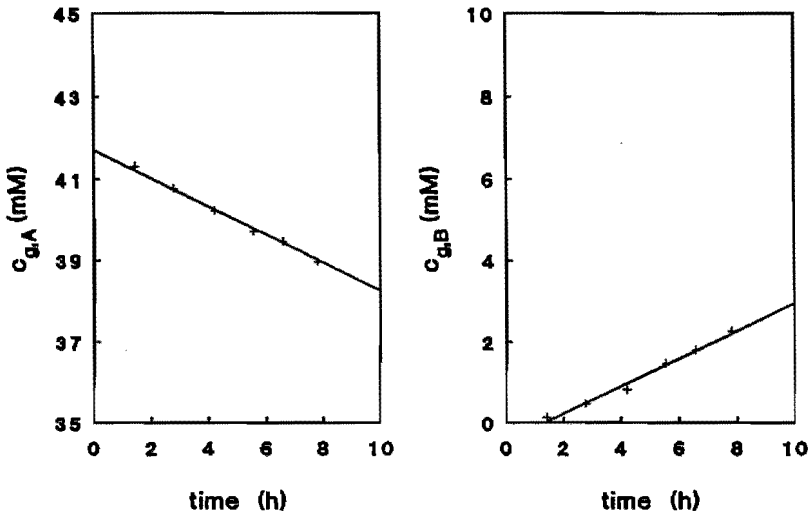


Figure 4.5: The glucose concentration in compartment A (left) and in compartment B (right) as a function of time in the case that a GO-containing membrane with a filter-paper on each side was mounted between the two compartments. Enzymatic reaction was prevented by nitrogen-saturation.

As only diffusion, and no reaction, takes place, the flux leaving compartment A (J_A) should be equal to the flux entering compartment B (J_B). The fact that this is indeed observed in the experiments ($J_A=0.73 \cdot 10^{-5} \text{ mol m}^{-2} \text{ s}^{-1}$ and $J_B=0.71 \cdot 10^{-5} \text{ mol m}^{-2} \text{ s}^{-1}$), means that saturation of both the compartments and the membrane with nitrogen is sufficient to prevent enzymatic reaction in the membrane. The flux has a

value of $0.72 \cdot 10^{-5} \text{ mol m}^{-2} \text{ s}^{-1}$, which means that, with $c_{g,A} - c_{g,B} = 40 \text{ mol m}^{-3}$, the total diffusional resistance ($1/k$) is equal to $5.6 \cdot 10^6 \text{ s m}^{-1}$. Subtracting the diffusional resistance of both the solution layers yields the diffusional resistance of the GO-containing membrane ($d_m/D_{\text{eff}} = 2.2 \cdot 10^6 \text{ s m}^{-1}$). As the diffusion coefficient of glucose in the membrane is known to be $0.047 \cdot 10^{-9} \text{ m}^2 \text{ s}^{-1}$ (Chapter 2, [10]) the, actually effective, thickness of the membrane is calculated to be $1.0 \cdot 10^{-4} \text{ m}$.

Kinetic parameters of immobilized enzyme

A number of diffusion cell experiments were carried out in order to determine the kinetic parameters of immobilized GO. Table 4.1 shows the average results for each of these experiments. An example of an accompanying plot is presented in Fig. 4.6. With the help of Eqn. (14), $c_{g,0}$ and $c_{g,\delta}$ were calculated, using the values of J_0 and J_δ .

To determine the kinetic parameters, the values of J_0 , J_δ , $c_{g,0}$ and $c_{g,\delta}$ have to be inserted in Eqn. (19). However, it is difficult to abstract $k_m^*(o)$, $k_m^*(g)$ and V_{max}^{**} from this rather complicated equation. Therefore, a computer program was written, which calculates two independent parameters. Eqn. (19) has to be rewritten as follows

$$J_0^2 - J_\delta^2 = 2D_{\text{eff}} \left[\frac{1}{a^*} (c_{g,0} - c_{g,\delta}) - \frac{b^*}{(a^*)^2} \ln \left[\frac{b^* + a^* c_{g,0}}{b^* + a^* c_{g,\delta}} \right] \right] \quad (21)$$

where $a^* = \frac{k_m^*(o) + c_{ox}}{V_{\text{max}}^{**} c_{ox}}$ and $b^* = \frac{k_m^*(g)}{V_{\text{max}}^{**}}$

The inherent kinetic parameters of immobilized glucose oxidase

The computer program (Appendix I) works with a least squares method, using the procedure Miniquad [11].

Table 4.1: Results for various diffusion cell experiments with an enzymatically active membrane.

$c_{g,A}$ (mM)	$c_{g,B}$ (mM)	c_{ox} (mM)	$J_0 \cdot 10^5$ (mol m ⁻² s ⁻¹)	$J_d \cdot 10^5$ (mol m ⁻² s ⁻¹)	$c_{g,0}$ (mM)	$c_{g,s}$ (mM)
20	0	1.05	0.55	0.26	10.3	4.5
20	0	0.22	0.53	0.22	10.6	3.8
40	0	1.05	0.96	0.41	23.1	7.2
40	0	0.22	1.01	0.35	22.2	6.2
100	0	1.05	2.28	1.56	60.0	27.5
100	0	0.22	2.48	2.17	56.3	38.2

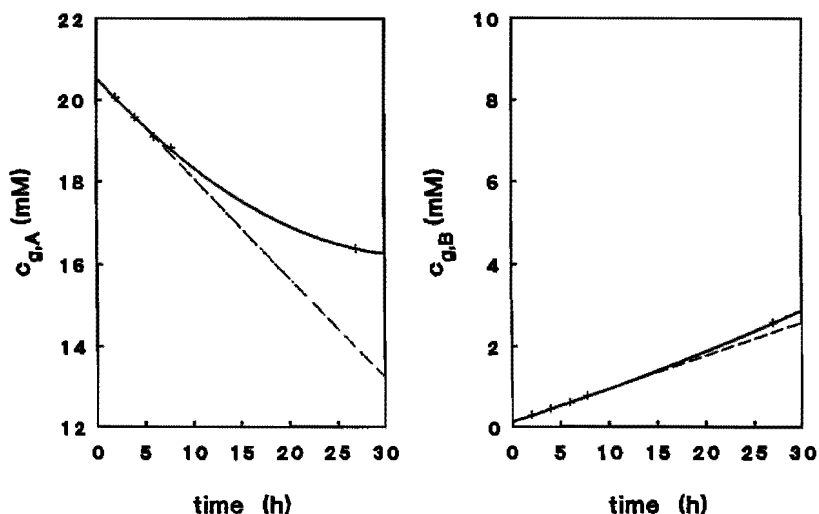


Figure 4.6: The glucose concentration in compartment A (left) and in compartment B (right) as a function of time in the case that a GO-containing membrane with a filter-paper on each side was mounted between the two compartments. Simultaneous diffusion and enzymatic reaction was obtained by saturation with pure oxygen.

From Table 4.1 it becomes clear that the oxygen concentration has a non-significant influence on the kinetics. This means that $k_m^*(o) \ll c_{ox}$ (for $c_{ox} \geq 0.22 \text{ mol m}^{-3}$), so that a^* is equal to $1/V_{max}^{**}$

The program calculates a^* to be $7.4 \text{ m}^3 \text{ s mol}^{-1}$, and b^* to be $1.6 \cdot 10^2 \text{ s}$. V_{max}^{**} can now be calculated as $0.14 \text{ mol m}^{-3} \text{ s}^{-1}$, and $k_m^*(g)$ as 22 mol m^{-3} . To compare k_{cat}^{**} of immobilized GO with k_{cat} of soluble GO, the concentration of GO in the gel should be known. As this value is difficult to obtain, an estimation is made. The assumption is made that the weight fraction of GO in a dry enzyme-containing

The inherent kinetic parameters of immobilized glucose oxidase

membrane is equal to that of the original gel solution, used for the membrane preparation. The weight fraction of GO was 0.00495. From the diffusion experiment (*vide supra*), d_m was calculated as $1.0 \cdot 10^{-4}$ m. The membrane, with a surface area, A_m , of $13.2 \cdot 10^{-4}$ m², weighs about 95 mg. This value has been determined before usage of the membrane, but after thoroughly rinsing it. As the molecular weight of the enzyme is known to be 150,000 g mol⁻¹, the concentration of enzyme in the membrane is calculated as 0.024 mol m⁻³. This is only valid for the situation that no enzyme has leaked out during rinsing the membrane, or, when it has, to the same extent as the other components present in the membrane. For this condition, k_{cat}^{**} is calculated as 6 s⁻¹. When GO has leaked out of the membrane k_{cat}^{**} will be ≥ 6 s⁻¹. In Table 4.2, the inherent kinetic parameters of immobilized GO and the intrinsic parameters of soluble GO are compared.

Table 4.2: The kinetic parameters for both soluble and immobilized GO.

unity	soluble		immobilized	
	parameter	value	parameter	value
mol m ⁻³	$k_m(o)$	0.80	$k_m^*(o)$	$\ll 0.22$
mol m ⁻³	$k_m(g)$	70	$k_m^*(g)$	22
s ⁻¹	k_{cat}	935	k_{cat}^{**}	≥ 6

The results of the determination of the kinetics of immobilized GO should be considered as preliminary. The method leaves room for improvements. The diffusional resistance of the solution layer is much too high as compared with the resistance of the membrane. This causes an inaccuracy in the calculation of the diffusional resistance of the membrane. The resistance of the solution layer could be

lowered by better stirring in the neighbourhood of the membrane, e.g., by an axial instead of a vertical gas inlet. Of course, the diffusional resistance of the solution as determined by an experiment with only two filter-papers placed between the two compartments, need not be the same as this resistance when a GO-containing membrane is placed between the filter-papers. Some interactions between the membrane and the filter-papers could take place. Usage of a hydrophilic membrane (e.g., cellulose acetate) instead of the filter-papers might give better results.

Although V_{\max}^{**} can be used for calculations with the sensor simulation program, a knowledge of k_{cat}^{**} is important because k_{cat}^{**} reflects the activity of the enzyme. Therefore, it is important to find a method to determine the concentration of GO in the membrane. Fortunately, this concentration is equal for membranes made on different days, and this makes V_{\max}^{**} reproducible for various membranes (prepared according to the same prescription).

Furthermore, $k_m^*(o)$ is negligible for oxygen concentration $\geq 0.22 \text{ mol m}^{-3}$. In the sensor, however, lower oxygen concentrations will occur, especially in the reaction zone. Therefore, experiments with lower oxygen tensions should be carried out.

In addition, a remark should be made on the meaning of the determined inherent kinetic parameters. Of course, these parameters do not strictly belong to covalently bound GO. In the membrane, most likely also adsorbed or completely inactive, denaturated GO is present. It is better to say that the determined kinetic parameters belong to GO immobilized in the specific membrane as described in this chapter.

Acknowledgment

I wish to acknowledge drs. A.J. Geurts and H. Willemsen from the Eindhoven University of Technology for their help to write the Miniquad-containing computer program.

References

1. J.F. Kennedy and J.M.S. Cabral, Enzyme Immobilization, in H.-J. Rehm and G. Reed (eds.), *Biotechnology, Enzyme Technology*, Vol. 7a, VCH, Weinheim, FRG, (1987), 347-404.
2. P.W. Carr and L.D. Bowers, Immobilized Enzymes in Analytical and Clinical Chemistry, Fundamentals and Applications, *Chemical Analysis*, Vol. 56, John Wiley & Sons, New York, (1980), 148-196.
3. J.-M. Engasser and C. Horvath, Diffusion and Kinetics with Immobilized Enzymes, in L.B. Wingard jr., E. Katchalski-Katzir and L. Goldstein (eds.), *Applied Biochemistry and Bioengineering*, Vol. 1, Academic Press, New York, (1976), 127-220.
4. J.A. DeSimone and S.R. Caplan, *Biochemistry*, 12 (1973) 3032-3038.
5. E. Sélégnny, G. Broun, J. Geffroy and D. Thomas, *J. Chim. Phys. et Physico-Chimie Biol.*, 66 (1969) 391-392.
6. E. Sélégnny, G. Broun and D. Thomas, *C.R. Acad. Sci. Paris*, 269 (Série D) (1969) 1330-1333.
7. E. Sélégnny, G. Broun and D. Thomas, *Physiol. Vég.*, 9 (1) (1971) 25-50.
8. Q.H. Gibson, B.E.P. Swoboda and J. Massey, *J. Biol. Chem.*, 239 (1964) 3927.
9. C. Walsh, *Enzymatic Reaction Mechanisms*, W.H. Freeman and Company, San Francisco, (1979), 220-224.
10. S.A.M. van Stroe-Biezen, F.M. Everaerts, L.J.J. Janssen and R.A. Tacken, *Anal. Chim. Acta*, 273 (1993) 553.
(This thesis, Chapter 2).
11. "Rekencentrum" of the Eindhoven University of Technology, PP-5.3, Non-linear regression without restrictions, TUE-RC 68438, (1989).

CHAPTER 5. TESTING THE PERFORMANCE OF A MACRO GLUCOSE SENSOR

5.1 The sensor simulation program

Whether the sensor provides the expected concentration profiles as roughly shown in Fig. 5.1, can be verified with the help of a simulation program. In addition, the influence of the diffusion coefficients and the kinetic parameters can be studied. The principle of the sensor includes a constant production rate of oxygen at the oxygen electrode. However, for experimental simplicity purposes, the simulation program uses a boundary condition of a constant oxygen concentration at the oxygen electrode. This boundary condition is easily changed into the original boundary condition (constant production rate of oxygen).

The structure of the computer simulation program is now described for the calculation of the oxygen concentration profiles. The procedure for glucose, hydrogen peroxide and gluconolactone is inherent to that of oxygen.

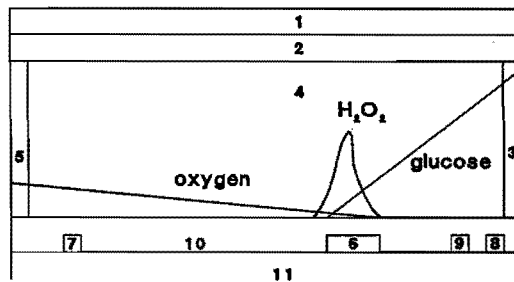


Figure 5.1: Expected concentration profiles of oxygen, glucose and hydrogen peroxide in the GO-containing hydrogel layer of the glucose sensor.

The simulation program is dealing with the concentration profiles for the instationary state:

$$\frac{\delta a}{\delta t} = D_a \frac{\delta^2 a}{\delta x^2} - v_0 \quad (1)$$

$$\frac{\delta b}{\delta t} = D_b \frac{\delta^2 b}{\delta x^2} - v_0 \quad (2)$$

$$\frac{\delta c}{\delta t} = D_c \frac{\delta^2 c}{\delta x^2} + v_0 \quad (3)$$

$$\frac{\delta d}{\delta t} = D_d \frac{\delta^2 d}{\delta x^2} + v_0 \quad (4)$$

where a, b, c en d denote the concentration (mol m⁻³) of oxygen, glucose hydrogen peroxide and gluconolactone, respectively. D is the diffusion coefficient (m² s⁻¹) and v₀ is the reaction velocity of the enzyme reaction (mol m⁻³ s⁻¹).

To describe the differential equation, the Crank-Nicolson formalism is used [1]. This formalism makes a discretion by placing a quadratic curve through three points,

$$\begin{aligned} a_{i,j} &= Ax_i^2 + Bx_i + C \\ a_{i-1,j} &= A(x_i - \delta)^2 + B(x_i - \delta) + C \\ a_{i+1,j} &= A(x_i + \delta)^2 + B(x_i + \delta) + C \end{aligned} \quad (5)$$

where the subscripts i and j denote a place and time index, respectively. Furthermore, $\delta = x_1$ (m) and $x_i = i * \delta$ (m).

From Eqn. (5) it follows that

$$2A = \frac{a_{i-1,j} + a_{i+1,j} - 2a_{i,j}}{\delta^2} = \frac{\delta^2 a_{i,j}}{\delta x^2} \quad (6)$$

This means that in the sensor,

$$\begin{aligned} \frac{a_{i,j+1} - a_{i,j}}{\delta t} = \frac{1}{2} D_s \left[\frac{a_{i-1,j} + a_{i+1,j} - 2a_{i,j}}{\delta x^2} + \frac{a_{i-1,j+1} + a_{i+1,j+1} - 2a_{i,j+1}}{\delta x^2} \right] \\ - \frac{V_{\max} \left[\frac{a_{i,j} + a_{i,j+1}}{2} \right] \left[\frac{b_{i,j} + b_{i,j+1}}{2} \right]}{k_m(o) \left[\frac{b_{i,j} + b_{i,j+1}}{2} \right] + k_m(g) \left[\frac{a_{i,j} + a_{i,j+1}}{2} \right]} \end{aligned} \quad (7)$$

where $k_m(o)$ and $k_m(g)$ are the Michaelis constants of oxygen and glucose, respectively, and V_{\max} is the maximal reaction velocity.

Eqn. (7) can also be written as

$$\begin{aligned} a_{i+1,j+1} + a_{i-1,j+1} - a_{i,j+1} \left[\frac{1}{\alpha_s} + 2 + \frac{\beta_1(b_{i,j} + b_{i,j+1})}{\alpha_s(\beta_2(b_{i,j} + b_{i,j+1}) + \beta_3(a_{i,j} + a_{i,j+1}))} \right] \\ = -a_{i+1,j} - a_{i-1,j} + a_{i,j} \left[-\frac{1}{\alpha_s} + 2 + \frac{\beta_1(b_{i,j} + b_{i,j+1})}{\alpha_s(\beta_2(b_{i,j} + b_{i,j+1}) + \beta_3(a_{i,j} + a_{i,j+1}))} \right] \end{aligned} \quad (8)$$

where

$$\alpha_a = \frac{D_a \delta t}{2 \delta x^2} \quad \beta_2 = \frac{k_m(o)}{2} \quad (9)$$

$$\beta_1 = \frac{V_{max} \delta t}{4} \quad \beta_3 = \frac{k_m(g)}{2}$$

Eqn. (8) can be simplified as follows

$$\begin{aligned} & - \text{conc1A}[i-1] + hA[i] \text{conc1A}[i] - \text{conc1A}[i+1] \\ & = \text{conc2A}[i-1] - h[i] \text{conc2A}[i] + \text{conc2A}[i+1] \end{aligned} \quad (10)$$

with $\text{conc1A}[i]$ and $\text{conc2A}[i]$ denoting the concentration of oxygen at $j=j$ and $j=j+1$ ($a_{i,j}$ and $a_{i,j+1}$), respectively, and

$$hA[i] = - \frac{1}{\alpha_a} + 2 + \frac{\beta_1(b_{i,j} + b_{i,j+1})}{\alpha_a (\beta_2(b_{i,j} + b_{i,j+1}) + \beta_3(a_{i,j} + a_{i,j+1}))} \quad (11)$$

$$h[i] = \frac{1}{\alpha_a} + 2 + \frac{\beta_1(b_{i,j} + b_{i,j+1})}{\alpha_a (\beta_2(b_{i,j} + b_{i,j+1}) + \beta_3(a_{i,j} + a_{i,j+1}))} \quad (12)$$

In the main program, $PA[i]$ is calculated:

$$- \text{conc1A}[i-1] + hA[1] \text{conc1A}[i] - \text{conc1A}[i+1] = PA[i] \quad (13)$$

The boundary conditions used are

At $x=0$ and $t \geq 0$, $a_{0,j} = \text{ANULL}$

At $x=N$ and $t \geq 0$, $da/dt=0$

Further, to calculate the concentration of oxygen at $j=2$, the timestep procedure is used. Therefore $\text{conc2A}[i]$ has to be written explicitly:

* According to Eqn. (5):

$$\begin{aligned} \text{conc2A}[N] &= A(N)^2 + B(N) + C \\ \text{conc2A}[N-1] &= A(N-\delta)^2 + B(N-\delta) + C \\ \text{conc2A}[N-2] &= A(N-2\delta)^2 + B(N-2\delta) + C \end{aligned} \quad (14)$$

It can be deduced that:

$$\text{conc2A}[N-2] - 4\text{conc2A}[N-1] + 3\text{conc2A}[N] = \left[\frac{d\text{conc2A}[i]}{dx} \right]_{x=N} = 0 \quad (15)$$

Therefore,

$$\text{conc2A}[N] = \frac{4}{3}\text{conc2A}[N-1] - \frac{1}{3}\text{conc2A}[N-2] \quad (16)$$

* According to Eqns. (10) and (13)

$$\text{conc2A}[N] - h[N-1]\text{conc2A}[N-1] + \text{conc2A}[N-2] = \text{PA}[N-1] \quad (17)$$

Combining Eqns. (16) and (17) gives

$$\text{conc2A}[N-1] = -AX[N-1] \left(\text{PA}'[N-1] - \frac{2}{3}\text{conc2A}[N-2] \right) \quad (18)$$

$$\text{with } AX[N-1] = \frac{1}{\left(h[N-1] - \frac{4}{3} \right)} \text{ and } \text{PA}'[N-1] = \text{PA}[N-1] - \text{PA}[N]$$

* Again, according to Eqns. (10) and (13)

$$\text{conc2A}[N-1] - h[N-2]\text{conc2A}[N-2] + \text{conc2A}[N-3] = \text{PA}[N-2] \quad (19)$$

Combining Eqns. (18) and (19) gives

$$\text{conc2A}[N-2] = -AX[N-2] \left(\text{PA}'[N-2] - \text{conc2A}[N-3] \right) \quad (20)$$

$$\text{with } AX[N-2] = \frac{1}{h[N-2] - \frac{2}{3}AX[N-1]}$$

$$\text{and } \text{PA}'[N-2] = \text{PA}[N-2] + AX[N-1]\text{PA}'[N-1]$$

* According to Eqns. (10) and (13)

$$\text{conc2A}[N-2] - h[N-3]\text{conc2A}[N-3] + \text{conc2A}[N-4] = \text{PA}[N-3] \quad (21)$$

From the combination of Eqns. (20) and (21) it follows that

$$\text{conc2A}[N-3] = -AX[N-3](\text{PA}'[N-3] - \text{conc2A}[N-4]) \quad (22)$$

$$\text{where } AX[N-3] = \frac{1}{h[N-3] - AX[N-2]}$$

$$\text{and } \text{PA}'[N-3] = \text{PA}[N-3] + AX[N-2]\text{PA}'[N-2]$$

The main program starts with calculating $\text{PA}[i]$ with the concentrations on $j=j$ ($\text{conc1A}[i]$), according to Eqn. (13). After calculation of $h[i]$, the timestep procedure is started. Here, after calculation of $AX[i]$ and $\text{PA}'[i]$, the concentrations on $j=j+1$ are calculated ($\text{conc2A}[i]$).

According to Eqn. (12), $h[i]$ is calculated using both $\text{conc1A}[i]$ and $\text{conc2A}[i]$. As $\text{conc2A}[i]$ is not known yet ($h[i]$ is calculated before the timestep procedure, $\text{conc2A}[i]$ is calculated in the timestep procedure), the value of $\text{conc1A}[i]$ is used for $\text{conc2A}[i]$. After the first timestep cycle, the value of $h[i]$ is recalculated, using the $\text{conc2A}[i]$ from the first cycle. Thereafter, the second timestep cycle is started. These cycles are repeated until the difference between the calculated $\text{conc2A}[i]$ and the $\text{conc2A}[i]$ from the former cycle as well as the difference between the calculated $\text{conc2A}[i]$ and that of two cycles before is negligible:

$$\begin{aligned} |\text{sum1} - \text{sum2}| &< 10^{-10} * \text{sum1} \\ |\text{sum1} - \text{sum3}| &< 10^{-10} * \text{sum1} \end{aligned} \quad (23)$$

where

$$\begin{aligned} \text{sum1} &= \sum_{i=0}^N (\text{conc1A}[i] - \text{conc2A}[i])^2 && (\text{cycle } j=j) \\ \text{sum2} &= \sum_{i=0}^N (\text{conc1A}[i] - \text{conc2A}[i])^2 && (\text{cycle } j=j+1) \\ \text{sum3} &= \sum_{i=0}^N (\text{conc1A}[i] - \text{conc2A}[i])^2 && (\text{cycle } j=j+2) \end{aligned} \quad (24)$$

When Eqn. (23) is obeyed, $\text{conc1A}[i]$ takes over the value of $\text{conc2A}[i]$, and for $j=j+2$ the whole procedure starts again.

All calculations are sent to a Lotusfile via the "Dump" procedure. With this Lotusfile a plot of the concentrations can be made.

The sensor simulation program is shown in Appendix II.

5.2 Calculations with the sensor simulation program

An example of a calculation with the sensor simulation program is shown in Fig. 5.2. Here, the values of the diffusion coefficients of oxygen, glucose, hydrogen peroxide and gluconolactone as determined in Chapter 2 are used. The kinetic parameters of immobilized GO as determined in Chapter 4 are inserted in the simulation program. As $k_m^*(o)$ is not exactly known, a range of values is inserted ($0.0001 \text{ mol m}^{-3} < k_m^*(o) < 0.02 \text{ mol m}^{-3}$), but this variation has no influence on the calculated concentration profiles. The total length of the sensor is chosen to be $3 \cdot 10^{-3} \text{ m}$ and the total time is six hours. At this time, the concentration profiles of glucose and oxygen are virtually stationary, whereas the concentrations of hydrogen peroxide and gluconolactone are, of course, still increasing with time. The boundary conditions are: $c_{ox} = 0.5 \text{ mol m}^{-3}$ at $i=0$, and $c_g = 5 \text{ mol m}^{-3}$ at $i=N$ ($i=20$).

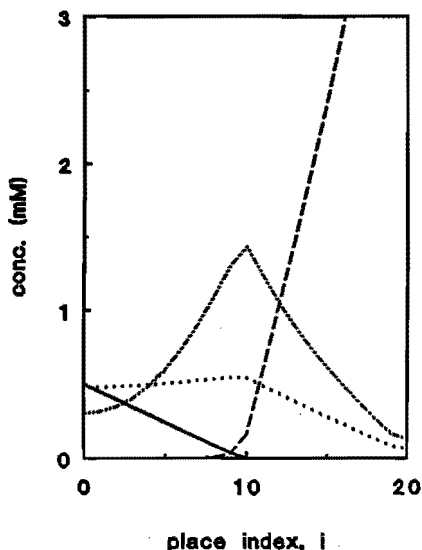


Figure 5.2: Example of a calculation with the sensor simulation program. Concentration profiles of oxygen (—), glucose (----), hydrogen peroxide (.....) and gluconolactone (-·-·-·-).

In Fig. 5.2 only a small peak in the concentration profile of hydrogen peroxide is observed. This is due to the fact that the diffusion coefficient of hydrogen peroxide is relatively high. Gluconolactone, with its much lower diffusion coefficient, shows much more of a peak in the concentration profile. The mentioned diffusional effect of hydrogen peroxide is of course eliminated in an operational sensor, because here the hydrogen peroxide is detected at an electrode before it can diffuse away.

It takes quite a long time before a pseudo-steady state for glucose and oxygen is reached. This is mainly a start up problem, as the sensor is completely deprived of oxygen and glucose. Once a steady state has established, the establishment of a new steady state after a change in the glucose boundary condition, will not take up such a

long time.

To diminish the time to reach a steady state, one could adapt the total length of the sensor. However, if the total length is chosen to be $1 \cdot 10^{-3}$ m instead of $3 \cdot 10^{-3}$ m, while leaving all other parameters unchanged (see Fig. 5.2), the whole sensor gets saturated with glucose. This is due to the fact that the diffusional supply on glucose is larger than the reactional discharge. An increase in the oxygen supply could solve the problem, but of course the dissolved oxygen concentration in the GO-containing hydrogel layer is limited to its saturation concentration, viz., about 1 mol m^{-3} . Production of oxygen bubbles in the sensor has to be prevented. In the example shown in Fig. 5.2, the ratio of the glucose concentration at $i=20$ and the oxygen concentration at $i=0$ is 10. Lowering this ratio could be performed e.g., by adding an extra diffusional resistance for glucose, before glucose enters the GO-containing layer. This diminishes the glucose concentration at $i=20$, whereas the glucose concentration in the test solution (e.g., blood) remains the same. Another possibility is to increase the activity of GO.

Calculations show that a decrease in both the total length of the sensor and the ratio of the initial concentrations of glucose ($i=20$) and oxygen ($i=0$) significantly lowers the duration of steady state establishment, whereas an increase in the activity of GO has no effect.

For example, for a sensor with a total length of $3 \cdot 10^{-3}$ m and a glucose/oxygen concentration ratio of 10 (Fig. 5.2), it takes six hours before a steady state is reached. A sensor of $3 \cdot 10^{-3}$ m with a concentration ratio of 5 needs three hours to reach a steady state and a sensor of $1 \cdot 10^{-3}$ m with a concentration ratio of 5 needs only one hour.

When the activity of GO becomes a hundred-fold higher, the production rate of hydrogen peroxide only increases with 17%.

If a sensor is required that responds within 10 min, the optimal design implies a total sensor length of $8 \cdot 10^{-4}$ m and a ratio of initial glucose and oxygen concentration of 2.5. As the maximal oxygen concentration in the gel layer is about

1 mol m^{-3} , the maximal glucose concentration at $i=20$ is 2.5 mol m^{-3} . This means that the glucose concentration range that can be determined with this design would be limited to $0\text{-}2.5 \text{ mol m}^{-3}$, unless an extra diffusional resistance is applied. This diffusional resistance, consequently, increases the response time, but this effect can be minimized.

The flux entering the GO-containing layer of the sensor is equal to that through the extra diffusional resistance layer. With the appropriate concentration drop over this layer (with a thickness d_r), the required diffusional resistance (D_r/d_r) can be calculated. The time it takes to reach the required concentration profile is equal to $d_r^2/\pi D$ (penetration theory, [2]). Hence, d_r is optional, D_r/d_r is not. For example, in the case mentioned (total sensor length is $8 \cdot 10^{-4} \text{ m}$ and the glucose-oxygen concentration ratio is 2.5) the flux entering the sensor under pseudo-steady-state conditions is $2.6 \cdot 10^{-7} \text{ m}^2 \text{ s}^{-1}$. To design a sensor that is able to detect glucose concentrations in a test solution (e.g., blood) up to 20 mol m^{-3} , the concentration drop over the diffusional resistance layer is 17.5 mol m^{-3} . To reach this concentration drop, the diffusion coefficient of glucose in the layer has to be $3.2 \cdot 10^{-13} \text{ m}^2 \text{ s}^{-1}$, in the case that d_r is chosen to be $1 \cdot 10^{-5} \text{ m}$. This means that the establishment of a steady concentration profile over the resistance layer will take about 2 min. When d_r is chosen to be $1 \cdot 10^{-6} \text{ m}$, the diffusion coefficient of glucose in the layer has to be $3.2 \cdot 10^{-14} \text{ m}^2 \text{ s}^{-1}$, and the establishment of the concentration profile over the layer will only take up 0.2 min.

5.3 Macro-sensor experiments

5.3.1 Introduction

To verify the calculations shown in paragraph 5.2, macro-sensor experiments have to be performed. For this purpose a Si wafer with a SiO_2 layer is used, which contains an array of ten Pt electrodes (Fig. 5.3a). The surface area is covered with a

GO-containing gel layer and the whole sensor is placed in an "envelope" of perspex (Fig. 5.3b). In this way, only from the left ($i=0$) and the right side ($i=N$), species can enter the gel layer of the sensor.

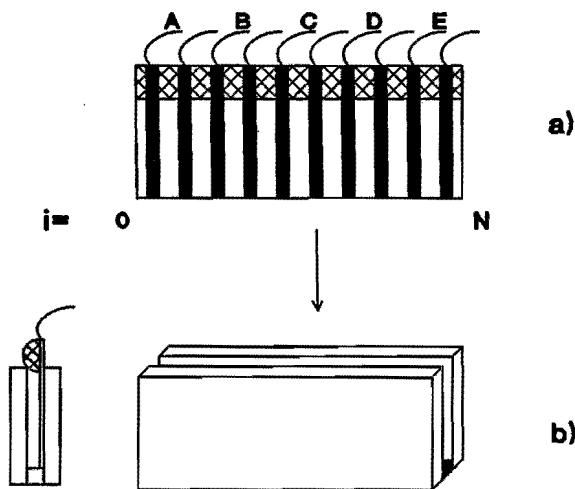


Figure 5.3: Configuration of macro-sensor (a) and perspex envelope (side-view and front view) (b). In the figure, platinum electrodes are drawn black and the epoxy resin is drawn in a checked pattern. The place index i (vide supra) is zero at the left side of the sensor and N at the right side of the sensor.

When one side of the sensor, e.g., the left side, is placed in a nitrogen-saturated glucose solution and the other side (the right side) is in contact with air, glucose and oxygen start to diffuse in counter flow towards each other. With each of the ten platinum electrodes the hydrogen peroxide concentration in the adjoining reaction zone can be determined. The results can be compared with the calculations of the sensor simulation program.

5.3.2 Experimental

Preparation of the macro-sensor [3, 4]

The sequence starts with the standard cleaning of a silicon wafer (radius 0.03 m and thickness 385 μm). The wafer is thermally oxidized, yielding a 0.5 μm thick SiO_2 layer. Then, a 50 nm thick Ti layer and 500 nm thick Pt layer are deposited on the wafer using a "US'gun II" sputter gun in a Balzers cryopumped sputter system. Thereafter, a photoresist mask is applied on the metal side, using standard photolithography. For patterning of the electrodes, a broad-beam ion source etcher is used (platinum was removed at areas that were not covered with photoresist). After etching, the remaining photoresist is stripped in an oxygen plasma. Finally, the wafer is diced, resulting in separate macro-sensors with a length of 30 mm and a width of 15 mm. The platinum electrodes have a length of 15 mm (=width of macro-sensor) and a width of 1 mm. The space between two electrodes is 2 mm. The thickness of the platinum electrodes is about 500 nm.

Connections were made by soldering electrical wires onto the top of each platinum electrode. The solder points were covered with an epoxy resin.

The whole surface area was covered with the same GO-containing hydrogel layer as described in Chapters 2 and 4, by spreading it with a spatula. The surface area of the gel layer was covered with a perspex plate, to avoid diffusion of oxygen and glucose over the surface area. The perspex envelope used for this purpose is shown in Fig. 5.3b.

The sensor was stuck in the envelope, owing to the fact that the epoxy resin just fits in the opening.

Sensor experiments

Preparation of the glucose solutions

To obtain 1000 ml of glucose-containing phosphate buffered saline (PBS), the proper amount of glucose was added to 9.22 g NaCl (0.16 mol), 17.8 g $\text{Na}_2\text{HPO}_4 \cdot 12\text{H}_2\text{O}$

Testing the performance of a macro glucose sensor

(0.050 mol) and 8.00 g $\text{NaH}_2\text{PO}_4 \cdot 2\text{H}_2\text{O}$ (0.050 mol) and diluted to 1000 ml with distilled, demineralized water. The pH was adjusted to 7.0 with 4 M NaOH. The glucose solutions were allowed to mutarotate for at least 3 hours before usage.

Calibration curve for hydrogen peroxide

The sensor was "packaged" in the perspex envelope and placed into a buffer solution (phosphate buffered saline, 0.16 M NaCl, 0.10 M phosphate, pH=7.0) Further, a platinum counter electrode with a surface area of $5 \cdot 10^{-4} \text{ m}^2$ and a saturated calomel reference electrode with a Luggin capillary were placed into the one-compartment cell.

After bringing the sensor at a certain hydrogen peroxide concentration ($c_{\text{H}_2\text{O}_2}$) by pipetting an aliquot of a 1.5 mM hydrogen peroxide solution into the buffer and letting it diffuse into the sensor for at least one hour, five electrodes were pulsed from +300 to +700 mV (vs. SCE) for 1 second. The pulse was repeated five times with intervals of 20 seconds (see Fig. 5.4). An Autolab General Purpose Electrochemical System (PGStat20, Ecochemie, Utrecht, Netherlands) was used.

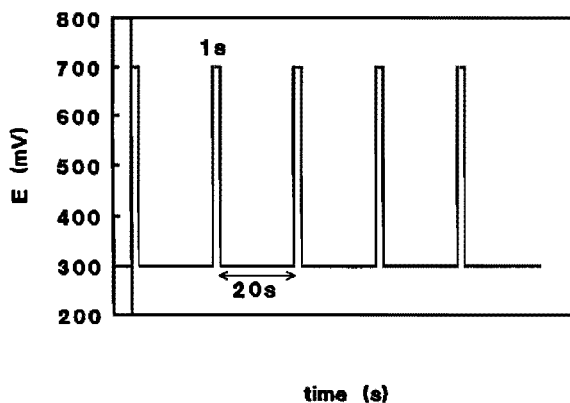


Figure 5.4: Pulse procedure for hydrogen peroxide measurements with electrodes from the macro-sensor.

The current was measured as a function of time, and the average current value of the five pulses, calculated over the last 0.2 s of each pulse, was used as a measure for the hydrogen peroxide concentration. The whole procedure was repeated for several hydrogen peroxide concentrations. In this way, for each of the five electrodes used, a calibration curve was obtained.

Testing the performance of the sensor

To reveal the agreement between the performance of the sensor and the calculation of the simulation program, two experiments were carried out.

1) Parallel-diffusion flow experiment.

For this experiment, a new perspex envelope was created. The envelope was also closed at the right side (Fig. 5.5), so that oxygen and glucose could only enter the sensor from the left side ($i=0$, parallel-diffusion flow).

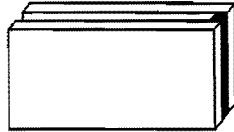


Figure 5.5: Perspex envelope used for parallel-diffusion flow experiments. The right side of the envelope is closed, while the left side remains open.

The sensor was saturated with pure oxygen while being placed in PBS. At time zero, the full sensor (with perspex envelope) was placed into an oxygen-saturated glucose solution (40 mM). At certain times, the pulse procedure as shown in Fig. 5.4 was carried out. The hydrogen peroxide concentration was measured as a function of time at the five electrodes A through E.

The measurements were compared with the results of calculations with the simulation program, using equal boundary conditions.

2) Counter-diffusion flow experiment

For this experiment, the same perspex envelope as for measuring the hydrogen peroxide calibration curve was used (both left and right side open).

The sensor was saturated with air, after it had been completely immersed in PBS. Subsequently, at time zero, the left side ($i=0$) of the sensor (with envelope) was placed in another one-compartment cell containing nitrogen-saturated 40 mM glucose solution. The right side ($i=20$) of the sensor remained in contact with air. In this way, glucose could enter the sensor at the left side, whereas oxygen could virtually only enter the sensor at the right side (counter-diffusion flow).

Again, the pulse procedure as shown in Fig. 5.4 was used to determine the hydrogen peroxide concentration as a function of time at 5 electrodes. The results were compared with the calculations of the simulation program.

5.3.3 Results and discussion

Calibration curve for hydrogen peroxide

Fig. 5.6 shows the calibration curve for one of the five electrodes, for a concentration range of hydrogen peroxide in the bulk solution (and so in the sensor) similar to that occurring in the experiments with the macro-sensor. Each electrode has its own calibration curve, but the differences are less than 10%. However, repeating the calibration curve measurement with the same macro-sensor yields a different result. No unambiguous relation between hydrogen peroxide concentration and measured current could be determined. Therefore, results from the simulation program and results from parallel-diffusion flow and counter-diffusion flow experiments with the macro-sensor were compared by adjusting, at a particular time t^* , both the concentration of the simulation curve and the corresponding current of the experimental curve to 100%. The adjustment factor is equal to $(I/I_{t^*,X})$ for the simulation curves and equal to $(c/c_{t^*,X})$ for the experimental curves, where the subscript X denotes

the electrode that shows the characteristic behaviour. The choice of t^* is limited to times where a characteristic behaviour in the curves is observed.

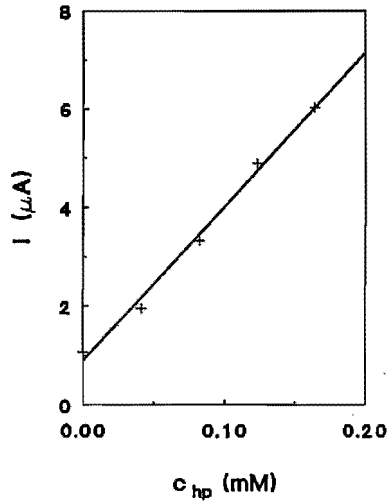


Figure 5.6: Calibration curve for hydrogen peroxide for one of the five electrodes of the macro-sensor, that are used to test the performance of the macro-sensor.

Parallel-diffusion flow experiment

For the parallel-diffusion flow experiment the simulation program used the following boundary conditions:

$$\begin{array}{llll} j=0 \text{ (} t=0 \text{)} & \text{for } i = 0 \text{ to } N & \text{conc1A}[i] & = 1 \text{ mol m}^{-3} \\ & \text{for } i = 0 \text{ to } N-1 & \text{conc1B}[i] & = 0 \text{ mol m}^{-3} \\ & \text{(for } i = 0 \text{)} & \text{conc1B}[0] & = 40 \text{ mol m}^{-3} \\ & \text{for } i = 0 \text{ to } N & \text{conc1C}[i] & = 0 \text{ mol m}^{-3} \\ & \text{for } i = 0 \text{ to } N & \text{conc1D}[i] & = 0 \text{ mol m}^{-3} \end{array}$$

$$\begin{array}{llll}
 j > 0 \quad (t > 0) & (\text{for } i = 0) & \text{conclA}[0] & = & 1 \text{ mol m}^{-3} \\
 & (\text{for } i = 0) & \text{conclB}[0] & = & 40 \text{ mol m}^{-3}
 \end{array}$$

The concentration-versus-time curve from the simulation program (simulation curve) and the current-versus-time curve from the macro-sensor experiment (experimental curve) from five electrodes are equalized and plotted in Fig. 5.7. As the characteristic time t^* serves $t=300$ min, because here, electrode B reaches a steady value in both the simulation curve and the experimental curve.

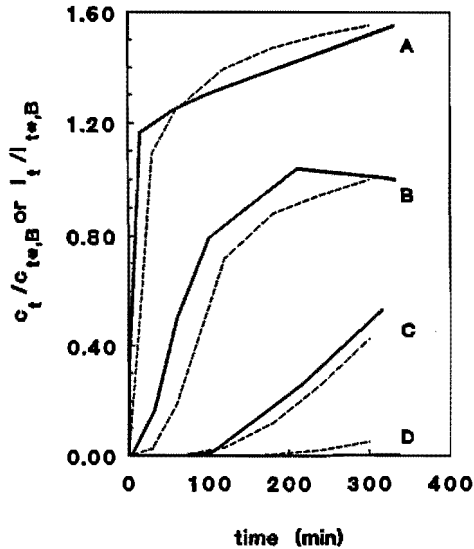


Fig. 5.7: Results of a parallel-diffusion flow macro-sensor experiment (solid lines) and calculations of the simulation program (dashed lines). The letters A through E denote the electrode concerned (see Fig. 5.3). $t^=300$ min and adjustment is carried out for I and c on t^* for electrode B.*

Some remarks should be made on the simulation curves. As the thickness of the GO-containing membrane is much thinner than the envelope opening, the envelope merely consists of a stagnant solution layer, and only a part consists of the enzymatic membrane. Therefore, if the diffusion coefficients of the species in the membrane (Chapter 2, [5]) were used in the simulation program, a clear time "gap" between the simulation curve and the corresponding experimental curve was observed (Fig. 5.8), although the shape of the curves were comparable. If, on the other hand, the diffusion coefficients of the compounds in solution (Chapter 2, [5]) were filled in in the simulation program, the time "gap" between the simulation curves and the experimental curves nearly vanished.

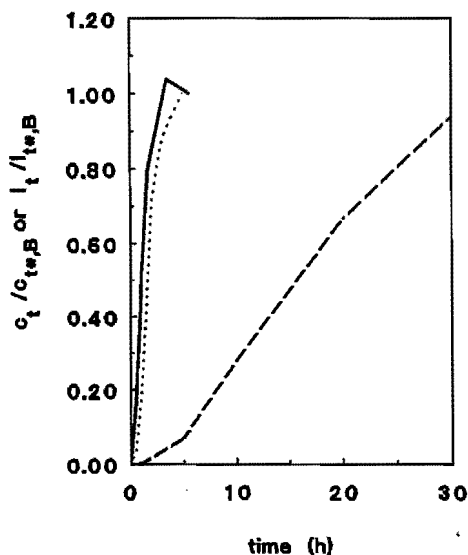


Figure 5.8: *Experimental curve for electrode B (solid line) and corresponding simulation curve with insertion of the diffusion coefficients in the solution (dotted line) or the diffusion coefficients in the membrane (dashed line).*

Testing the performance of a macro glucose sensor

Furthermore, the simulation program requires a value for $k_m^*(o)$. From the experiments described in Chapter 4, the exact value of $k_m^*(o)$ can not be elucidated. It is only known that $k_m^*(o) \leq 0.22 \text{ mol m}^{-3}$. To check the influence of the varying this value, calculations were made with $0.0001 \text{ mol m}^{-3} < k_m^*(o) < 0.02 \text{ mol m}^{-3}$. It turned out that the value of $k_m^*(o)$ in this range had no influence on the shape or concentration values of the simulation curve.

Counter-diffusion flow experiment

For the counter-diffusion flow experiment, the following boundary conditions were used:

$j=0$ ($t=0$)	for $i = 0$ to N	$\text{conc1A}[i]$	=	0.2 mol m^{-3}
	for $i = 0$ to $N-1$	$\text{conc1B}[i]$	=	0 mol m^{-3}
	(for $i = 0$)	$\text{conc1B}[0]$	=	40 mol m^{-3}
	for $i = 0$ to N	$\text{conc1C}[i]$	=	0 mol m^{-3}
	for $i = 0$ to N	$\text{conc1D}[i]$	=	0 mol m^{-3}
$j>0$ ($t>0$)	(for $i = N$)	$\text{conc1A}[N]$	=	0.2 mol m^{-3}
	(for $i = 0$)	$\text{conc1B}[0]$	=	40 mol m^{-3}

After equalizing the simulation curves and the experimental curves, a plot as shown in Fig. 5.9 was made. The characteristic behaviour is now observed at $t=240 \text{ min}$ (t^*), because here both the experimental curves and the simulation curves for electrodes B and C intersect.

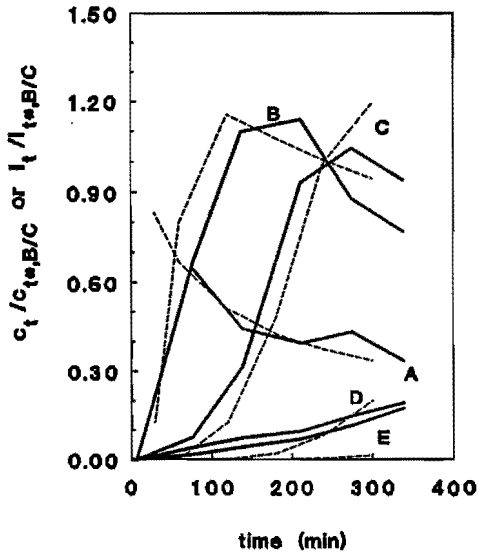


Figure 5.9: Results of a counter-diffusion flow macro-sensor experiment (solid lines) and calculations of the simulation program (dashed lines). The letters A through E denote the electrode concerned (see Fig. 5.3). $t^* = 240$ min and adjustment is carried out with I and c on t^* for electrodes B and C.

Again, a good agreement is observed between the experimental curves and the simulation curves. This means that the one-dimensional approach used here, gives satisfying results.

5.4 Concluding remarks

Both the parallel-diffusion flow and the counter-diffusion flow experiments show that the macro-sensor behaves, qualitatively, according to the sensor simulation program

forecast.

Exact values of the hydrogen peroxide concentrations formed in the macro-sensor can not be determined, because the hydrogen peroxide calibration curve is not constant over several experiments. The currents measured during macro-sensor experiments can not be related to the concentration calculated with the sensor simulation program. The usage of other electrode materials could improve the reproducibility of the calibration curve for hydrogen peroxide. This would make a quantitative comparison of simulation curves and experimental curves possible.

When the principle is tested to be valid, further design of e.g., the geometry of the sensor is necessary.

Diminishing the total length of the sensor has the advantage of shortening the duration of steady state establishment, but it also requires a decrease in the ratio of the initial concentrations of oxygen and glucose. To nevertheless have a sufficiently large detectable glucose concentration range (e.g., 0-20 mol m⁻³), the use of an extra diffusional resistance layer is indispensable. This also requires an accurate choice of material and geometry.

The sensor has theoretically a chance of success. This is shown by the computer calculations. Practically, the performance of a macro-sensor is in a qualitative way in accordance with the computer calculations. Still, a lot of practical problems have to be surmounted. Adaptations and extensions of the design, related to experimentally demonstrated difficulties, are now of major concern.

Acknowledgment

I wish to acknowledge dr. ir. M.C.A. Donkersloot from the Eindhoven University of Technology for his contribution to the simulation program and drs. D.J. Sprangers and ir. E.L. de Weerd from Twente Technology Transfer B.V. (3T B.V., Enschede, Netherlands) for their advice on and contribution to the preparation of the macro-sensor.

References

1. J. Crank, *The mathematics of diffusion*, 2nd edition, Clarendon Press, Oxford, (1975), 144-146.
2. Southampton Electrochemistry Group, *Instrumental methods in electrochemistry*, John Wiley and Sons, New York, (1985), 30.
3. US, Inc., U.S. Patent No. 4,434,042.
4. F.A. Smidt, *International Materials Reviews*, 35 (1990) 61-128.
5. S.A.M. van Stroe-Biezen, F.M. Everaerts, L.J.J. Janssen and R.A. Tacken, *Anal. Chim. Acta*, 273 (1993) 553-560.

CHAPTER 6. THE USAGE OF MEMBRANES IN GLUCOSE SENSORS. A REVIEW

6.1 Immobilization of glucose oxidase for usage in a glucose sensor

6.1.1 Introduction

In the work, described in this thesis, usage is made of the quite satisfying covalent immobilization technique of poly(vinyl alcohol) with the cross-linkers DTS-18 and glutaraldehyde. Presumably, this technique has the disadvantage of a low GO yield in the membrane, which is reflected in a low V_{max} . Therefore, other immobilization techniques should not be ruled out. In fact, not until research is conducted on or with a particular technique (in this case the GO-immobilization technique), one acquires an insight into the usability of this technique. Because of this, a purposive literature study on other techniques, while aiming at the evidently important issues, can be carried out.

Immobilization of enzymes has some important advantages [1,2]. Firstly, an enhanced stability towards chemical and physical conditions (e.g., pH, temperature) occurs. Secondly, the enzyme can be reused several times. Further, leakage of the enzyme out of the sensor is prohibited.

However, immobilization can effect the activity of the enzyme in a negative way due to [1,2]:

- changes in enzyme configuration
- steric hindrance
- diffusional resistance
- modified micro environment of the enzyme

As an exception to the generally observed decrease in activity, Cabral *et al.* [3]

reported that the maximal initial velocity (V_{max}) of the immobilized enzyme gluco-amylase is about ten times higher than V_{max} of the native enzyme.

It is obvious that the chosen immobilization technique plays an important role with respect to the stability and activity of the enzyme.

In principle three immobilization techniques are available (Fig. 6.1):

- 1) adsorption (including Carbon Paste Electrodes)
- 2) gel entrapment
- 3) covalent binding, with or without the use of a cross-linker

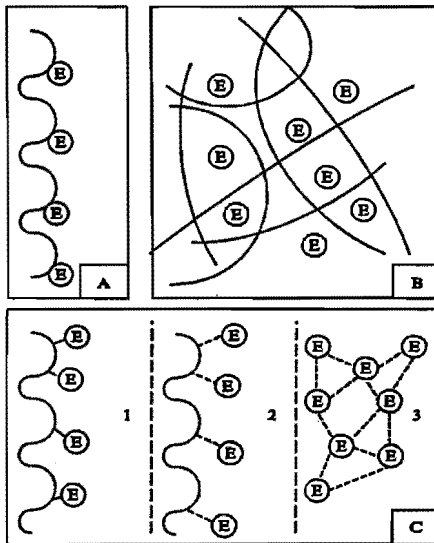


Figure 6.1: Three possible immobilization techniques: A) Adsorption, B) Gel Entrapment and C) Covalent Binding (1. direct covalent binding onto a carrier, 2. covalent binding onto a carrier with a cross-linker, 3. intermolecular cross-linking)

In this review, the immobilization possibilities for the relatively stable enzyme glucose oxidase (GO, EC 1.1.3.4) are considered. A lot of papers have been published on this subject and the available information on the different immobilization techniques is listed and discussed. The papers mainly date from the period between 1985 and 1992.

6.1.2 Immobilization of glucose oxidase

The enzyme glucose oxidase (GO) plays an important role in the development of glucose sensors. The immobilization of the enzyme is one of the major difficulties here. GO is derived from either *Aspergillus niger*, *Penicillium amagasakienses* or *Penicillium notatum*. GO is a flavoprotein and contains two FAD-units (flavin adenine dinucleotide) per molecule. The FAD-units serve as redox-centra and are indispensable for the specific oxidation of glucose by GO. It is highly important to avoid binding and steric hindrance of the active FAD-centra. Covalent binding should therefore occur for instance via lysine groups.

GO catalyses the oxidation of glucose by oxygen:



Instead of electron transfer via oxygen, it is also possible to make use of a mediator that takes over the function of oxygen. In addition, a redox polymer can replace oxygen.

6.1.2.1 GO-immobilization by adsorption

Koopal [4] developed a glucose sensor in which GO is adsorbed onto poly(pyrrole). In the pores of a poly(carbonate) track-etch membrane pyrrole is

chemically polymerized. The obtained poly(pyrrole) microtubules were used as a mediator. GO was adsorbed onto the zigzag microstructure of the poly(pyrrole) layer. A sensor in which this immobilization technique is used, is able to amperometrically measure glucose concentrations ranging from 1-40 mM, under steady state conditions. One of the advantages is that no oxygen is used and no hydrogen peroxide is formed. Hydrogen peroxide could damage GO. Electron transfer is carried out directly from the enzyme, via the oxidized (and so conducting) poly(pyrrole) layer, to the electrode.

Bianco *et al.* [5] describe GO immobilization based on adsorption on a pyrolytic graphite electrode. Benzoquinone, present in solution, is used as a mediator. The technique is quite fast. However, the enzyme seems to lose its activity with time. The authors compared this method, based on adsorption, with an almost identical covalent method (*vide infra*). The responses with the adsorbed GO appeared to be less stable than those with the covalently bound GO. Progressive lack of enzymatic activity is for the adsorbed GO due to slow desorption and/or reformation from the native enzyme to an inactive form.

Wang and Angnes [6] immobilized GO by electrochemical codeposition with rhodium on a carbon fiber electrode. The electrode shows excellent catalytic properties towards hydrogen peroxide. Catalytic platinumized carbon glucose sensors usually operate at +0.6 to +0.8 V (versus Ag/AgCl), whereas the Rh/GO modified carbon-fiber electrodes response at +0.3 V (versus Ag/AgCl). The lowering of the operating potential permits minimization of interferences from acetaminophen. Some interference, however, was observed in the presence of ascorbic and uric acids (oxidation starting at +0.25 V (versus Ag/AgCl)). Concentrations of glucose up to 50 mM were measured with this technique.

Carbon paste electrodes

In a carbon paste electrode (CPE), GO is mixed with paraffine oil and graphite powder. It is also possible that the paste contains a mediator or a mediator-modified

polymer.

The one-electron mediator system ferrocene/ferricinium is used by several authors. As it is highly toxic, the system is not applicable for *in vivo* glucose sensors.

Hale *et al.* [7] describe a glucose sensor based on a conventional carbon paste electrode (CPE). Graphite powder is mixed with paraffin oil, GO and polymer-bound ferrocene. Ferrocene is covalently attached to an insoluble siloxane polymer. As this siloxane backbone is highly flexible and able to rotate easily, it allows the covalently bound ferrocene mediators into close contact with the FAD/FADH₂ centers of GO. Oxygen interference is very strong at low glucose concentrations. At glucose concentrations higher than 25 mM this effect is negligible. The storage stability of a GO/siloxane modified CPE is excellent. Under dry conditions at 4°C a decrease in activity of less than 20 % has been observed after 7 months. Under wet conditions leakage of enzyme into the storage solution causes a larger decrease.

From the same research group, Gorton *et al.* [8] report a similar sensor, but with the carbon paste electrode surface coated with an extra poly(ester sulfonic acid) cation exchanger membrane. The coating showed not to be detrimental to the enzyme, but prevents active anionic interferences, such as ascorbate and urate, from reaching the electrode surface. It also prevents GO from leaking out of the carbon paste and protects the electrode surface from fouling agents from body fluids. The coating increased the strictly linear range from 5 mM to 20 mM glucose, while the response current is maintained.

A glucose sensor based on ferrocene-modified poly(ethylene oxide) and GO was used by Hale *et al.* [9]. They prepared a carbon paste by mixing graphite powder and poly(ethylene oxide) with covalently bound ferrocene. GO was incorporated into the matrix, while retaining its activity. The mediator ferrocene makes oxygen-deficiency unimportant and better, present oxygen does not influence the measurement when the glucose concentration is higher than 5 mM. The whole polymer redox system serves as an "electrical wire" for the enzyme, taking care of a flow of electrons from the enzyme to the electrode. A (non-linear) calibration curve

was measured up to 35 mM of glucose. The sensor, when stored under dry conditions at 5 °C, shows less than 10 % decrease in response after six months.

Wang *et al.* [10] prepared a modified carbon paste electrode by mixing graphite powder, paraffin oil, GO and a (non polymer-bound) ferrocene derivative. Usage of the ferrocene derivative t-pentylferrocene yields response times (95 %) of 18 seconds. In the presence of a membranous diffusion barrier (e.g., a CPE with membrane entrapped GO), response times of 2 minutes are found. Addition of stearic acid to the enzyme containing carbon paste seems to strongly reduce the interfering effects of ascorbate.

Hale *et al.* [11] use the same system as Wang *et al.* [10], but instead of a ferrocene derivative, they use a viologen (4,4'-bipyridyl) derivative. The advantage of these derivatives are their cathodic redox potentials, so that a sensor using this mediator operates at potentials where the common electroactive species are not interfering. Still, the redox potentials of these mediators are anodic enough to reoxidize the FAD-centers of GO.

6.1.2.2 GO-immobilization by gel entrapment

Kierstan and Bucke [12] use calcium alginate gels in which GO can be immobilized under extremely mild conditions. The activity of the entrapped GO is reduced to 10-20 % of the activity of the native enzyme. The gel shows only a little barrier to diffusion of neutral substrates up to a molecular weight of 5000. Phosphates (20 mM) appear to disrupt the gel structure.

Vopel *et al.* [13] entrapped GO in a photo polymer system. In this way, patterned enzyme membranes could be produced. As a polymeric binder, a partially hydrolysed poly(methyl methacrylate) (PMMA) was used. Further, the bifunctional monomer bisphenol A-bis(2-hydroxypropyl methacrylate) (BBHM) and the initiator Michler's ketone-benzophenone (MK-BP) were used. GO was added to a solution of PMMA, BBHM and MK-BP. Glucose was detected by measuring hydrogen perox-

ide. A calibration graph was made for glucose concentrations ranging from 1-6 mM. The GO activity of the membrane decreased by 50 % within eight days. The measured response curve, however, only changed by 5 % in this time.

Malitesta *et al.* [14] claim to present the first membrane that is capable, at the same time, of entrapping GO and rejecting ascorbate. They used a poly(*o*-phenylenediamine) (PPD) with a thickness less than 10 nm. PPD was electrochemically polymerized onto a platinum electrode. The PPD-electrode showed a lower response time and a higher limiting current than a comparable poly(pyrrole) (PPy) electrode. Further, hydrogen peroxide could damage the poly(pyrrole) matrix. A non-linear calibration curve of glucose concentrations ranging from 2 to 100 mM was obtained. Storage of the Pt/PPD/GO electrode at pH=7.0 and T=4 °C for nine days did not give a decrease in the measured current. The sensor was able to measure for about twenty hours before starting to show a decrease in response.

Wang *et al.* [15] describe a simple and fast immobilization technique for GO. The enzyme was incorporated into a matrix of the cation exchanger poly(ester-sulfonic acid), commercially available under the trademark Eastman AQ polymers. A sensor using this membrane shows little interference of ascorbic and uric acid. Acetaminophen is only slightly hindered by the membrane. The resulting sensor yields a very fast and sensitive response to glucose concentrations ranging from 25 to 200 μ M.

Shaolin *et al.* [16] use poly(aniline) to entrap glucose. The poly(aniline) film was electrochemically deposited on a platinum foil. The resulting sensor has a fast response time (20-40 s) and high storage and operational stability (> 60 days). The maximum current response for the poly(aniline)/GO electrode is obtained at pH= 5.6, T=40 °C and 0.60 V. A phosphate buffer is preferred to an acetate buffer. As the electrochemical activity of poly(aniline) decreases with increasing pH of the solution, it is difficult to incorporate GO in poly(aniline) at high pH values. A linear relationship between response current and glucose concentration was measured for glucose concentrations ranging from 0.1 to 1.0 mM. A non-linear increase in

response current with increasing glucose concentration was observed from 1.0 to 50 mM. Above 50 mM glucose, the increase in response current with increasing glucose concentration was not significant.

6.1.2.3 GO-immobilization by covalent binding

The most frequently used immobilization technique concerns the covalent binding of GO onto a carrier. This can be achieved by directly coupling GO and a carrier via their (non-essential) functional groups or by using a spacer or cross-linker to couple GO with the carrier. It is also possible to only use GO and a cross-linker, without a carrier. This technique is called intermolecular cross-linking. Because of a non-selective binding reaction, where also intramolecular reactions take place, intermolecular cross-linking is not very popular. Covalently binding the enzyme onto a carrier can prohibit these intramolecular reactions, because in this way the ratio between the number of functional groups available and the quantity of cross-linker is increased.

Still, the differentiation between the various types involving covalent binding of GO is very subtle. For instance, cross-linking of GO by glutardialdehyde (GA) would be an example of intermolecular cross-linking. When GO is co-cross-linked with bovine serum albumin (BSA) by GA, one could again speak of intermolecular cross-linking. However, BSA can also be considered to be a carrier, so that it is a case of covalent binding of the enzyme onto a carrier via a cross-linker. This paragraph therefore deals with non-strictly divided immobilizations techniques, where GO is, in one way or the other, covalently bound.

The division in this paragraph, however, is based on the way of electron transfer from the reduced GO to the electrode. There are three possibilities, as stated before:

- 1) Oxygen re-oxidizes GO and the glucose measurement is based on the formation and detection of hydrogen peroxide.
- 2) Electrons evolving from the glucose oxidation are transferred to the electrode by a mediator. No hydrogen peroxide is formed.
- 3) GO is covalently bound onto a conducting polymer. No hydrogen peroxide is formed and the electrons are directly transferred from GO, via the polymer, to the electrode.

Electron transfer via oxygen

Broun *et al.* [17] describe intermolecular cross-linking with glutardialdehyde (GA). When cross-linking was stopped early enough, the obtained soluble enzyme oligomers could be included in an agarose-poly(acrylamide) gel. The activity yield under optimal conditions was 10 %. When, however, GO was co-cross-linked with an inactive protein (albumin), an activity yield of 80 % was obtained. This effect can be explained by the prevention of intramolecular reaction in the presence of albumin (*vide supra*). Only a restricted number of amino groups of each GO molecule is involved in the cross-linking.

Kuijpers *et al.* [18] immobilize GO on a poly(vinyl alcohol) (PVA) matrix by adding glutardialdehyde (GA) and the polyazonium salt DTS-18. DTS-18 cross-links PVA under UV-radiation. Directly after radiation the non-radiated areas are flushed out. As DTS-18 does not provide enough cross-linking, GA is added. The cross-linking of GA is established during 24 hours at 4 °C, after radiation and flushing.

Koudelka *et al.* [19, 20] use bovine serum albumin (BSA) as a carrier protein and GA as a cross-linking agent for the immobilization of GO. The glucose concentration was determined by measuring the hydrogen peroxide concentration. The sensor was covered by a 3 μm poly(urethane) membrane to slow glucose diffusion and the response was linear between 3.5 and 13.8 mM. For *in vivo*

experiments the sensor showed an acceptable time lag of about 5 minutes between subcutaneous glycaemia and the actual one measured in the plasma by using a conventional method.

An activity drop to 25 % of the native activity is observed by Alva *et al.* [21] when GO is immobilized in a BSA-GA matrix. The stability of the enzyme, however, is greatly improved. The produced sensor has a shelf life (storage life) of more than 60 days. In addition, co-immobilization of 1 M urea seems to increase the activity to 39 % of the native activity. 3 M urea, on the other hand, has a detrimental effect. Alva *et al.* also checked the impact of several metal ions on the activity of immobilized GO. Manganese has an enhancing effect, magnesium has no effect and copper shows to be an inhibitor.

Also Ruger *et al.* [22] use BSA and GA to immobilize GO for a glucose sensor. Immobilization with GA was chosen because it is fast, easy to perform and results in sensitive and stable sensors. Adhesion of the enzyme layer to the platinum electrode is sufficient. However, silanization of the electrodes improves the stability of the construction. A cellulose acetate membrane covers the GO-membrane to prevent interferences of electroactive species, such as the oxidizable substrate ascorbic acid. The lower determination limit is 1 μM and the linear range goes up to 1 mM.

Kimura *et al.* [23] use the same immobilization technique and the enzyme layer was spin coated on to an ISFET wafer, which was cut into individual devices. About 2 % of the enzyme activity is assumed to be retained in the fabricated enzyme membrane. The sensor is restricted to glucose concentrations below 11 mM.

Mullen *et al.* [24] describe a sensor in which again the BSA-GA immobilization technique is used. They covered the enzyme membrane with organosilane-treated membranes in order to achieve pH- and temperature-independence and a stable output in unstirred solutions. Combination of the BSA-GA-GO layer with a silanized cover membrane (poly(carbonate)) extended the linear range enormously compared with the combination of a BSA-GA-GO layer and a non-silanized

poly(carbonate). The silane-treated membrane markedly decreases glucose diffusion. In addition, organosilanes are widely used to improve the blood compatibility. Interference of electroactive species was substantially decreased by interposing a cellulose acetate membrane between the enzyme layer and the electrode surface.

Shichiri *et al.* [25] describe a successful sensor where GO is attached onto cellulose acetate using GA. To slow glucose diffusion a poly(urethane) membrane was used. *In vitro*, a 90 %-response time of 16 seconds is observed and a linear range of 0-28 mM is obtained. Subcutaneous *in vivo* tests with human volunteers showed good correlation with blood values between 3 and 22 mM glucose. The concentrations in the subcutaneous tissue were about 20 % lower than the blood concentrations.

A cellulose acetate matrix, cross-linked with GA was also used by Weiß [26]. It seemed that after six weeks at room temperature and pH=7, still 71 % of the enzyme activity was present. Again, poly(urethane) showed to slow glucose diffusion, which results in the extension of the linear range.

Alves da Silva *et al.* [27] examined immobilization of GO on hydrolyzed nylon-6,6. Various spacers were introduced on the support before coupling the enzyme. The best spacer turned out to be hexamethylenediamine (HMD). A strong improvement of the immobilization technique was obtained by covering the nylon-6,6 with denatured BSA before spacer coupling. BSA provided the enzyme with a good biological environment. Best combinations showed to be: nylon-6,6/BSA/GO, nylon-6,6/BSA/HMD/GO and nylon-6,6/BSA/HMD/HMD/GO. For all these methods about 20 % of the enzyme used is actually coupled. Retention of the activity (ratio U/mg immobilized GO and U/mg native enzyme) is about 50 %. The stability of the enzyme is depending upon the storage solution. In distilled water (pH=6.0) as well as in 0.1 M acetate buffer (pH=5.0)

+ 5 mM glucose +20 mM sodium azide the retention of the activity is 50 % after 60 days at room temperature. In addition, the activity of immobilized GO seems to be sensitive to the pH and the ionic strength of the buffer solution.

Schalkhammer *et al.* [28] couple GO onto substituted poly(pyrrole) films. The terminal carboxyl and nitro groups of the polymer are activated by water-soluble carbodiimides and chloranil, which can also establish the covalent enzyme coupling. In this way a porous poly(pyrrole) layer with covalently coupled GO can be developed, which has no redox activity. Two main advantages appear to be a significant increase of response per unit area and a significant increase in selectivity due to permeation control of interfering electroactive species. Polymerization of substituted pyrrole monomers yields an unstable, water-soluble film. To avoid this problem the modified pyrrole monomers are co-polymerized with pyrrole to obtain an aqueous stable, porous film with an optimal enzyme load.

Collagen membranes are used by Coulet *et al.* [29]. The collagen membranes undergo an acyl-azide activation process, which makes them suitable for enzyme coupling. When measuring glucose *in vitro* (blood sample) two electrodes are used, one containing the GO-collagen membrane, the other with a non-enzymatic collagen membrane. The first electrode detects hydrogen peroxide and possible interfering species, such as ascorbic acid, uric acid and tyrosine. The second electrode only measures the interfering species. This differential method allows to accurately measure glucose concentrations in the range $1 \cdot 10^{-4}$ -2 mM.

Abel *et al.* [30] use sepharose-bound GO on a cuprophan membrane. The enzyme layer was covered by another cuprophan membrane. The linear range of this construction is only small and therefore an additional membrane was added (poly(urethane), poly(ethylene) or cellulose acetate). This cover membrane is able to restrict glucose permeation relatively to that of oxygen. For glucose measurements *in vitro* and *ex vivo* a disc shaped electrode was used, for measurements in subcutaneous tissue a pencil shaped electrode was used. The storage stability of the enzyme layer was very high, i.e., three years at 4 °C. For both disc and pencil shaped electrodes a linear range of more than 40 mM was obtained *in vitro*. The 95 %-response time was 360 s for the disc shaped and 600 s for the pencil shaped electrode. The oxygen partial pressure was of no influence on the sensors' output up

to a glucose concentration of 10-15 mM. At an oxygen partial pressure of 2 kPa a linear range of 0-15 mM was obtained. This means that in subcutaneous tissue, where experiments show an oxygen partial pressure of 2-5 kPa, the physiological range of glucose concentration is guaranteed. The pencil shaped electrode was used for measurements in dogs. Simultaneously performed plasma measurements showed great agreement with the tissue measurements.

Kawaguchi *et al.* [31] immobilized GO on aminated styrene-acrylamide latex particles by using sodium meta-periodide and borohydride. A bond between the amino group of the latex particle and a carboxyhydrate unit of the enzyme seems to be a satisfactory coupling method, as about 40 % of the enzyme activity is retained. The specific activity of the enzyme is reduced when the amount of immobilized enzyme per latex particle is too large. A maximum activity of immobilized GO was observed when it occupies approximately the same molecular surface area as the native GO (120 nm²/molecule). Too loose or too tight immobilization causes a decrease in specific activity, perhaps due to an expansion or compression of the enzyme conformation.

Electron transfer via a mediator

A mediator takes care of the electron transport from GO to the electrode. This means that oxygen is superfluous and hydrogen peroxide, which could damage GO, is no longer formed. However, present oxygen can now interfere with the measurement based on the mediator.

Bianco *et al.* [5] do not only describe the adsorption of GO onto pyrolytic graphite (*vide supra*), but also the covalent attachment on glassy carbon using a carbodiimide activation. A amino group of GO is coupled with a carboxyl group of the glassy carbon surface. Benzoquinone is used as a mediator. The stability of the covalently bound GO is much higher than the stability of adsorbed GO. The authors

think that loss of activity of the covalently bound GO could be due to enzyme layer wash-out, enzyme denaturation or possibly both.

Electron transfer via a conducting polymer

Oxidoreductases, such as glucose oxidase, can be covalently attached to electrodes via a redox polymer. In this way the electrons flow from the enzyme, through the polymer, to the electrode. This method is called electrical wiring of an enzyme onto an electrode.

Gregg and Heller [32, 33] accomplish electrical wiring based on a cross-linkable poly(vinylpyridine) complex of $[\text{Os}-(2,2'\text{-bipyridyl})_2\text{Cl}]^{+2+}$, that communicates with the FAD centers of GO. Here Os(III) takes over the role of oxygen. GO is cross-linked onto the redox polymer with poly(ethylene glycol diglycidyl ether) (PEG). The method is simple and effective. The enzyme containing films are stable, selective and highly active for the catalytic oxidation of glucose. Although this results in a high current density, oxygen can still interfere with Os(III). For air-saturated conditions, only 20 % of the active enzyme is directly oxidized by the polymer. In addition, the authors report that the maximum steady state current is apparently limited by redox polymer kinetics rather than by enzyme kinetics.

Pishko *et al.* [34] from the same department as Gregg and Heller, use the same redox polymer. Instead of a glassy carbon macro-electrode, Pishko *et al.* use a bevelled carbon-fiber micro-electrode. This results in a 10-fold increase in current density and a significantly reduced sensitivity to oxygen. Radial charge transport, through the redox hydrogel, to the electrode is sufficiently fast to effectively compete with oxidation of the enzyme by oxygen. Under aerated conditions an only 2 % lower current is observed than under anaerobic conditions.

6.1.3 Non-immobilization method

Till sofar, several methods were described for immobilizing GO for usage in a glucose sensor.

Schmidt [35], however, developed an implantable glucose sensor where GO is not immobilized, but solved in saline. The sensor is based on the principle of microdialysis. A hollow fiber is placed subcutaneously. Glucose diffuses from the tissue into the microdialysis system, where a GO-solution is circulated. The difference in the oxygen concentration of the GO-solution before entering and after leaving the tissue is in relation with the subcutaneous glucose concentration. The measuring device is a Clark-type oxygen electrode. The detrimental hydrogen peroxide is eliminated by the enzyme catalase, which is also present in the GO-solution.

6.1.4 Concluding remarks

The most popular immobilization techniques are undoubtedly gel entrapment and covalent attachment via a cross-linker. Gel entrapment yields a reduced stability of the enzyme and covalent methods yield a reduced activity. Still, a reduced but stable signal seems more useful than a (in the beginning) high but drifting signal. For this reason, it is not surprising that most researchers use covalent techniques. As a natural environment is important to limit reduction in enzyme activity, a BSA carrier/spacer appears to be quite suitable. The use of BSA with GA as cross-linker predominates the literature. Activity retentions of 80 % are mentioned. The method used by Kawaguchi *et al.* [31], i.e., immobilization of GO on latex particles, yields 40 % retention of the enzyme activity and the possibility to use the particles in a mobile (flow-)system.

6.2 Coating membranes in a glucose sensor

Coating membranes can have various (combined) functions. Most important are:

- biocompatibility
- barrier for interfering species
- restriction of glucose diffusion

However, some researchers use GO-containing membranes, which include (one of) these functions, so that an extra coating membrane is not necessary.

Biocompatibility

For *in vivo* use it is very important that the outer membrane of the sensor is biocompatible. The polysaccharide heparin has anti-coagulating properties.

Merrill *et al.* [36] and Goosen and Safton [37] reported in respectively 1970 and 1983 the possibilities of a poly(vinyl alcohol)-heparin hydrogel. Clot-inhibiting (nonthrombogenic) properties were assessed by both *in vitro* and *in vivo* tests, despite the fact that the release rate of covalently bound heparin is negligible.

Brinkman [38] immobilizes heparin in a poly(vinyl alcohol) (PVA) hydrogel with the cross-linkers DTS-18 and GA (cfr. Kuijpers [18]) for use in medical sensor catheters. He also describes the use of biocompatible materials (without heparin), such as poly(ethylene oxide) (PEO) grafted onto a carrier (pellethane). In addition, he gives a review on biocompatible materials.

Further it seems that poly(urethane) has interesting biocompatible characteristics (Shichiri *et al.* [25]) and the same is reported about organosilanes (Mullen *et al.* [24]).

Barrier for interfering species

To control permeation of interfering species, such as acetaminophen, uric and ascorbic acid, different coating layers can be used.

Gorton *et al.* [8] found that coating their sensor with poly(ester sulfonic acid) could prevent electroactive species to reach the electrode surface. Wang *et al.* [15] use poly(ester sulfonic acid) not as a coating membrane but as a gel to entrap GO. In this way the versatile membrane has a double function: enzyme immobilization and exclusion of interfering species. Wang *et al.* [10] mention the reduction of ascorbic acid interference due to addition of stearic acid.

Other membranes that inhibit the interference of electroactive species are a cellulose acetate coating [Rüger 22, Mullen 24] or a Nafion membrane [Chen 39]. Further, poly(pyrrole) is considered to control the permeation of electroactive substances [Malitesta 14, Schalkhammer 28]. Also poly(o-phenylenediamine) (PPD) has a permselective character, which allows removal of ascorbate interference [Malitesta 14].

Restriction of glucose diffusion

A big problem for *in vivo* glucose measurements is the oxygen limitation due to the low oxygen concentration in subcutaneous tissue. To extend the linear glucose concentration range of a sensor and to make it less dependent on the oxygen concentration the glucose diffusion has to be retarded relatively to oxygen diffusion by an extra membrane. Poly(urethane) is the most commonly used membrane to slow glucose diffusion [Koudelka 19, 20, Shichiri 25, Weiß 26, Abel 30]. Mullen *et al.* [24] describe a silane-treated GO-membrane, which also slows glucose diffusion. Further, poly(ethylene) and cellulose acetate are mentioned for this purpose [Abel 30, Chen 39]. Finally, Van Stroe-Biezen *et al.* [40] showed that a PVA/GA/DTS-18 hydrophilic membrane restricts glucose diffusion relatively to oxygen with a factor 2.9.

References

1. J.F. Kennedy and J.M.S. Cabral, Enzyme Immobilization, in H.-J. Rehm and G. Reed (eds.), *Biotechnology, Enzyme Technology*, Vol. 7a, VCH, Weinheim, FRG, (1987), 347-404.
2. P.W. Carr and L.D. Bowers, *Immobilized Enzymes in Analytical and Clinical Chemistry, Fundamentals and Applications*, Chemical Analysis, Vol. 56, John Wiley & Sons, New York, (1980), 148-196.
3. J.M.S. Cabral, J.M. Novais and J.P. Cardoso, *Chem. Eng. J.*, 27 (1983) B47.
4. C.G.J. Koopal, Thesis, University of Nijmegen, (1992).
5. P. Bianco, J. Haladjian and C. Bourdillon, *J. Electroanal. Chem.*, 293 (1990) 151-163.
6. J. Wang and L. Angnes, *Anal. Chem.*, 64 (1992) 456-459.
7. P.D. Hale, L.I. Boguslavsky, T. Inagaki, H.I. Karan, H.S. Lee, T.A. Skotheim and Y. Okamoto, *Anal. Chem.*, 63 (1991) 677-682.
8. L. Gorton, H.I. Karan, P.D. Hale, T. Inagaki, Y. Okamoto and T.A. Skotheim, *Anal. Chim. Acta*, 228 (1990) 23-30.
9. P.D. Hale, H.L. Lan, L.I. Boguslavsky, H.I. Karan, Y. Okamoto and T.A. Skotheim, *Anal. Chim. Acta*, 251 (1991) 121-128.
10. J. Wang, L.-H. Wu, Z. Lu, R. Li and J. Sanchez, *Anal. Chim. Acta*, 228 (1990) 251-257.
11. P.D. Hale, L.I. Boguslavsky, H.I. Karan, H.L. Lan, H.S. Lee, Y. Okamoto and T.A. Skotheim, *Anal. Chim. Acta*, 248 (1991) 155-161.
12. M. Kierstan and C. Bucke, *Biotechnol. Bioeng.*, 19 (1977) 387-397.
13. T. Vopel, A. Ladde and H. Müller, *Anal. Chim. Acta*, 251 (1991) 117-120.
14. C. Malitesta, F. Palmisano, L. Torsi and P.G. Zambonin, *Anal. Chem.*, 62 (1990) 2735-2740.

15. J. Wang, D. Leech, M. Ozsoz and S. Martinez, *Anal. Chim. Acta*, 245 (1991) 139-143.
16. M. Shaolin, X. Huaiguoa and Q. Bidong, *J. Electroanal. Chem.*, 304 (1991) 7-16.
17. G. Broun, D. Thomas, G. Gelff, D. Domurado, A.M. Berjonneau and C. Guillon, *Biotechnol. Bioeng.*, 15 (1973) 359-375.
18. M.H. Kuijpers, G.F.J. Steeghs and E. Brinkman, *U.S. Patent No. 5 134 057*, (1992)
19. M. Koudelka, F. Rohner-Jeanrenaud, J. Terrettaz, E. Bobbioni-Harsch, N.F. de Rooij and B. Jeanrenaud, *Biosensors and Bioelectronics*, 6 (1991) 31-36.
20. M. Koudelka-Hep, F. Rohner-Jeanrenaud, E. Bobbioni-Harsh, J. Terrettaz, N.F. de Rooij and B. Jeanrenaud, *Adv. in Biosensors*, 2 (1992) 131-149.
21. S. Alva, S.S. Gupta, R.S. Phadke and G. Govil, *Biosensors and Bioelectronics*, 6 (1991) 663-668.
22. P. Rüger, U. Bilitewski and D. Schmid, *Sensors and Actuators B*, 4 (1991) 267-271.
23. J. Kimura, A. Saito, N. Ito, S. Nakamoto and T. Kuriyama, *J. of Membr. Sci.*, 43 (1989) 291-305.
24. W.H. Mullen, F.H. Keedy, S.J. Churchouse and P.M. Vadgama, *Anal. Chim. Acta*, 183 (1986) 59-66.
25. M. Shichiri, R. Kawamori, N. Hakui, N. Asakawa, Y. Yamasaki and H. Abe, *Biomed. Biochim. Acta*, 43 (1984) 561-568.
26. T. Weiß, Thesis, München University of Technology, (1989).
27. M. Alves da Silva, M.H. Gil, J.S. Redinha, A.M. Oliveira Brett and J.L.C. Pereira, *J. Pol. Sci.*, 29 (1991) 275-279.
28. T. Schalkhammer, E. Mann-Buxbaum, F. Pittner and G. Urban, *Sensors and Actuators B*, 4 (1991) 273-281.
29. P.R. Coulet, R. Sternberg and D.R. Thévenot, *Biochim. Biophys. Acta*, 612 (1980) 317-327.

30. P. Abel, A. Müller and U. Fischer, *Biomed. Biochim. Acta*, 43 (1984) 577-584.
31. H. Kawaguchi, N. Koiwai and Y. Ohtsuka, *J. Appl. Pol. Sci.*, 35 (1988) 743-753.
32. B.A. Gregg and A. Heller, *Anal. Chem.*, 62 (1990) 258-263.
33. B.A. Gregg and A. Heller, *J. Phys. Chem.*, 95 (1991) 5976-5980.
34. M.V. Pishko, A.C. Michael and A. Heller, *Anal. Chem.*, 63 (1991) 2268-2272.
35. F.J. Schmidt, Thesis, University of Groningen, (1991).
36. E.W. Merrill, E.W. Salzman, P.S.L. Wong, T.P. Ashford, A.H. Brown and W.G. Austen, *J. Appl. Physiol.*, 29 (1970) 723-730.
37. M.F.A. Goossen and M.V. Sefton, *J. Biomed. Mat. Research*, 17 (1983) 359-373.
38. E. Brinkman, Thesis, University of Twente, (1989).
39. G. Chen, Thesis, University of Twente, (1991).
40. S.A.M. van Stroe-Biezen, F.M. Everaerts, L.J.J. Janssen and R.A. Tacke, *Anal. Chim. Acta*, 273 (1993) 553-560.

APPENDIX I. THE MINIQUAD PROGRAM

```
program "miniquad"(input, output, invoer, uitvoer);
{$F+}
type array1dr = array[1..10] of real;
   array2dr = array[1..10,1..2] of real;
   VIString = String[80];
   ResiduProc = Procedure (Var X : Array1dr;
                           Var G : Real;
                           I : Integer);
   GradientProc = Procedure (Var X, Dg : Array1dr;
                              I : Integer);
var D, S2, epsabs, epsrel, x1, x2           :real;
    k, m, n, info, method, stopcr, imax, out,l :integer;
    x, S0, Sd, J0, Jd                       :array1dr;
    varcov                                  :array2dr;
    invoer, uitvoer                         :text;
    finame, foname                          :string[12];

procedure residu(var x:array1dr; var res:real; i:integer);
var u, v, w:real;
begin
    u := ((J0[i] - Jd[i]) * (J0[i] + Jd[i]))/(2 * D);
    v := S0[i] - Sd[i];
    w := ln((x[1] * S0[i] + x[2])/(x[1] * Sd[i] + x[2]));
    res := (u * x[1] - v) * x[1] + x[2] * w;
end;

procedure grdres(var x, grad:array1dr; i:integer);
var u, v, w, t :real;
begin
    u := ((J0[i] - Jd[i]) * (J0[i] + Jd[i]))/(2 * D);
    v := S0[i] - Sd[i];
```

```
w := ln((x[1] * S0[i] + x[2])/(x[1] * Sd[i] + x[2]));
t := (x[2]*v)/((x[1] * S0[i] + x[2]) * (x[1] * Sd[i] + x[2]));
grad[1] := 2 * u * x[1] - v + x[2] * t;
grad[2] := w - x[1] * t;
end;
  {$I A:miniqd.pas}
begin
  write('name of the input file: '); readln(finame); writeln;
  write('name of the output file: '); readln(foname); writeln;
  {finame:='test.dat'; foname:='test.out';}
  assign(invoer, finame); reset(invoer);
  assign(uitvoer, foname); rewrite(uitvoer);
  writeln(uitvoer, 'Program results of vdloo');
  readln(invoer, D, S2);
  readln(invoer, m, n);
  for k := 1 to m do read(invoer, S0[k], Sd[k], J0[k], Jd[k]);
  readln(invoer, x1, x2);
  writeln(uitvoer, 'info method stopcr      x[1]          x[2]');
  writeln(uitvoer);
  for k:= 1 to 4 do for l:= 1 to 3 do
  begin
    epsabs := 1e-5; epsrel := 1e-5;
    info := 1; stopcr := 1;
    imax := 50; out:=0;
    x[1]:=x1; x[2]:=x2;
    method:=10*k+l;
    miniqd(m, n, x, residu, grdres, info, method, stopcr,
      epsabs, epsrel, imax, out, varcov, uitvoer);
    write(uitvoer, ' ', info, ' ', method, ' ', stopcr);
    writeln(uitvoer, ' ', x[1], ' ', x[2]);
  end; close(uitvoer)
end.
```

APPENDIX II. THE SENSOR SIMULATION PROGRAM

PROGRAM SensorSimulation;

{Numerical solution of a diffusion problem which includes constant concentration of one reactant (oxygen, A) at the left hand boundary and at the right hand boundary a constant concentration of the other reactant (glucose, B). In the region where the reactants meet reaction takes place with Ping-Pong mechanism reaction kinetics. The reaction products (C and D) may also diffuse away. The method is based on a modified and generalized Crank/Nicolson algorithm. }

{ \$N- } { +/- does/doesn't use the mathematical coprocessor }
{ \$R+ } { + checks array boundaries }
{ \$M 49152,0,655360 } { stack adjustment is essential }

USES

Crt,Dos,Printer;

CONST

MaxX = 580; { maximum number of layers;
MaxX > 600 causes memory problems }

TYPE

FileNameType = string[20];
layers = array[0..MaxX] of real;

VAR

year,month,day,DoW,
hr,min,sec,sec100 : word;
DA1,DB1,DC1,DD1,DA,DB,DC,DD : real;
NX,NTime : integer;
PathLength,TotalTime : real;
DelX,DelT : real;
ANULL,VA,BNULL : real;
AINIT : real;

```

                VAA                : real;
                CA,CB               : real;
k1a,k1,k2,k3,Beta1,Beta2,Beta3    : real;
                AlphA,AlphB,AlphC,AlphD : real;
                ij                  : integer;
                X,Y,Z              : real;
Conc1A,Conc1B,Conc1C,Conc1D       : layers;
Conc2A,Conc2B,Conc2C,Conc2D       : layers;
                hA,hB,hC,hD        : layers;
                h                   : layers;
                PA,PB,PC,PD        : layers;
                Lotus               : text;
                Lotusfile           : FileNameType;
                prntr               : char;
                Sum1,Sum2,Sum3      : real;
                DumpInt             : byte;
                NRand               : integer;
                SumA,SumB,SumC,SumD : real;
```

```
PROCEDURE TimeStepA (N:integer;var P,Conc,h:layers); {OXYGEN,A}
```

```
Var
```

```

i,k    : integer;
AX     : layers;
```

```
begin
```

```

AX[N-1]:=1/(h[N-1]-4/3);P[N-1]:=P[N-1]-P[N];
AX[N-2]:=1/(h[N-2]-2*AX[N-1]/3);P[N-2]:=P[N-2]+AX[N-1]*P[N-1];
for i:=N-3 downto 1 do
begin AX[i]:=1/(h[i]-AX[i+1]);P[i]:=P[i]+AX[i+1]*P[i+1] end;
Conc[1]:=AX[1]*(P[0]-P[1]);
for k:=2 to N-2 do
begin i:=k; Conc[i]:=-AX[i]*(P[i]-Conc[i-1]) end;
```

The sensor simulation program

```
Conc[N-1]:=-AX[N-1]*(P[N-1]-2*Conc[N-2]/3);
Conc[N]:=P[N]+(4*Conc[N-1]-Conc[N-2])/3;
Conc[0]:=P[0];
end;      {End TimeStepA}
```

```
PROCEDURE TimeStepB(N:integer;var P,Conc,h:layers);  {GLUCOSE, B}
```

```
Var
```

```
  i,k : integer;
```

```
  AX  : layers;
```

```
begin
```

```
  AX[1]:=1/(h[1]-4/3);P[1]:=P[1]-P[0];
```

```
  AX[2]:=1/(h[2]-2*AX[1]/3);P[2]:=P[2]+AX[1]*P[1];
```

```
  for i:=3 to N-1 do
```

```
    begin AX[i]:=1/(h[i]-AX[i-1]);P[i]:=P[i]+AX[i-1]*P[i-1] end;
```

```
  Conc[N-1]:=AX[N-1]*(P[N]-P[N-1]);
```

```
  for k:=2 to N-2 do
```

```
    begin i:=N-k;Conc[i]:=-AX[i]*(P[i]-Conc[i+1]) end;
```

```
  Conc[1]:=-AX[1]*(P[1]-2*Conc[2]/3);
```

```
  Conc[0]:=P[0]+(4*Conc[1]-Conc[2])/3;
```

```
  Conc[N]:=P[N];
```

```
end;  {End TimeStepB}
```

```
PROCEDURE TimeStepC(N:integer;var P,Conc,h:layers); {Products, C and D}
```

```
Var
```

```
  i,k : integer;
```

```
  AX  : layers;
```

```
begin
```

```
  AX[1]:=1/(h[1]-4/3);P[1]:=P[1]-P[0];
```

```
  AX[2]:=1/(h[2]-2*AX[1]/3);P[2]:=P[2]+AX[1]*P[1];
```

```
  for i:=3 to N-1 do
```

```
begin AX[i]:=1/(h[i]-AX[i-1]);P[i]:=P[i]+AX[i-1]*P[i-1] end;
Conc[N-1]:=AX[N-1]*(P[N]-P[N-1]);
for k:=2 to N-2 do
begin i:=N-k;Conc[i]:=-AX[i]*(P[i]-Conc[i+1]) end;
Conc[1]:=-AX[1]*(P[1]-2*Conc[2]/3);
Conc[0]:=P[0]+(4*Conc[1]-Conc[2])/3;
Conc[N]:=P[N]+(4*Conc[N-1]-Conc[N-2])/3;
end; {End TimeStepC}
```

```
PROCEDURE Dump(Time:real;N:integer;CA,CB,CC,CD:layers);
```

```
var i : integer;
begin
writeln(Lotus,Time,"s");
for i:=0 to N do
writeln(Lotus,i,CA[i],CB[i],CC[i],CD[i]);
writeln(Lotus," ")
end; {End Dump}
```

```
begin {MAIN PROGRAM}
ClrScr;
Randomize;NRand:=Random(10000);
DA:=0.37E-9 {zuurstof, m2.s-1};
DB:=0.047E-9 {glucose} ; {diffusion coefficients;}
DC:=0.27E-9 {H2O2} ;
DD:=0.04E-9 {gluconolactone} ; {estimation}

DA1:=DA*1E9; DB1:=DB*1E9;
DC1:=DC*1E9; DD1:=DD*1E9;
k1:=0.14E-3 {kmol.m-3.s-1} ; {Vmax}
k2:=0.01E-3 {kmol.m-3} ; {ko} {kinetic parameters;}
k3:=22E-3 {kmol.m-3} ; {kg}
```

```
k1a: =k1*1E3;
TotalTime: =600 ; {s}
LotusFile: ='c:\reken\123\dif1';
Assign(Lotus,LotusFile + '.prn');rewrite(Lotus);
Writeln(Lotus,'"Name:"',N Rand);
Writeln(Lotus,'"DA= "',DA1,'"**E-9"');
Writeln(Lotus,'"DB= "',DB1,'"**E-9"');
Writeln(Lotus,'"DC= "',DC1,'"**E-9"');
Writeln(Lotus,'"DD= "',DD1,'"**E-9"');
Writeln(Lotus,'"Vmax= "',k1a,'"**E-3"');
Writeln(Lotus,'"ko= "',k2);
Writeln(Lotus,'"kg= "',k3);
Writeln(Lotus,'"tot.tijd="',TotalTime,'"s"');
ANULL: =1E-3 ;      {constant concentration of A at left boundary}
BNULL: =5E-3 {kmol.m^-3} ; {constant concentration of B at right
                           boundary}
AINIT: =0 {1e-3} {kmol.m^-3} ; {constant initial conc. of A all over the sample}

prnr: ='n';          {'y' if output wanted on the printer}

NX: =20;              {number of layers used}
if NX < 2 then
begin
  ClrScr;writeln;
  writeln('****Not enough layers: increase the value of NX****');
  Halt
end;

if NX > MaxX then
begin
  ClrScr;writeln;writeln('****Too many layers: adjust NX or MaxX ****');
  Halt
```

```
end;
PathLength:=8E-4 {m};
DelX:=PathLength/NX;
NTime:=100;
DelT:=TotalTime/NTime;
GetDate(year,month,day,DoW);GetTime(hr,min,sec,sec100);
writeln;writeln;
writeln('date: ',year,'.',month,'.',day
      ','; time: ',hr,':',min,':',sec);
writeln;
writeln('Input: ');writeln;
writeln('DA = ',DA:15,'m^2.s^-1');
writeln('DB = ',DB:15,'m^2.s^-1');
writeln('DC = ',DC:15,'m^2.s^-1');
writeln('DD = ',DD:15,'m^2.s^-1');
writeln;
writeln('A0 = ',ANULL:15,'kmol.m^-3');
writeln('B0 = ',BNULL:15,'kmol.m^-3');
writeln;
writeln('k1 = ',k1:15,'kmol.m^-3.s^-1');
writeln('k2 = ',k2:15,'kmol.m^-3');
writeln('k3 = ',k3:15,'kmol.m^-3');
writeln;
writeln(NX:5,'layers of thickness',DelX:15,'m');
writeln('total pathlength: ',PathLength:15,'m');
writeln;
writeln(NTime:5,' periods of ',DelT:15,'s');
writeln('total time: ', TotalTime:15,'s');
writeln;
writeln('****PROGRAM IS RUNNING****');
writeln;writeln;
if prntr = 'y' then
```



```
begin
  writeln(lst);writeln(lst);
  writeln(lst,'date: ',year,' ',month,' ',day
    ,';time: ',hr,':',min,':',sec);
  writeln(lst,'Name: ',NRand);
  writeln(lst);
  writeln(lst,'Input: ');writeln(lst);
  writeln(lst,'DA = ',DA:15,' m^2.s^-1');
  writeln(lst,'DB = ',DB:15,' m^2.s^-1');
  writeln(lst,'DC = ',DC:15,' m^2.s^-1');
  writeln(lst,'DD = ',DD:15,' m^2.s^-1');
  writeln(lst);
  writeln(lst,'A0 = ',ANULL:15,'kmol.m^-3');
  writeln(lst,'B0 = ',BNULL:15,'kmol.m^-3');
  writeln(lst);
  writeln(lst,'k1 = ',k1:15,'kmol.m^-3.s^-1');
  writeln(lst,'k2 = ',k2:15,'kmol.m^-3');
  writeln(lst,'k3 = ',k3:15,'kmol.m^-3');
  writeln(lst);
  writeln(lst,NX:5,'layers of thickness',DelX:15,'m');
  writeln(lst,'total pathlength: ',PathLength:15,'m');
  writeln(lst);
  writeln(lst,NTime:5,'periode of ',DelT:15,'s');
  writeln(lst,'total time: ',TotalTime:15,'s')
end;

X:=0.5*DelT/(DelX*DelX);AlphaA:=DA*X;AlphaB:=DB*X;
      AlphaC:=DC*X;AlphaD:=DD*X;

X:=DelT/4;Beta1:=X*k1;Beta2:=k2/2;Beta3:=k3/2;

X:=0.0;          {setting the initial concentrations}
```

```
for i:=0 to NX do
begin
  Conc1A[i]:=AINIT;Conc1B[i]:=X;Conc1C[i]:=X;Conc1D[i]:=X;
  Conc2A[i]:=AINIT;Conc2B[i]:=X;Conc2C[i]:=X;Conc2D[i]:=X;
end;

Conc1B[NX]:=BNULL;Conc1A[0]:=ANULL;
PA[0]:=ANULL;PA[NX]:=0.0;
PB[0]:=0.0;PB[NX]:=BNULL;
PC[0]:=0.0;PC[NX]:=0.0;
PD[0]:=0.0;PD[NX]:=0.0;

DumpInt:=1;
for j:=1 to Ntime do
begin
  writeln(NRand,'; Cycle:'j,' from ',NTime,'); Conc1A[1] = ',Conc1A[1],
'Conc1A[3] = ',Conc1A[3], 'Conc1A[7] = ',Conc1A[7], 'Conc1A[10] = ',Conc1A[10],
'Conc1A[13] = ',Conc1A[13], 'Conc1A[9] = ',Conc1A[9], 'Conc1A[17] = ',Conc1A[17],
'Conc1A[20] = ',Conc1A[20], 'Conc1A[5] = ',Conc1A[5]);
  Sum2:=1.0E9;

  REPEAT
    Sum3:=Sum2;Sum2:=Sum1;

    for i:=1 to NX-1 do
    begin
      hA[i]:=Beta1*(Conc1A[i]+Conc2A[i]);
      hB[i]:=Beta1*(Conc1B[i]+Conc2B[i]);
      hC[i]:=Beta2*(Conc1B[i]+Conc2B[i]);
      hD[i]:=Beta3*(Conc1A[i]+Conc2A[i]);
      if (hC[i]+hD[i])=0.0 then X:=0.0 else X:=hB[i]/(hC[i]+hD[i]);
      PA[i]:=(2-1/Alpha+X/Alpha)*Conc1A[i]-Conc1A[i+1]-Conc1A[i-1];
```

```
if (hC[i]+hD[i])=0.0 then X:=0.0 else X:=hA[i]/(hC[i]+hD[i]);
PB[i]:=(2-1/AlphB+X/AlphB)*Conc1B[i]-Conc1B[i+1]-Conc1B[i-1];
if (hC[i]+hD[i])=0.0 then X:=0.0 else X:=-hB[i]*hA[i]/(hC[i]+hD[i]);
PC[i]:=X/(AlphC*Beta1)
      +(2-1/AlphC)*Conc1C[i]-Conc1C[i+1]-Conc1C[i-1];
PD[i]:=X/(AlphD*Beta1)
      +(2-1/AlphD)*Conc1D[i]-Conc1D[i+1]-Conc1D[i-1]
end;

for i:=1 to NX-1 do begin
if (hC[i]+hD[i])= 0.0 then X:=0.0 else X:=hB[i]/(hC[i]+hD[i]);
h[i]:=(1/AlphA+2+X/AlphA) end;
TimeStepA(NX,PA,Conc2A,h);
for i:=1 to NX-1 do begin
if (hC[i]+hD[i])= 0.0 then X:=0.0 else X:=hA[i]/(hC[i]+hD[i]);
h[i]:=(1/AlphB+2+X/AlphB) end;
TimeStepB(NX,PB,Conc2B,h);
for i:=1 to NX-1 do h[i]:=(1/AlphC+2);
TimeStepC(NX,PC,Conc2C,h);
for i:=1 to NX-1 do h[i]:=(1/AlphD+2);
TimeStepC(NX,PD,Conc2D,h);
Sum1:=0.0;
for i:=0 to NX do
begin
X:=Conc1A[i]-Conc2A[i];Sum1:=Sum1+X*X;
{writeln('Conc2A,Sum1,i=',Conc2A[i],Sum1,i);}
X:=Conc1B[i]-Conc2B[i];Sum1:=Sum1+X*X;
{writeln('Conc2B,Sum1,i=',Conc2B[i],Sum1,i);}
X:=Conc1C[i]-Conc2C[i];Sum1:=Sum1+X*X;
X:=Conc1D[i]-Conc2D[i];Sum1:=Sum1+X*X
end;
```

```
X:=Abs(1.0E-10*Sum1)

UNTIL (Abs(Sum1-Sum2)<X) and (Abs(Sum1-Sum3)<X);

for i:=0 to NX do
begin
  Conc1A[i]:=Conc2A[i];Conc1B[i]:=Conc2B[i];
  Conc1C[i]:=Conc2C[i];Conc1D[i]:=Conc2D[i]
end;

{ if (j=Round(NTime/6.0*DumpInt)) and (k1 < > 0.0) then
begin
  X:=j*DelT;
  Dump(X,NX,Conc1A,Conc1B,Conc1C,Conc1D);
  DumpInt:=DumpInt+1 end; }

end;
X:=TotalTime;
Dump(X,NX,Conc1A,Conc1B,Conc1C,Conc1D);
writeln;writeln;
write('      [A]  ','      [B]  ');
writeln('    [C]  ','    [D]  ')
  if prntr='y' then
begin
  writeln(1st);writeln(1st);
  write(1st,'      [A]  ','      [B]  ');
  writeln(1st,'    [C]  ','    [D]  ')
end;
write(Lotus,chr(26));Flush(Lotus); Close(Lotus)

end.      {END MAIN PROGRAM}
```

LIST OF SYMBOLS

(with the exception of symbols used in the sensor simulation program)

α	partition coefficient at the interface hydrogel/bulk solution
α_g, α_{ox}	partition coefficient of glucose and oxygen, respectively
η	dynamic viscosity of the overall solution ($\text{kg m}^{-1} \text{s}^{-1}$)
η_a, η_b, η_c	dynamic viscosity of an aqueous solution of compound 1, 2 and 3, respectively ($\text{kg m}^{-1} \text{s}^{-1}$)
η_1, η_2, η_3	apparent dynamic viscosity of compound 1, 2 or 3, respectively ($\text{kg m}^{-1} \text{s}^{-1}$)
η_s, η_w	dynamic viscosity of the overall solution and pure water, respectively ($\text{kg m}^{-1} \text{s}^{-1}$)
ν	kinematic viscosity of a solution ($\text{m}^2 \text{s}^{-1}$)
ν_{dl}	kinematic viscosity of the diffusion layer ($\text{m}^2 \text{s}^{-1}$)
ρ	density (kg m^{-3})
ω	angular rotation rate (rad s^{-1})
a^*, b^*	parameters defined by Eqn. (21) in Chapter 4
A_o	geometrical electrode area (m^2)
A_m, A_f	surface area of membrane and filter-paper, respectively (m^2)
C	constant ($\text{mol}^2 \text{m}^{-3}$)
c'_A, c'_B	concentration at the diffusion layer/filter-paper interface next to compartment A and B, respectively (mol m^{-3})
c^*_{dl}, c^*_{hl}	concentration at the diffusion layer/hydrogel layer interface, at the diffusion layer and hydrogel layer side, respectively (mol m^{-3})
c_A, c_B	concentration in compartment A and B, respectively (mol m^{-3})
c_b, c_{dl}, c_{hl}	concentration in, respectively, bulk solution, diffusion layer and hydrogel layer (mol m^{-3})
c_g, c_{hp}, c_{ox}	concentration of glucose, hydrogen peroxide and oxygen, respectively (mol m^{-3})
$c_{g,a}, c_{g,b}$	glucose concentration at the filter-paper/membrane interface next to compartment A and B, respectively (mol m^{-3})

$c_{g,A}$ $c_{g,B}$	glucose concentration in compartment A and B, respectively (mol m ⁻³)
c_{GO}	glucose oxidase concentration (mol m ⁻³)
c_t	concentration at time t (mol m ⁻³)
$c_{t^*,X}$	concentration at characteristic time t^* and characteristic electrode X (mol m ⁻³)
D	diffusion coefficient in the bulk solution (m ² s ⁻¹)
D_{eff}	effective diffusion coefficient (m ² s ⁻¹)
D_{dl} , D_{hl} , D_m , D_r , D_{sl}	diffusion coefficient in, respectively, the diffusion layer, the hydrogel layer, the membrane, the resistance layer and the solution layer (m ² s ⁻¹)
d_{dl} , d_r , d_{hl} , d_m , d_t , d_{sl}	thickness of, respectively, the diffusion layer, the filter-paper, the hydrogel layer, the membrane, the resistance layer and the solution layer (m)
F	the Faraday, i.e., the charge on one mole of electrons (C)
h_A , h_B	initial slope of concentration versus time curve of compartment A and B, respectively (mol m ⁻³ s ⁻¹)
i	place index
I^*	intercept of a current versus square root of the angular rotation rate curve (A)
I_{lim}	diffusion controlled limiting current (A)
I_t	current at time t (A)
$I_{t^*,X}$	current at characteristic time t^* and characteristic electrode X (A)
j	time index
J	flux (mol m ⁻² s ⁻¹)
J_0 , J_δ	flux in the membrane at membrane/filter-paper interface next to compartment A and B, respectively (mol m ⁻² s ⁻¹)
J_A , J_B	flux leaving compartment A and entering compartment B, respectively (mol m ⁻² s ⁻¹)
J_{dl} , J_{hl} , J_m	flux through a diffusion layer, a hydrogel layer and a membrane, respectively (mol m ⁻² s ⁻¹)

List of symbols

k	total mass transfer coefficient (m s^{-1})
$k_{bl}, k_{dl}, k_f,$ k_{hl}, k_m	mass transfer coefficient in, respectively, the buffer layer, the diffusion layer, the filter-paper, the hydrogel layer and the membrane (m s^{-1})
k_1, k_2	rate constant of a particular reaction step ($\text{m}^3 \text{mol}^{-1} \text{s}^{-1}$)
k_{-1}, k_{-2}	rate constant of a particular reaction step (s^{-1})
k_{cat}	(intrinsic) catalytic constant of turnover number (s^{-1})
k_{cat}^*	inherent catalytic constant, determined by inserting D_m (s^{-1})
k_{cat}^{**}	inherent catalytic constant, determined by inserting D_{eff} (s^{-1})
$k_m(g)$	(intrinsic) Michaelis constant for glucose (mol m^{-3})
$k_m(o)$	(intrinsic) Michaelis constant for oxygen (mol m^{-3})
$k_m^*(g)$	inherent Michaelis constant for glucose (mol m^{-3})
$k_m^*(o)$	inherent Michaelis constant for oxygen (mol m^{-3})
m_{GO}	number of moles of GO present (mol)
n	number of electrons involved in the electrode reaction
P_{dl}, P_{hl}	permeability of the diffusion layer and the hydrogel layer, respectively (m s^{-1})
P_{eff}	effective permeability (m s^{-1})
t	time (s)
V	volume (m^3)
v_0	initial reaction velocity ($\text{mol m}^{-3} \text{s}^{-1}$)
V_{max}	(intrinsic) maximal reaction velocity ($\text{mol m}^{-3} \text{s}^{-1}$)
V_{max}^{**}	inherent maximal reaction velocity, determined by inserting D_{eff} ($\text{mol m}^{-3} \text{s}^{-1}$)
x	distance (m)
$x_{1,a}, x_{2,b}, x_{3,c}$	mole fraction of compound 1, 2 and 3 in the related aqueous solutions a, b and c, respectively
x_1, x_2, x_3	mole fraction of compound 1, 2 and 3 in the overall solution
x_w	mole fraction of water in the overall solution
$x_{w,a}, x_{w,b}, x_{w,c}$	mole fraction of water in the aqueous solutions a, b and c, respectively

SUMMARY

This thesis describes the design of a new short-term *in vivo* glucose sensor for diabetic patients. Like the present glucose sensors, the new sensor uses the enzyme glucose oxidase (GO) to catalyse the reaction of glucose and oxygen to gluconolactone and hydrogen peroxide. Hydrogen peroxide is detected amperometrically. The new principle of the sensor implies the creation of a counter-diffusion flow of glucose and oxygen through a GO-containing hydrogel layer. As a result, hydrogen peroxide is only formed in a restricted hydrogel zone. When the detection electrode for hydrogen peroxide is placed adjoining to this zone, the major part of hydrogen peroxide is detected, whereas in other sensors loss of hydrogen peroxide is one of the most disturbing problems. To determine the optimal geometry of the sensor the concentration profiles of the participating compounds have to be calculated. This can be carried out with the help of a computer program that simulates the sensor. This program requires knowledge of the diffusion coefficients of the compounds in the GO-containing hydrogel layer and the kinetic parameters of the enzyme reaction.

Determination of the diffusion coefficients of oxygen and hydrogen peroxide was performed using a rotating disc electrode (RDE), covered with a GO-containing hydrogel layer. The diffusion of both species appeared to be slowed to the same extent by the gel. The diffusion coefficient of the electrochemically inactive glucose was determined by simultaneous diffusion of glucose and hydroquinone through the hydrogel. As the diffusion coefficient of hydroquinone in the gel was determined with the RDE-hydrogel method, the diffusion coefficient of glucose in the hydrogel could be calculated. Glucose appeared to be slowed to a larger extent than oxygen and hydrogen peroxide.

Before determining the inherent kinetic parameters of immobilized GO, the (intrinsic) parameters of soluble GO were determined for comparison. The *initial* reaction velocity was determined by measuring the hydrogen peroxide concentration as a function of time, after injection of GO. With the construction of Lineweaver-Burk plots the kinetic

Summary

parameters were obtained.

The inherent kinetic parameters of immobilized GO were determined with a diffusion cell. Between two compartments (A and B) containing solutions with different glucose concentrations, a GO-containing hydrogel membrane was placed. The flux leaving compartment A was not equal to the flux entering compartment B, owing to simultaneous diffusion through and enzymatic reaction in the GO-containing membrane. By deducing an equation for this situation, the kinetic parameters of immobilized GO could be determined. The inherent turnover number of immobilized GO was considerably larger than the (intrinsic) turnover number of soluble GO. Presumably, this is a result of GO-leakage out of the membrane, mainly before cross-linking with glutaraldehyde occurs. This means that the turnover number is calculated from the maximal initial velocity V_{\max} using a higher GO-concentration than it actually might be.

From calculations with the sensor simulation program the conclusion can be drawn that when the total length of the sensor (from oxygen producing electrode to glucose window) is too small, diffusion control is replaced by kinetic control, which leads to saturation of the sensor with oxygen and glucose. To reach steady state diffusion controlled concentration profiles, the sensor must have a minimum total length of $8 \cdot 10^{-4}$ m. The adjustment of the steady state takes about 10 min for a sensor with this minimum total length. The glucose concentration range that can be measured is 0-5 mM. Applying an extra diffusion barrier for glucose could significantly increase this range. The time needed to reach steady state with this extra diffusional resistance is extended by less than 2 min.

A macro sensor with an array of ten electrodes was used to compare the experimental performances with the calculations of the sensor simulation program. Both parallel-diffusion flow and counter-diffusion flow experiments show good agreement with the simulation forecast.

The new principle of counter-diffusion flow appears to have the potential to yield a suitable glucose sensor. A lot of practical problems, however, have not been solved yet and they now should become our major concern.

SAMENVATTING

Dit proefschrift beschrijft het ontwerp van een nieuwe short-term *in vivo* glucosesensor voor diabetespatiënten. Net zoals de huidige glucosesensoren gebruikt de nieuwe sensor het enzym glucoseoxidase (GO) om de reactie van glucose met zuurstof tot gluconolacton en waterstofperoxyde te katalyseren. Waterstofperoxyde wordt dan amperometrisch gedetecteerd. Het nieuwe principe van de sensor behelst het doen ontstaan van een tegenstroom van glucose- en zuurstofdiffusie door een GO-bevattende hydrogellaag. Hierdoor wordt waterstofperoxyde slechts in beperkte hydrogel-zone gevormd. Door nu hier de detectie-elektrode te plaatsen wordt het overgrote deel van de waterstofperoxyde daadwerkelijk gedetecteerd. Bij de huidige sensoren is juist het verlies aan waterstofperoxyde uit de sensor en dus een lage detectiestroom een van de grootste problemen. Om de optimale geometrie van de sensor te bepalen, zullen de concentratieprofielen van alle stoffen die bij de glucosemeting betrokken zijn berekend moeten worden. Dit kan gedaan worden met behulp van een computer simulatieprogramma. Als invoerparameters voor dit programma dienen zowel de diffusiecoëfficiënten van de participerende stoffen in een GO-bevattende hydrogel als de kinetische parameters van de enzymatische reactie in de hydrogel.

De bepaling van de diffusiecoëfficiënten van zuurstof en waterstofperoxyde werd uitgevoerd met een roterende schijf elektrode (RDE) die bedekt was met een GO-bevattende hydrogellaag. De diffusie van beide stoffen bleek in dezelfde mate afgeremd te worden door de gel. De diffusiecoëfficiënt van het elektrochemisch inactieve glucose werd bepaald door simultane diffusie van glucose en hydrochinon door de hydrogel. Daar de diffusiecoëfficiënt van het elektroactieve hydrochinon met de RDE-hydrogel methode bepaald kon worden, kon de diffusiecoëfficiënt van glucose in de hydrogel berekend worden. De diffusie van glucose bleek veel sterker geremd te worden door de hydrogel dan de diffusie van zuurstof en waterstofperoxyde.

Alvorens de inherente kinetische parameters van geïmmobiliseerd GO te bepalen, werden ter vergelijking de (intrinsic) kinetische parameters van GO in de oplossing bepaald. De *initiele* reactiesnelheid werd bepaald door de waterstofperoxyde-concentratie

na injectie van GO als functie van de tijd te meten. Via Lineweaver-Burk plots konden de kinetische parameters berekend worden.

De inherente kinetische parameters van geïmmobiliseerd GO werden bepaald met behulp van een diffusiecel. Tussen twee compartimenten (A en B) werd een GO-bevattend membraan geplaatst. De compartimenten bevatten oplossingen met verschillende glucoseconcentraties. Bij verzadiging met zuurstof is de flux, die compartiment A verlaat groter dan de flux, die compartiment B ingaat, omdat er gelijktijdig diffusie door het membraan en enzymatische reactie in het membraan plaatsvindt. Door een relatie voor deze situatie af te leiden, kunnen de kinetische parameters van geïmmobiliseerd GO bepaald worden. Het inherente turnover number van geïmmobiliseerd GO is aanmerkelijk lager dan het turnover number van GO in oplossing. Hoogstwaarschijnlijk is dit te wijten aan het uitlekken van GO uit het membraan, voornamelijk in de fase voordat cross-linking met glutaaraldehyde plaatsvindt. Dit betekent dat de GO-concentratie in het membraan veel lager is dan de concentratie waarmee het turnover number is berekend.

Uit berekeningen met het sensor simulatieprogramma kan de conclusie getrokken worden dat bij een te klein gekozen totale sensorlengte (diffusie weglengte) diffusie-limitering overgaat in kinetische limitering, waardoor de sensor verzadigd raakt met glucose en zuurstof. Diffusie-gelimiteerde stationaire profielen worden bereikt als de sensorlengte minimaal $8 \cdot 10^{-4}$ m is. Het instellen van de (pseudo)stationaire toestand duurt ongeveer 10 min voor een sensor met deze minimale lengte. De glucose-concentratierange die dan gemeten kan worden is 0-5 mM. Door het aanbrengen van een extra diffusiebarrière voor glucose kan deze range aanzienlijk vergroot worden. De extra tijdsduur die nodig is om met deze extra diffusieweerstand een (pseudo)stationaire toestand te bereiken is minder dan 2 min.

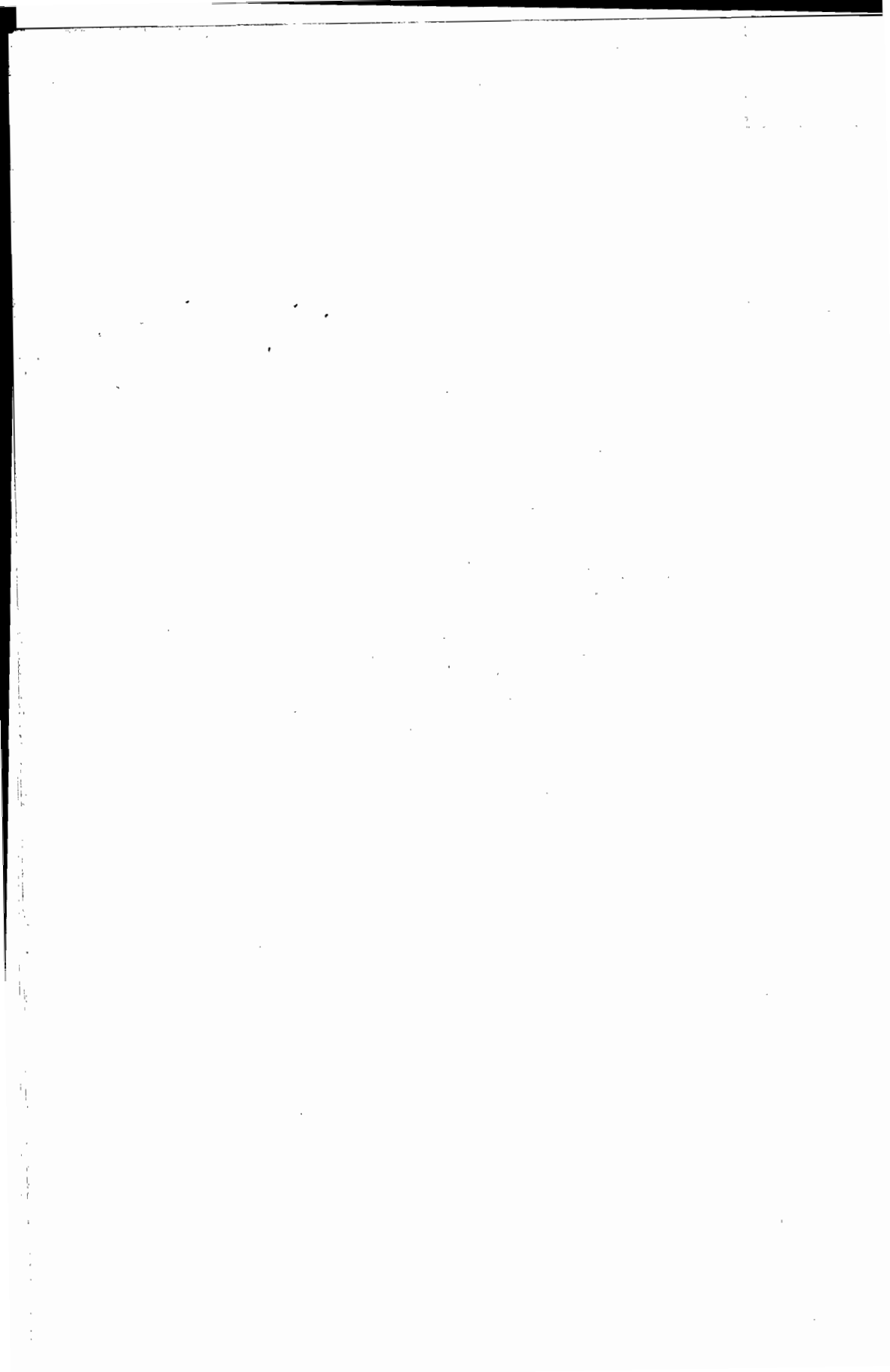
Een macrosensor met een rij van tien elektroden werd gebruikt om de experimentele prestaties te vergelijken met de berekeningen van het simulatieprogramma. Zowel meestroom- als tegenstroomexperimenten vertonen een goede overeenkomst met de uitkomsten van het simulatieprogramma. Het nieuwe tegenstroomprincipe blijkt mogelijkheden te hebben om een goede glucosesensor op te leveren. Toch bestaan er nog een aantal praktische problemen, welke nu onze grootste aandacht verdienen.

CURRICULUM VITAE

De schrijfster van dit proefschrift werd geboren op 27 augustus 1967 te Eindhoven. In mei 1985 werd het VWO-diploma behaald aan het Maurick-college te Vught. In september van hetzelfde jaar werd aangevangen met de studie Scheikundige Technologie aan de Technische Universiteit Eindhoven. In september 1986 werd het propedeutisch examen afgelegd. Het ingenieursexamen (afstudeerrichting bio-organische chemie) werd in oktober 1989 cum laude afgelegd.

Van november 1989 tot september 1990 was zij als assistent in opleiding (A.I.O.) werkzaam binnen de vakgroep Organische Chemie van de Technische Universiteit Eindhoven.

Het in dit proefschrift beschreven onderzoek werd uitgevoerd in de periode september 1990 tot september 1993 bij de subgroep Elektrochemie van de vakgroep Instrumentele Analyse, aan dezelfde universiteit. Het onderzoek, onder leiding van prof.dr.ir. F.M. Everaerts en dr. L.J.J. Janssen, werd financieel ondersteund door de Stichting voor de Technische Wetenschappen (STW).



STELLINGEN

behorende bij het proefschrift

**Heading for a glucose sensor
Designing and testing a new principle**

van

Saskia A.M. van Stroe-Biezen

1. De randvoorwaarde die Tse *et al.* gebruiken, dat in een zowel zuurstof- als waterstofperoxyde-bevattende oplossing onder anodische omstandigheden de afgeleide van het concentratieprofiel van zuurstof aan het elektrode-oppervlak gelijk zou zijn aan nul, is discutabel. Bij de anodische oxidatie van waterstofperoxyde wordt immers zuurstof aan het elektrode-oppervlak gevormd.

P.H.S. Tse, J.K. Leyboldt en D.A. Gough, Biotechn. and Bioeng., 29 (1987) 696-704.

2. Daar bij enzymatische sensoren het activiteitsverlies van het enzym vaak één van de grootste problemen vormt, moet men zorgen dat deze activiteit geen limiterende rol vervuld.

Dit proefschrift, Hoofdstuk 1.

3. De meer dan twintig jaar oude ADI's (Acceptable Daily Intake) van zowel nitraat als nitriet zijn met de huidige kennis van zaken totaal verouderd en zouden opnieuw moeten worden vastgesteld.

M.W.P.L. Baars and E.H.H. Snellen, Investigations of nitrate in leafy vegetables. A critical view on the "ADI", Case-study verslag, Technische Universiteit Eindhoven, Laboratorium voor Instrumentele Analyse, (1993).

P.J.P. Janssen, Onderzoek naar het effect van nitriet op hormoonmetaboliserende P450 enzymen uit de runder bijnierschors, afstudeerverslag, Technische Universiteit Eindhoven, (1993).

4. Het vergelijken van de effectieve kinetische parameters van een geïmmobiliseerd enzym met de (intrinsieke) kinetische parameters van een enzym in oplossing zegt feitelijk niets over het effect van de immobilisatie op het enzym zelf.

Dit proefschrift, Hoofdstuk 4.

5. Het herinvoeren van de rekenliniaal zou het gevoel voor (significantie van) getallen, wat door het gebruik van de rekenmachine duidelijk onder peil is geraakt, aanzienlijk vergroten.
6. De onderzoeker komt zichzelf tegen, op het moment dat hij zijn werk wil gaan publiceren.
7. Het uitbesteden van niet-kernactiviteiten en het vergroten van de betrokkenheid en de individuele verantwoordelijkheid van de werknemers ("lean management") zou voor vele bedrijven een middel kunnen zijn om te overleven.
8. Technische opleidingen zouden meer bedrijfskundige en commerciële elementen moeten bevatten.
9. Het is danstechnisch en historisch gezien onjuist om Fred Astaire, Ginger Rogers en Gene Kelly aan te merken als de grondleggers van de moderne dans. Dit zou Harold en Fayard Nicholas (The Nicholas Brothers) te kort doen.
10. Iemand die een goede daad verricht om er daarna over op te kunnen schepen, verricht deze daad ter eer en glorie van zichzelf. Iemand die in alle bescheidenheid en anonimiteit een ander helpt, getuigt pas werkelijk van een oprechte goedheid.

Amisum non flet cum sola est Gellia patrem;
si quis adest, iussae prosiliunt lacrimae.

Non luget quisquis laudari, Gellia, quaerit.

Ille dolet vere, qui sine teste dolet.

Martialis, epigram 1,33.